Università degli Studi di Firenze

DOTTORATO DI RICERCA IN
"Scienze del Suolo e Climatologia"

CICLO XXV

COORDINATORE Prof. Luca Calamai

Assessment of weather impact on Durum wheat and forecasting of grain yield and quality

Settore Scientifico Disciplinare AGR / 02

Dottorando
Dott. (*Orlando Francesca*)
(firma)

Tutore
Prof. (*Orlandini Simone*)
(firma)

Co-Tutore
Prof. (*Motha Raymond*)
(firma)

Anni 2010/2012

Ai miei amici e alla mia famiglia,
in particolar modo ai nuovi
arrivati, Mariateresa e Marco

TABLE OF CONTENT

Section 2 *"Performance of remotely sensed indices in monitoring the variability of harvest quantity and quality and integration with crop modeling tools"*

1. DURUM WHEAT

1.1. Durum wheat production in Italy

Italy is among the top twenty wheat producing countries in the world. Despite this, during the years, Italy is slowly losing its high ranking, moving from 6th place in 1961 to 18th place in 2010 (Fig. 1.1.1, FAOSTAT). However, Italian wheat production is still relatively consistent, especially taking into account the lower available arable lands compared others countries, this trend highlights the crisis that agriculture is going through for the cereal sector. The consequence is for Italy to increase foreign grain importation, losing its world leadership.

The decline of wheat production during the last 50 years (1961-2010) is confirmed by the recorded trends for the harvested quantity and dedicated area (Fig. 1.1.2, FAOSTAT data elaboration). In both cases, significant decreasing ($P \leq 0.001$) trends are shown, with R^2 values of 0.43 and 0.95, respectively.

A smaller decrease was observed for the harvested quantity compared to the dedicated area. This is due to the parallel improvement of yield that was partially able to compensate the reduction of cultivated lands (Fig. 1.1.3, FAOSTAT data elaboration). The yields increase was due to technological enhancements, principally in cultivation techniques (e.g. soil tillage, crop rotation, etc.), cultivar patterns (plants breeding and genetic improvement) and chemical input (e.g. fertilizers, pesticides, herbicides, etc.).

Despite the decreasing production, the relevance of wheat in the agricultural sector remained constant. From 1961 to 2010 this crop was among the first four main agricultural products of Italy, together with grapes, maize and sugar beet (FAOSTAT). Indeed the wheat flour is the main raw material for the bread and pasta-making industry and for the confectionery industry. In particular, durum wheat (*Triticum turgidum* L. var. *durum*) has a main role, in terms of national annual consumption and for the export market, since it is the only species able to provide the raw material for pasta making. Durum wheat provides a coarse granulated flour, called ‘semolina’. This flour, compared to that from ordinary wheat, contains more crude protein and gives particular

baking and nutritional qualities to the final product (Salmon and Clark, 1913). The latest data from the International Pasta Organization (2011) shows a world pasta production of about 13 million tons, spread over 44 countries. In this context, the Italian industry accounts for almost 25%. For this reason durum wheat remains the most important cereal for Italy, with more than 1 million of cultivated hectares and about 4 million tons of annual production (ISTAT, 2011). The durum wheat Italian production is concentrated in the southern and central regions (ISTAT, 2011).

In particular, in Tuscany (central Italy) durum wheat is considered an important quality production. The regional cultivated surface with durum wheat was during the last 5 years (2007-2011) on average of 100,000 ha, equal to about 15% of the total Tuscan arable lands. In 2011 (ISTAT, 2011) the Tuscan annual production of durum wheat was more than 300,000 tons with a cultivated surface that covered more than half of the arable lands dedicated to cereals in the region (Fig. 1.1.4).

The greater importance of durum wheat compared to common wheat is also underlined by the different trends of harvested quantity that these two crops had in Tuscany over the years (Fig. 1.1.5, ISTAT data elaboration). From 1952 to 2011, durum wheat showed an increasing trend, despite the general crisis of the local cereal sector, while the ordinary wheat had a marked decrease.

Fig. 1.1.1 Wheat production in Metric Ton-USA system (1 MT =1000 kg) in 2010, from the top 20 producing countries. Source: FAOSTAT, 2010.

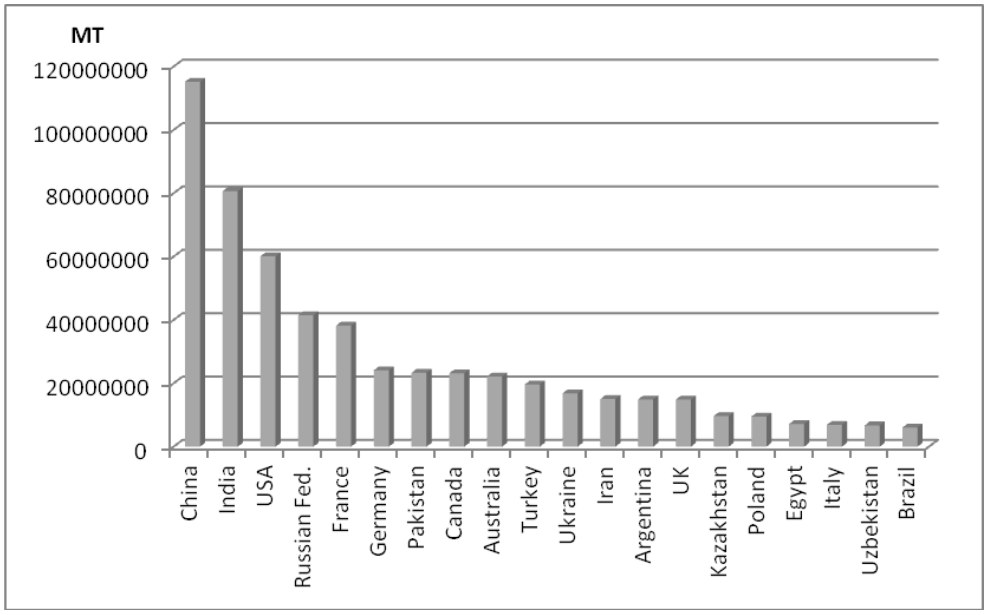

Fig. 1.1.2 Wheat harvested quantity and dedicated area in Italy from 1961 to 2010. Source: FAOSTAT, 1961-2010, data elaboration.

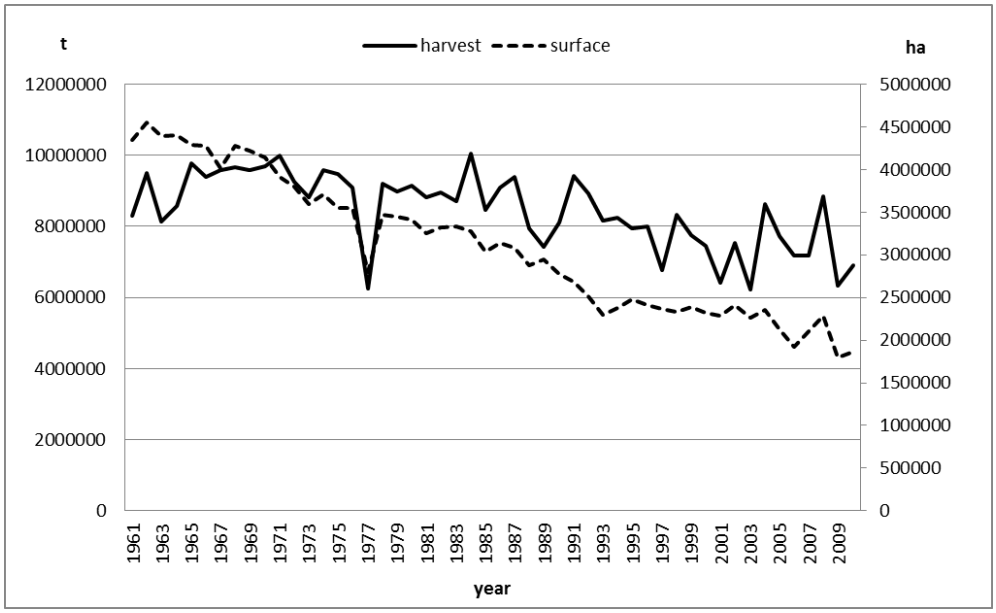

Fig. 1.1.3 Wheat yield and dedicated area in Italy from 1961 to 2010.

Source: FAOSTAT, 1961-2010, data elaboration.

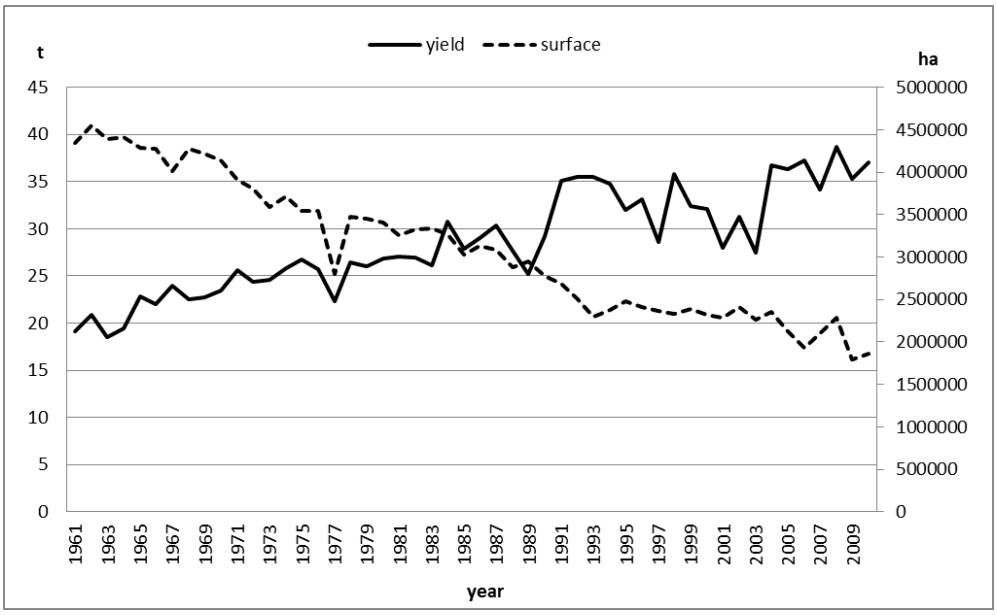

Fig. 1.1.4 Arable lands (%) dedicated to cereal crops in Tuscany in 2011.

Source: ISTAT, 2011.

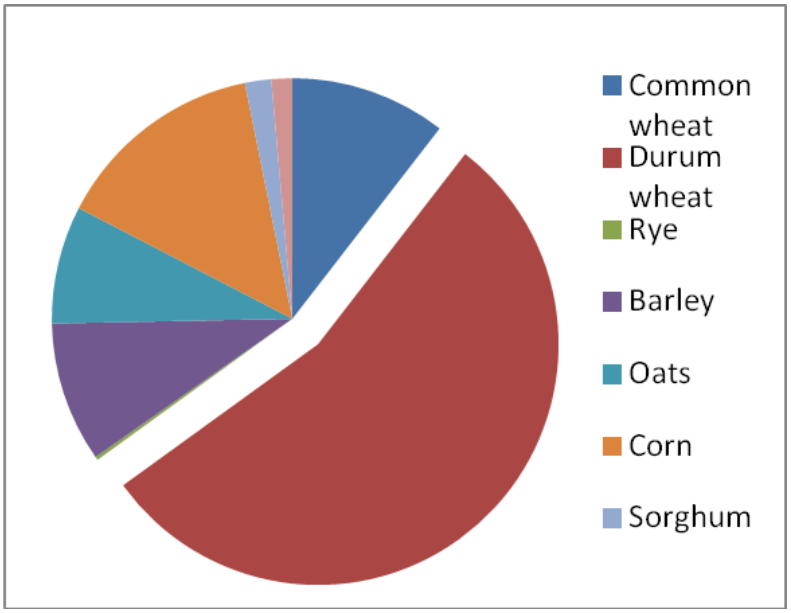

Fig. 1.1.5 Durum wheat and common wheat harvested quantity in Tuscany from 1952 to 2011. Source: ISTAT, 1952-2011, data elaboration.

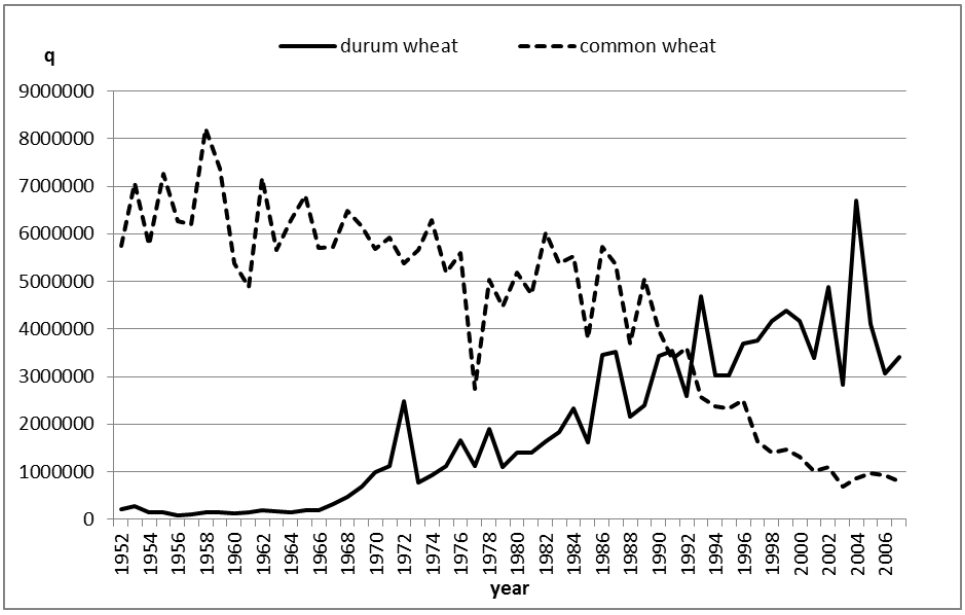

1.2. Durum wheat, development and production

Durum wheat (*Triticum turgidum durum* L.) was developed by the spontaneous breeding between two wild species, with chromosome pattern 2n = 14 each, and through the following artificial selection and genetic improvement. It represents the only tetraploid species (2n = 28) of wheat with commercial relevance. This genetic trait distinguishes this species from the common wheat or soft wheat (*Triticum aestivum* L.), that instead is hexaploid (2n = 42). In comparison with *Triticum aestivum*, durum wheat shows at maturity glassier and harder kernels, higher grain protein content and a different protein pattern. Durum wheat is also richer in gluten that makes its flour suitable for the pasta production.

Large fluctuations of wheat production were recorded in Mediterranean environment for both yield and grain protein content (Borghi et. al., 1997). As discussed in the following paragraphs, several studies have been carried out about the impact of climate variability on wheat performance. The results confirmed that the thermal and water conditions strongly affect the duration of each crop stage, the plant growth rate and the quality and quantity of the harvest. In particular, the Italian durum wheat production shows high variability in terms of yield and grain quality (De Vita et al., 2007).

Compared to the ordinary wheat, durum wheat is less subject to smut and rust, and, it is better adapted to semiarid climates being more drought resistant. For these reasons, durum wheat has had an important role in all margin marginal areas of Mediterranean environment (Salmon and Clark, 1913), where stresses, such as high temperature and water scarcity, are common constraints.

Ordinary wheat and durum wheat have different responses to the same environment, in line with expectations from the goals of their breeding (Cossani et al., 2011). Comparing the two species, durum wheat showed on average higher grain weight, yield and grain nitrogen concentration (Cossani et al., 2011). Moreover, durum wheat has a higher productive responsiveness to Mediterranean climate, with a wider variability of both rate and duration of grain filling stage, and a less stable grain final size and weight

(Cossani et al., 2011). As a consequence, a larger variability of yield and final grain protein concentration was observed in durum wheat (Cossani et al., 2011).

In Italy durum wheat is a fall-winter sown crop. In particular in Val d' Orcia (Tuscany) it can be sown over the period from October to January. The crop normally reaches the flowering period between April and May. The harvesting typically occurs in the summer, from beginning of June to the end of July.

The beginning of the crop cycle and the phenological phases development provide the temporal framework within which the climate and cropping system constraints, impact final harvest, as a percentage of the potential performance. Photoperiod and temperature are the main environmental factors that directly control the duration of each crop phenological stage (Fisher, 1985; Slafer and Rawson, 1994; Whitechurch and Slafer, 2002; Fischer, 2011).

The variation in anthesis date represents the primary adaptative response of wheat to the environment, and only a few days difference in its onset can be significant for the crop performance (Fischer, 2011). Furthermore, the timing of key events, within periods such as floral initiation, terminal spikelet, end of tillering, start of stem elongation, flag emergence, grain meiosis and grain filling, has a significant role in the harvest determining (Slafer et al. 2009; Fischer, 2011).

The table 1.2.1. (Miller, 1992) and the figure 1.2.1 (Acevedo et al., 2002) supply a description of the main development stages of wheat.

Fig. 1.2.1 Schematic diagram of wheat growth and development stages, periods of initiation or growth of specific organs and periods of different components of grain yield (Acevedo et al., 2002). Legend: sowing (S), germination (G), emergence (E), double ridge appearance (DR), terminal spikelet initiation (TS), heading (HD), anthesis (A), beginning of grain filling (BGF), physiological maturity (PM), growth stage (GS).

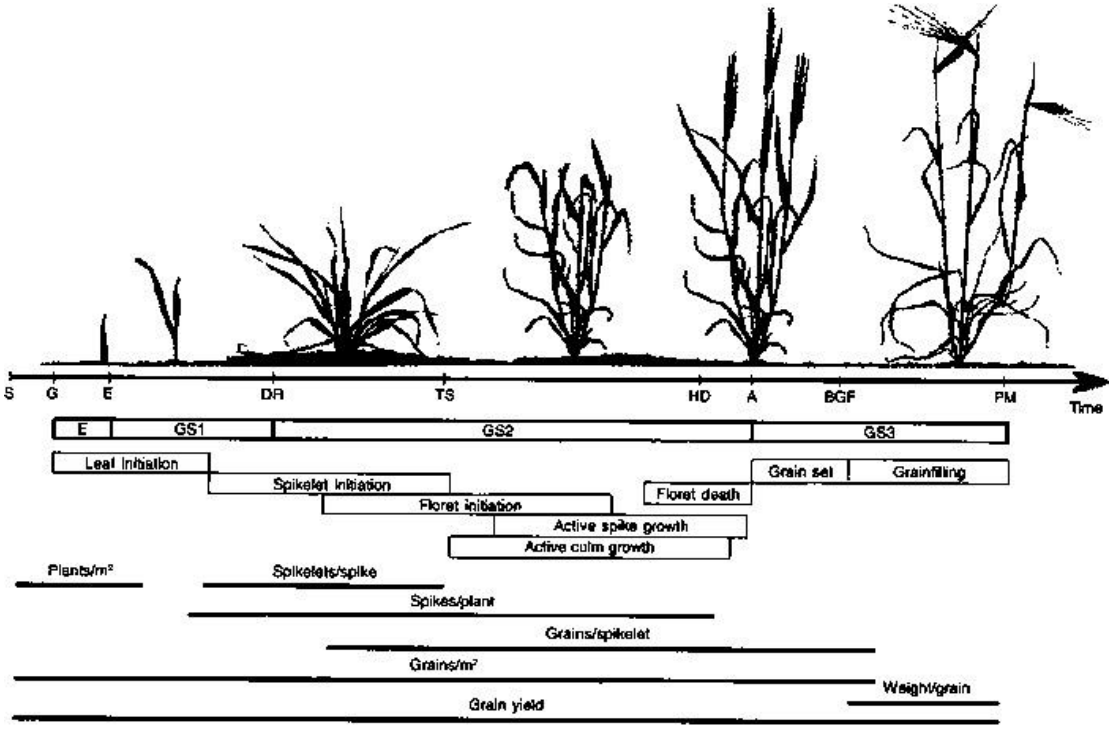

Tab. 1.2.1. Description of the main phenological stages in wheat and matching between Feekes-scale and BBCH-scale (Miller, 1992).

BBCH	Feekes	Stage	Description
2.0-2.n	2.0–3.n	Tillering I	Tiller is a shoot which originates in the axil of a leaf or at the coleoptilar node; it shares the same root mass with the original shoot or main stem. During this stage, most of the tillers are formed. Late sowing involves less time to tiller and, then, lower final plants density. On the other hand, early nitrogen applications may enhance the tillering rate, encouraging a higher number of ears at harvest.
1.0-1.n	4.0–5.n	Tillering II	The seedling changes its status from prostate to erect (Fig. 1.2.2). During this stage the leaves grow, lengthening the sheaths, and the number of potential spikelets per spike is determined. Nitrogen applications can affect the number of seeds per ear and the seed size, while they not affect the number of ears at harvest. The water availability can be critical during the spikelet differentiation process and a water stress can reduce the potential number of seeds per ear.
3.0-3.n	6.0–7.n	Stem elongation	The stem growth starts when the first node is visible (Fig. 1.2.3). Even if the spike is already fully differentiated, containing all potential spikelets and florets, the biomass development during this stage affects the final grain size. Nitrogen applications can enhance the final grain size.
4.0-4.n	8.0-9.n	Booting	This growth stage starts when the last leaf (flag leaf) begins to emerge from the whorl. The good status of the flag leaf is important since it makes up approximately 75 % of the effective leaf area that will contribute to grain filling. From this stage, nitrogen applications are able to enhance the grain protein concentration while have poor influence on the yield.
5.0-5.n	10.0-10.5	Ear emergence	The ear is fully developed and begins to be visible emerging through slit of flag leaf sheath until it is completely emerged (Fig. 1.2.4).
6.0-6.n	10.5.1-10.5.3	Flowering	The florets are pollinated and the final grains number is setted. This stage begins since the first anthers are visible and follows with the anthers maturity and the spikelets flowering.
7.0-7.n 8.0-8.n	10.5.4-11.3	Grain filling	The nutrients move from the vegetative parts to fill the grains and the final kernel mass is determined. The grain starts the ripeness until the maturity (Fig. 1.2.5).

Fig. 1.2.2 Tillering stage (II): the seedlings change their status from prostate to erect (monitoring of 20 March).

Fig. 1.2.3 Stem elongation stage: the stem starts to growth (monitoring of 10 April).

Fig. 1.2.4 Ear emergence stage: the ear begins to be visible emerging through slit of flag leaf sheath (monitoring of 10 May).

Fig. 1.2.5 Grain filling stage: the grain starts the ripeness until the maturity (monitoring of 30 May).

The grain filling stage represents a relatively short phase of the crop cycle, occupying the last 20-30 days until the grain maturity (Jenner et al., 1991). Despite this, it is a critical period and a complex phase, during which key processes occur in determining of the qualitative and quantitative performance of the crop. The stage can be subdivided into three consecutive phases (Vos, 1981).

- Within the first 1–2 weeks after anthesis the rate of dry matter accumulation in the grain is relatively small. Enlargement of the grain begins from the anthesis and it is mainly related to the water availability (Schnyder and Baum, 1992). During this initial phase the grain structure enlarges and the capacity of the grain to accumulate dry matter, in particular starch, is established (Jenner et al., 1991).
- The second period, the 'linear phase', extends over most of the grain filling stage. During this phase the growth rate is almost constant and most of the starch and protein are accumulated in the grain.
- During the third period, the 'maturity phase', the rate of starch deposition declines rapidly (Jenner et al., 1991), while the incorporation of N tends to proceed for longer and at a higher rate (Vos, 1981). Finally, both processes finish at grain maturity.

Jenner et al. (1991) suggested that the rate and duration of both starch and protein deposition are essentially independent events, controlled by different mechanisms and influenced by different factors.

Under adequate growing conditions, the rate and duration of starch deposition are determined mainly by factors that operate within or close to the grain itself. Therefore, the starch accumulation in the grain is mainly sink-limited and depends on the grain number (Jenner et al., 1991; Jamieson and Semenov, 2000).

On the other hand, the rate and duration of protein deposition are determined mainly by factors of supply external to the grain. Therefore, the protein accumulation in the grain is mainly source-limited and depends on the total N content in the crop biomass (Jenner et al., 1991; Jamieson and Semenov, 2000).

Starch in the endosperm of grain wheat is the major form of carbon reserves and represents between 60% and 75% of the final dry weight (Hurkman et al., 2003).

Therefore, biosynthesis and accumulation of starch in grain is a key process in determining grain yield. During the grain filling starch is synthesized in the grain from sucrose. This latter derives mostly from CO_2 assimilation (Rawson and Evans, 1971) and from mobilization of stored soluble carbohydrates in stem, spikes and leaves (Spiertz and Van De Haar, 1978; Van Herwaarden et al., 1998).

On the other hand, the proteins have a key role in determining the harvest quality. They are synthesized in the grain starting from aminoacids, which in turn derive from the catabolism of proteins in the vegetative organs or current nitrogen uptake (S. Asseng et al., 2002). Leaves and stem represent the most important reserve of N, with smaller contribution by glumes (about 15% of grain N) and roots (about 10% of grain N) (Dalling, 1985). Regarding this issue, a positive relationship was found between protein or N grain concentration and the total leaf N at anthesis (Huang et al., 2004; Wang et al, 2003) and at 2 weeks after anthesis (Li et al., 2005).

A positive relationship has been established between the duration of various phenological phases and the production and survival of numerical components of wheat grain per m^2 (tillers, spikes, spikelets, florets, grains) (Slafer and Whitechurch, 2001; Gonzalez et al., 2005; Fischer, 2011). Therefore, the yield variability is associated with the number of grain per m^2 and with the dry matter accumulation in spikes at flowering and at grain filling stage (Bingham, 1969; Fisher, 1984; Miralles and Slafer, 2007; Reynolds et al., 2009; Fischer, 2011).

On the other hand, the final grain protein content is derived from the ratio of grain N and grain yield (S. Asseng et al., 2002). About this, the literature widely reports the negative correlation between wheat yield and grain protein concentration (Spiertz, 1977; Johnson et al., 1985; Fischer et al., 1993; Feil, 1997; Novaro et. at, 1997; Rharrabti et al., 2001a).

1.3. Impact of nitrogen fertilizer

The rate and timing of nitrogen fertilizer applications play a main role in obtaining good wheat performance. The optimization of the fertilizer plan can improve the grain quality and the yield.

The wheat growth, from anthesis to maturity, depends on the nitrogen assimilated prior to anthesis (Garabet et al.; 1998). Most of the N uptake occurs during tillering to anthesis (Garabet et al.; 1998). The assimilated N during this period represents about 80% of the total N assimilated by the crop at maturity (Cox et al, 1985). Therefore, the productive response of wheat in terms of yield can be maximized with fertilizer applications at onset of stem elongation (Gusta and Chen, 1987; Mossedaq and Smith, 1994).

About this, Abedi et al. (2011) showed that N fertilizers applied during the crop vegetative growth, from tillering to steam elongation stages, allowed to reach higher yield, with a particular responsiveness by the crop to N application at tillering. The absence of N supply at grain filling did not affect yield negatively, while the lack of nitrogen input at tillering stage involved lower yields (Abedi et al., 2011). Since the number of spikes per unit area is set before steam elongation (Li et al., 2001), the N fertilization in tillering stage was found to have a significant impact on the quantitative components of the harvest.

On the other hand, Abedi et al. (2011) showed that a removal of fertilization at grain filling led to a lower amount of protein in the grain. Many studies confirmed that N applications, later in the season, at ear emergence and close to anthesis, were effective in enhancing grain protein content of wheat (Timms et al., 1981; Luo et al., 2000; Ottman et al., 2000; Bly and Woodard, 2003; Brown and Petrie, 2006; Weber et al., 2008).

2. IMPACT OF CLIMATE ON WHEAT GROWTH, DEVELOPMENT AND YIELD

2.1. Temperature

Temperature affects both wheat phenological development and growth, representing a determinant factor for the production with direct and indirect effects on yield components.

Temperature has its primary impact on the phenological development, influencing the duration and onset of each plant stage. In relationship to temperature, the wheat development rate shows a sigmoidal trend: the development starts at 1-5 °C, rising slowly as temperature increases, and then more rapidly until a threshold of 30 °C, and after that it rapidly slows down (Shaykewich, 1995). The effect of temperature on wheat development are described by a thermal time approach. An average increase of about 1 °C reduces the entire wheat cycle of 21 days and the period from anthesis to grain maturity of 3 days, with considerable differences responses among varieties (Batts et al., 1998a; Batts et al., 1998b; Lawlor and Mitchell, 2000).

On the other hand, an increase of biomass growth rate was recorded with an increase of temperature (Lawlor and Mitchell, 2000). Temperature impacts the photosynthesis activity of wheat. Photosynthesis is smaller at values below 5 °C, rises with the temperature until a optimum around 25 °C, and then decreases progressively until finally ceasing at about 40 °C (Lawlor and Mitchell, 2000).

However, even if high temperatures are able to promote the rate of vegetative biomass growth, in general they result in lower biomass production and yield. Warmer conditions shorten the duration of all growth stages and accelerate leave maturation and senescence. As result for the plant, there is a reduction of the available period to intercept the solar radiation and to capture the water and nutrients resources, necessary to biomass accumulation through photosynthesis (Mitchell et al 1993, Mearns et al. 1997).

The magnitude of the impact of warm temperatures depends on which crop stage is affected. High temperatures at early growth stage are less damaging for biomass production and grain yield, compared to those that occur later during the period of plant higher growth rate (Lawlor and Mitchell, 2000). Furthermore, thermal stresses severely affect the reproductive period, influencing the anthesis and grain filling, with significant repercussions on the harvest.

Ferris et al. (1998) studied the effects on wheat of an average increase of 2 °C during anthesis. No significant correlation was found between mean temperature and above ground biomass, grain weight and yield. However, the temperature rise involved a faster decline of the roots biomass. On the other hand, maximum temperature was found to be significantly and negatively correlated with the grains number per ear and yield (Ferris et al., 1998).

Likewise, Mitchell et al. (1993) highlighted the negative impact of a brief exposure to hot temperatures during wheat anthesis. At maximum temperature of 27 °C, an increase of sterile grains percentage was observed. Others studies confirm the susceptibility of wheat anthesis to extreme temperatures (> 30 °C). The extreme temperatures are critical and able to damage the pollen formation, which in turn reduces the grain-set and involves a yield decrease (Dawson and Wardlaw ,1989; Tashiro and Wardlaw, 1990).

Studies found an interaction between the effect of warm temperatures over the period close to anthesis and the air humidity (Dawson and Wardlaw, 1989, Tashiro and Wardlaw, 1990). When a thermal stress (31 °C - 36 °C) was associated to high relative air humidity (50%), it caused a higher frequency of sterile grains compared to the lower humidity condition (35%) (Tashiro and Wardlaw, 1990). On the other hand, ar smaller temperatures (18 °C - 30 °C), high humidity did not impact the grain-set, indicating the absence of interaction between these two environmental variables (Tashiro and Wardlaw, 1990).

Grain filling stage is another critical period for wheat production, and it is susceptible to changes in temperature, with consequences on yield. Contrary to anthesis, in the post-anthesis period, the yield component most sensitive to temperature is the individual kernel mass, rather than the number of grain per ear but (Stone et al., 1994).

The rate of grain filling, and the increase of grain dry weight, are principally determined by temperature with a positive correlation (Sofield et al., 1977; Angus et al., 1981; Hunt et al., 1991; Jenner, 1991; Wardlaw and Moncur, 1995). On the other hand, the temperature determines the rate of progress to grain maturity, and warm conditions shorten the duration of this phase (Sofield et al. 1977; Wardlaw et al. 1980; Al-Khatib and Paulsen 1984; Hunt et al. 1991, Jenner 1991, Slafer and Rawson 1994; Wardlaw and Moncur 1995, Wheeler et al. 1996).

Many studies confirmed that, even if high temperatures are associated with an increase in grain growth rate, this process does not compensate the negative effects due to warm conditions. Indeed, high temperatures involve a shortening of the available period for the deposition of nutrients into the grain, resulting in smaller kernel weight and lower yield (Sofield et al. 1977, Al-Khatib and Paulsen 1984, Orlandini et al. 2011).

Stone et al. (1994) highlighted that also a brief exposure to extreme temperature (> 35 °C) during grain filling causes a significant reduction of individual kernel mass with marked effect on grain yield.

2.2. Water availability

The water supply represents a main factor affecting the wheat harvest, and limiting the production potential of the crop, especially in Mediterranean regions (Giunta et al., 1993; Garabet, 1998; Zang and Oweis, 1999). Under Mediterranean climate, water stresses result from low precipitation or not enough rainfall to compensate the evapotranspiration water losses due to high temperature.

In Mediterranean environment, the drought involves in durum wheat a significant decrease of the harvest index and a yield reduction between 25 - 87 % (Giunta et al., 1993). On the other hand, the irrigation significantly increases the total biomass production and grain yield of wheat (Garabet et al., 1998; Li et al., 2010).

Drought conditions, from seedling to maturity, are able to affect many growth and productive components of the wheat, resulting in a reduction of plant height, number of spike per unit area, number of spikelets per spike, spike weight, grain weight, and then in a decrease of yield (Kiliç and Yağbasanlar, 2010). A lengthening of the drought periods over the crop cycle involves a decrease of leaf area index, biomass dry matter accumulation and grain yield (Dalirie et al., 2010).

Giunta et al. (1993) found that the effect of drought on the yield components depends on the intensity of the water stress. Severe water stress mainly influenced the number of fertile ears per unit area and the number of grains per ear, with a reduction of 60% and 48% respectively. On the other hand, a mild water stress involved a yield reduction solely due to a low grain weight.

The water availability affects not only the biomass growth but also the phenological development of wheat. Regan et al. (1992) found that water limited conditions led to a late onset of the crop reproductive stages. In particular, the water stress involves a reduction of the available time from heading stage to grain maturity and shortens the grain filling stage (Kiliç and Yağbasanlar, 2010). The disadvantages resulting from less number of available days for the grain filling are additional to those due to the water stress impact on biomass growth, with the harmful consequences for the harvest.

The wheat yield is affected not only by the total water use during the crop cycle, but also by the water supply during each growth stage. The crop productive response to the drought depends on in which development stage the water stress occurs (Zhang, 1998; Zhang and Oweis, 1999; Lopez et al., 2003; Li et al., 2010).

During the seedlings stage the number of tillers and the number of spikelets per spike are determined, as well as the leaves growth, with the lengthening of the sheaths, occurs (Miller, 1992). The negative impact on wheat yield due to water stress during the seedling stage was described by many authors (Zhang et al., 1998; Guttieri et al., 2001; Zhang et al., 2004; Li at al., 2010). The lack of rainfall over this period was pointed out as the major cropping risk to wheat producers in Mediterranean environment (Dalirie et al., 2010). A reduction of yield, between 16 % and 48 %, due primarily to lower kernel weight, and secondarily to less kernel per spike, was associated to water deficit imposed after tiller initiation (Guttieri et al., 2001).

Water stress during tillering stage involves for the crop the inability to produce adequate dry matter (Regan et al., 1992; Zhang et al., 1998). Regan et al. (1992) showed the relevance of the seedlings early vigour for the yield. The plants with larger leaves or with higher number of tillers reached a higher growth rate and green area index. The large degree of ground cover, and the higher light interception, resulted in higher biomass accumulation and yield (Regan et al., 1992). Similarly, Zhang et al. (1998) showed that water limited conditions at the beginning of the crop development affected the epigeal biomass production in the following periods. The crop showed a smaller leaf area growth, with a reduction of the upper leaves size and of the leaf area index. The lower plant photosynthetically active surface resulted in a decrease of the grain weight and grain number per ear, and then, of the yield (Zhang et al., 1998).

Zhang et al. (2004) showed that aid irrigation in the winter-autumn was more important in improving the wheat yield, than the irrigation in spring. The study underlined the relevance for the yield enhancement of the water supply at early vegetative growth stages. On the other hand, the results suggested that the water deficit over the period from spring green up to early grain filling stage limits the production less severely (Zhang et al., 2004).

Nevertheless, not all studies detected the tillering stage as the most critical period for wheat production in relationship to the water supply (Zhang and Oweis, 1999).

The disagreement can be explained by the different effect of water deficit during the early crop period on the epigeal biomass growth, on one hand, and on the roots system development, on the other hand. Indeed, water stress at seedling stage can promote the root expansion, resulting in a relatively larger and deeper root system (Zhang et al., 1998). This positive effect of water stress can compensate, in some cases, its negative impact on the above-biomass accumulation (Kang et al. 2002), leading to point out other development stages as the most critical in relationship to the water availability.

Kang et al. (2002) analyzed the wheat responses to different soil moisture treatments. Compared to the high-moisture treatment, a yield rise was associated to a mild water deficit during the seedling stage, when drought conditions occurred, during the following periods of the crop cycle. Therefore, in some cases, an early drought is able to support the production, encouraging the water extraction by the plant from the deeper soil storages, when the water limited conditions persisted, during the later period of the vegetative growth and grain development (Kang et al., 2002).

Studies found that the water stress from steam elongation to booting was able to impact the wheat yield more than the water limited conditions occurred during the following or previously periods (Zhang and Oweis, 1999; Li et al., 2010). Zhang and Oweis (1999) identified as most critical period the ‘stem elongation-booting’ stage, followed by the anthesis and third by grain filling stage. Li et al. (2010) considered the period from the beginning of steam elongation to grain milk maturity. The authors found that the water stress, at steam elongation and heading stage, affected the yield more that at grain filling stage. Compared to the irrigations during these two vegetative growth stages, the irrigation applied only during the later period, at grain filling, involved a higher grain weight but lower spikes number. The increase of grain weight was not able to compensate for the spikes reduction, with a net result of lower yield (Li et al., 2010).

On the other hand, studies pointed out the grain filling stage as a critical period, during which the water stress involves a reduction in grain weight and a significant decrease of yield (Kobata et al., 1992; Zhang et al., 1998; Eitzinger et al., 2003).

These results are apparently in disagreement with the studies described above that showed the water availability during the pre-anthesis stages more relevant compared to that of the post-anthesis periods. This can be explained by taking into account the different susceptibility to water stress of the translocation and deposition processes that occur during the grain filling (Zhao et al., 2009; Gooding et al., 2003). In some cases, water limited conditions during the grain development can promote the harvest quantity or not affect it.

Zhao et al. (2009) found a yield increase associated to a mild water deficit during grain filling, compared to condition of severe drought, as well as of more water supply. The authors suggested that, the mild water stress has been able to enhance the remobilization of stored reserves from the vegetative tissues to the grain, supporting the biosynthesis and accumulation of starch more than those of the other compounds. Since the starch represents 60-75% of grain weight, the mid water stress during the grain development can involve a yield increase (Zhao et al., 2009).

Furthermore, Gooding et al. (2003) did not find impacts on the harvest due to water stress during the late period of grain filling (second and third phase), unless it was associated with thermal stress. The water limited conditions was able to affect the harvest only when they occurred in the early period of grain filling, during the first 2 weeks after anthesis, when the cell division and the liner grain growth starts.

2.3. Interaction between temperatures and water availability

The results described in the previous paragraphs, show that the temperature has its main impact on the progress and timing of the phenological development , while the water supply affects more the biomass growth and accumulation within each crop stage. Several studies analyzed the individual effect of these two weather variables on wheat yield. On the other hand, the interactions among thermal and water conditions, and the resulting impact on the crop, are less investigated. Recently studies tried to deepen this aspect. When warm and drought conditions are focused on the grain filling period, the combined effect among the two stress factors lead to a reduction of the grain weight with a yield decrease (Gooding et al., 2003). On the other hand, when warm and drought conditions characterize the entire crop cycle they can result positive for the harvest (Prasad et el., 2008; Van Ittersum et al., 2003; Xiao et al., 2008). About this, the long-term study of Xiao et al. (2008) found a non-linear relationship between yield and the rise in annual average temperature, and a linear and negative correlation between yield and annual rainfall reduction. However, an overall yield increase was observed in relationship to warming temperature and rainfall changes. These results were explained by taking into account that the higher temperature over the crop cycle, involving earlier flowering, shifted the grain filling period toward a cooler and wetter season. This allowed to the crop avoiding the water and thermal stresses, more severe in the later part of the crop cycle (Xiao et al., 2008). Van Ittersum et al. (2003) showed similar conclusions. Even if, the high temperature during the crop cycle commonly results in a yield decrease, it was able to shift the flowering onset, and then improved the yield in case of terminal drought. Moreover, thermal stress during plant development causes a reduction of biomass accumulation, and then smaller leaf surface(Prasad et el., 2008). The lower plant LAI involves a decrease of transpiration and water losses that can promote the crop if a drought condition follows in the second part of the crop cycle. This aspect can explain the performances shown by some wheat cultivars. The cultivars that exhibit greater resistance to thermal stress, with less impact of warm condition on the biomass growth, conversely are highly susceptible to drought (Prasad et el., 2008).

3. WHEAT QUALITY

3.1. Grain protein in durum wheat production

The grain protein content and pattern play a critical role in determining the physical and nutritional characteristics of flour and then the quality of the derived product.

The grain protein concentration (GPC) and the gluten quality affect the cooked pasta visco-elasticity, determining the pasta firmness and its cooking quality (D'Egidio et al., 1993; Troccoli et al. 2000; Oak et al., 2006; Cubadda et al., 2007). Similarly, for the bread production, a good protein level and gluten content confer to the flour the properties of plasticity, strength and elasticity that are needed to make bread rise (Stone and Savin, 1999; Shewry, 1995).

For these reasons, the grain protein is one of the most important traits in quality evaluation and breeding of durum wheat. In world wheat trade, the higher the GPC, the higher the price will be paid for farmers (Li et al., 2012).

Even if in the Mediterranean areas durum wheat is traditionally grown, the locally produced wheat suffers the competition with the imported wheat grain. The unpredictability of climatic condition in many Mediterranean countries makes difficult to guarantee the quality standards requested by the grain dealers (Troccoli et al., 2000). In this context, the farmers are under the pressure from the marketing strategies of the durum wheat exporting countries (e.g. Canada, Australia) and the quality has become an ever more important issue (Troccoli et al., 2000).

The grain protein is the result of the combination of wheat genotype (G) and environmental factors (E). These components show an additive effect. However, the interaction between G x E was found small or negligible and the environmental impacts override those of genotype in the determining of GPC (Peterson et al., 1992; Mariani et al., 1995; Novaro et al., 1997; Uhlen et al., 1998). Therefore, the environment, particularly the weather conditions and the nitrogen availability, has the main influence on wheat quality (Troccoli et al., 2000).

3.2 Relationship between grain protein concentration and yield

The environment impact on GPC is intrinsically linked to the modalities in which the environment variables affect the yield. Many studies showed the negative correlation between yield and GPC (Spiertz, 1977; Johnson et al., 1985; Fischer et al., 1993; Feil, 1997; Novaro et. at, 1997; Rharrabti et al., 2001a; Rharrabti et al., 2001b).

However, the inverse relationship between yield and GPC is not a universal rule. The correlation between the two harvest components depends on the yield level (Stoddart and Marshall, 1990), soil fertility (Kramer, 1979), the N input and sowing date (Ehdaie and Waines, 2001).

The primary cause for this negative correlation seemed to be the dilution of protein by non-nitrogen compounds in the grain (Pleijel et al., 1999).

Moreover, 1 g of glucose, produced with the photosynthesis, can be used by the crop to synthesize 0.83 g of carbohydrates or 0.4 g of protein (Penning De Vries et al., 1974). Therefore, an increase of grain protein, using more photosynthate, can lead to a decrease of photosynthate availability for the carbohydrates, resulting in a relative decrease of yield (Rharrabti et al., 2001a).

Last but not least, the starch translocation and deposition in the grain appear to be more sensitive to adverse environmental conditions, than the nitrogenous compounds translocation and protein synthesis (Campbell et al., 1981; Bhullar and Jenner, 1985; Garcia del Moral et al., 1995; Fernandez-Figares et al., 2000; Rharrabti et al., 2001a). Therefore, conditions of low rainfall and high temperature during the crop vegetative growth were found associated to an improvement of protein deposition and to a decrease of yield (Campbell et al., 1981; Erekul and Köhn, 2006; Orlandini et al., 2011). Similarly, drought and warm stresses during the grain development shorten the grain filling stage but affect the starch accumulation more than that of the protein, resulting in a relatively increase of GPC (Bhullar and Jenner, 1985; Garcia del Moral et al., 1995; Fernandez-Figares et al., 2000; Rharrabti et al., 2001a; Zhao et al., 2009).

The genetic differences between wheat species and cultivars have been shown by several authors as an intrinsic factors capable of affecting grain protein formation in the

different production conditions (Bhatia, 1975; Kramer, 1979; Johnson et al., 1985; Rostami and O'Brein, 1996; Jamieson et al., 2004).

About this, the inverse relationship between yield and GPC is emphasized more in durum wheat compared to common wheat (Cossani et al., 2011). In durum wheat an increase of grain weight is accompanied by a higher pronounced decrease of grain N percentage. This results in the lower stability of GPC observed in durum wheat grown in Mediterranean environment compared to ordinary wheat (Cossani et al., 2011).

3.3 Impact of climate on grain protein concentration

In general, the climate conditions that suppress the yield are able to improve the wheat GPC. Therefore, GPC increases with a temperature rise and rainfall reduction (Troccoli et al., 2000; Erekul and Köhn 2006).

Many studies focused on terminal stress during the post-anthesis. Drought and high temperatures during the grain filling stage have a key role in determining wheat quality since they are able to negative affect the yield, and, hence, to involve a significant increase of GPC (Kolderup, 1975; Sofield et al., 1977; Blumenthal et al., 1982; Bhullar and Jenner, 1985; Garcia del Moral et al., 1995; Porter et al., 1999; Fernandez-Figares et al., 2000; Troccoli et al., 2000; Rharrabti et al., 2001a; Zhao et al., 2009).

The issue of weather impact on ordinary wheat is been widely discussed. However, the literature is quite poor of specific studies on durum wheat responsiveness to Mediterranean climate.

3.3.1. Temperature

During the late period, heat stress involves a reduction of carbohydrate accumulation into the grain higher than that of nitrogen (Troccoli et al., 2000).

A reduction in the size and number of grain starch granules was found associated to warm conditions (Tester et al., 1995). On the other hand, higher temperatures are able to promote the nitrogen mineralization in the soil and the N uptake by the plant (Russel et al., 1973). Warm conditions are able also to increase the rate of the nitrogen relocation from the vegetative organs to the grain (Neales et al., 1963). Finally, high temperatures, although they shortening the grain filling stage, they involve a relative increase of nitrogen to the detriment of starch, resulting in higher GPC

However, in case of temperature extremes during the grain development, the GPC also suffers a reduction (Stone and Nicolas, 1996). The exposition of wheat to temperatures of 40 °C for five days at grain filling stage involved a significant GPC decrease (Stone and Nicolas, 1996). This result can be explained in relationship to the inhibition of the

RuBisCo enzyme activity observed in wheat at temperature above 30 °C (Feller et al., 1998).

The impact on GPC of temperature rising during the crop vegetative growth is less clear. Erekul and Köhn (2006), from a long-term analysis on wheat production, found a positively relationship between GPC and temperature. In 2003, when from March to July the temperatures exceeded the average by 1.65 °C, an average increase of 5 % of GPC was observed. (Erekul and Köhn, 2006).

Campbell et al. (1981), in an experiment in controlled environment, have found an increase by 33 % of GPC at a constant daily temperature regime of 27 °C during the crop cycle, compared to the treatments at 22 °C and 17 °C. Despite this, no significant differences were found in GPC, as a consequence of the increase of 5 °C in the thermal regime from the treatment at 22 °C to that at 17 °C.

The long-term study (1999-2009) of Orlandini et al. (2011) showed a positive relationship between GPC of durum wheat and the temperatures computed on the multi-monthly periods, from February to June, in particular during spring and early summer. However, no significant correlations were found between GPC and the monthly temperatures (Orlandini et al.; 2011).

The study of Smith and Gooding (1996), on seven regions per seven years, showed that only the temperature trend in late summer was able to explain the GPC temporal and spatial variability. Similarly, Garrido-Lestache et al. (2005) did not find any correlations between GPC and temperature during the crop cycle, except with the maximum temperature at anthesis and milk ripening stage.

Ludwig and Asseng (2006) in a long-term study on 50 years analyzed the impact on wheat of a rise of average temperature. The authors found that high temperatures during the crop cycle could involve an increase, as well as a decrease of the GPC. Under wet conditions, higher temperatures increased the GPC. However, at lower regime of rainfall, the warmer climate involved a GPC reduction (Ludwig and Asseng, 2006).

Finally, the literature highlights a well-established relationship between GPC improvement and rising temperature during the grain filling stage. Despite this, there are not many studies that take into account the effect of the temperature trend during the

other crop development stages. Moreover, in this case, the results not always showed a positive correlation between GPC and temperature, especially when long-term analyses were carried out.

3.3.2. Water availability

Concerning the impact of water availability on GPC, the mechanisms underlying the effects of rainfall and soil moisture are complex (Troccoli et al., 2000).

Many studies confirm the positive effect of water stress on grain protein accumulation during the grain filling (Garcia del Moral et al., 1995; Fernandez-Figares et al., 2000; Rharrabti et al., 2001a; Zhao 2009; Gooding et al., 2003). Gooding at al. (2003) showed that water stress during grain filling period was able to increase the GPC, compared to the optimum water conditions. The moisture restrictions during the first 14 days of grain filling involved the higher amount of grain N.

Also the studies that took into account the water deficit during the other periods of wheat cycle showed similar conclusions. The drought conditions tend to reduce the size and weight of grain, involving a relatively increase of GPC (Troccoli et al., 2000; Rharrabti et al., 2003a; Rharrabti et al., 2003b; Ludwig and Asseng, 2006; Rharrabti et al., 2003b; Erekul and Köhn, 2006; Orlandini et al., 2011).

Moisture stress, that occurred in rainfed crop system, was found able to increase GPC, compared to the irrigated system (Rharrabti et al., 2003a; Rharrabti et al., 2003b). Similarly, Erekul and Köhn (2006) detected a significant GPC increase in the growing season characterized by a higher deficit in precipitation. These results are confirmed by the long-term study of Ludwig and Asseng (2006). The authors assessed an average increase of GPC related to a rainfall reduction. Similarly, other studies showed the negative correlation between GPC and the rainfall in the winter-spring season (Smith and Gooding, 1996; Garrido-Lestache et al., 2005; Orlandini et al., 2011).

On the other hand, high level of water supply during the crop cycle can increase the final GPC, since it positively affects on N availability and N uptake by the plant. The soil moisture promotes the nitrogen mineralization, the plant root growth and the

movement of nitrogen fertilizer into the root-zone, increasing the mass flow of water and nitrogen towards the plant (Sander et al., 1987; Garabet et al., 1998; Troccoli et al., 2000). The results shown by some studies can be explained by taking into account the relevance of this increase in N availability when the nitrogen supply has its larger impact on GPC. Authors found a significant and positive correlation between GPC and the precipitation that occur in early summer, during the grain filling stage (Smith and Gooding, 1996), or in April when anthesis and milk ripening stage take place (Garrido-Lestache et al. 2005).

The significant interaction between water and nitrogen can change the effect on GPC of water deficit conditions. The effect of water conditions on the nitrogen availability can overcoming the influence due to the inverse relationship between yield and GPC (Campbell et al., 1981; Garabet et al., 1998; Troccoli et al., 2000; Garrido-Lestache et al., 2005).

The study of Campbell et al. (1981) in controlled environment highlighted that the relationship between water availability and GPC is determined in a complex way by the interaction with the nitrogen supply. Moreover, impact of water stress depends on the level of water stress and on the affected development stage.

The increase of GPC per unit of N input was lower for plants grown at optimum moisture level, compared to the plants suffering high and medium water stress (Campbell et al., 1981). On the other hand, when water deficit was imposed only during the late period (from late flowering to maturity) no GPC rise was observed, unless high water stress was combined with high nitrogen input (Campbell et al., 1981). At low nitrogen input, only high water stress, from tillering or from boot stage until grain maturity, involved a GPC increase. On the other hand, medium water stress or terminal water stress were found unable to improve the grain quality (Campbell et al., 1981). Similar GPC was found for the plant stressed from boot or tillering stage with two exceptions. The combination between high water stress, from boot stage, and low nitrogen input involved the lowest GPC. Conversely, the combination between high water stress, from boot stage, and high nitrogen input resulted in highest GPC (Campbell et al., 1981).

The authors explained the failure of late drought and the effectiveness of the earlier water stress in improving GPC, on the basis of the inhibition of nitrogen assimilates redistribution during grain filling stage (Campbell et al., 1981). Plants stressed earlier would have had the opportunity to adapt their physiology to drought conditions. O the other hand, late water deficit, during the period of most active nitrogen distribution in wheat, disadvantaged the grain protein accumulation (Campbell et al., 1981).

Garrido-Lestache et al. (2005) carried out a field experiments on durum wheat. The study highlighted the lack of any clear response by the crop to timing and splitting of N fertilizer. The authors explained these results on the basis of the interaction between the annual variability in rainfall amount and distribution and the N uptake and N fertilizer efficiency at various crop stages.

These latter considerations underline the difficulties that will be attempting to predict the levels of GPC under field condition from year to year.

4. CROP MODELING TOOLS

4.1 Crop models to analyze the weather variables affecting the crop

As has been shown in previous paragraphs, the combined effects of the environmental variables involve different results for the wheat harvest quantity and quality. In particular, water availability and temperature do not have a univocal and linear effect on wheat performance. The weather impact changes in relationship to the timing, intensity and progress of the water and heat stresses during the crop cycle.

In general, a temperature rise (Mitchell et al., 1993; Shaykewich, 1995; Mearns et al., 1997; Lawlor and Mitchell, 2000) and water supply reduction (Giunta et al., 1993; Garabet et al., 1998; Kiliç and Yağbasanlar, 2010; Dalirie et al., 2010) involve a decrease of yield. However, the magnitude and direction of the climate impact on yield, strictly depend on the affected growth stages (Zhang, 1998; Zhang and Oweis, 1999; Lawlor and Mitchell, 2000; Li et al., 2010), the intensity of weather stresses (Mitchell et al., 1993; Ferris et al., 1998; Zhao et al.; 2009), the interaction between the degree of water availability and temperatures variability during the crop cycle (Van Ittersum et al., 2003; Prasad et al, 2008; Xiao et al., 2008).

The interactions between the environmental variables are also more complex and less known in determining the GPC. In general, climate conditions that depress the yield, as warm and drought, are able to improve the grain quality, on the basis of the inverse relationship between GPC and yield (Spiertz, 1977; Feil, 1997; Troccoli et al., 2000; Rharrabti et al., 2001a; Erekul and Köhn, 2006). The positive effect on GPC of warm temperature during grain filling stage is well-established (Neales et al., 1963; Russel et al., 1973; Tester et al., 1995). On the other hand, the magnitude and direction of weather impact on grain quality due to the temperature trend during the other crop stages, is still not clear (Garrido-Lestache et al., 2005; Ludwig and Asseng, 2006; Orlandini et al., 2011). Similarly, the timing of water stress and its interaction with the nitrogen dynamics involve different responses in term of wheat quality. A reduction of water

availability does not always result in an increase of GPC (Campbell et al., 1981; Smith and Gooding, 1996; Garrido-Lestache et al, 2005).

Finally, the impact of temperatures rise and rainfall changes on harvest quantity and quality is in general non-linear and not univocal, diversifying significantly in relationship to soil types and locations (Ludwig and Asseng, 2006).

For these reasons, the results from field experiments are highly changeable from site to site and season to season (Asseng et al., 2002). The complexity of plant growth and development processes, which interact with one another and with the prevailing environmental variables, has made rather difficult the interpretation of the results, especially from field experiments about wheat quality (Asseng et al., 2002).

In this context, a complex deterministic model represents a useful means to study the 'soil - atmosphere – plant' system. Differently from a statistical approach, the crop modeling tools are able to describe the interactions between the environmental variables. Capturing the key physiological processes in a simulation model would greatly aid both the interpretation and extrapolation of the experimental study results.

For this reason, the complex model CERES has been used by agricultural researchers from different disciplines (Jones et al., 2003). After calibration and validation, CERES can be used in a long-term study. In this context, unlike the recorded historical data series of crop production, the crop models allow to discern the weather effects from the confounding influences of the technology development (e.g. new high-yielding varieties, intensive use of fertilizers, etc.). Furthermore, unlike the field experiments, that cover a limited series of years, the crop model analyses the plant responses to the meteorological variables over many years. In this way, the study of the interactions between plant and environment is not influenced by the typical weather patterns that characterize only a few growing seasons. Therefore, the crop simulation models can aid in the identification of the more susceptible plant development stages and the main weather variables affecting the harvests.

In the last years, the crop simulation models have been widely used to investigate the crop growth, development, and productive responses to pedo-climatic conditions. However, most of the studies have been addressed to ordinary wheat performance in

relationship to climate (Triticum aestivum L.). The literature survey about the use of modeling to forecast and to assess of durum wheat harvest in typical Mediterranean areas is quite poor (Pala et al., 1996; Pecetti and Hollington, 1997; Rinaldi, 2004; Rezzoug et al., 2008; Latiri et al., 2010; Richter et al., 2010; Dettori et al., 2011; Toscano et al., 2012), and overall any of these studies deals with the issue of GPC simulation.

Therefore, durum wheat responsiveness to weather conditions during the development cycle is an issue yet be investigated, especially taking into account the larger variability of the harvest quantity and quality that was observed for this crop in Mediterranean areas (Cossani et al., 2011). The identification of major weather variables affecting the GPC plays a key role in the achievement of good quality standards in pasta making (D'Egidio et al., 1993; Troccoli et al. 2000; Oak et al., 2006; Cubadda et al. 2007) and bread making (Stone and Savin, 1999; Shewry, 1995) and, thus, for the farmers (Li et al., 2012 Troccoli et al., 2000).

4.2. Crop models for operational applications

The possibility to forecast both yield and GPC before the beginning of grain filling stage can be important to ensure the quality of durum wheat production. Assessments of harvest in advance support the decision-making for a proper management of nitrogen fertilizer at anthesis.

The rates and timing of nitrogen applications represent a decisive factor to enhance the quality and quantity of wheat harvest (Timms et al., 1981; Gusta and Chen, 1987; Mossedaq and Smith, 1994; Luo et al., 2000; Ottman et al., 2000; Bly and Woodard, 2003; Brown and Petrie, 2006; Weber et al., 2008; Abedi et al.; 2011). In year when a high yield can lead to low GPC (Spiertz, 1977; Johnson et al., 1985; Fischer et al., 1993; Feil, 1997; Novaro et. at, 1997; Rharrabti et al., 2001a; Rharrabti et al., 2001b), the farmer has the opportunity to improve the grain quality with late applications of nitrogen (Timms et al., 1981; Luo et al., 2000; Ottman et al., 2000; Bly and Woodard, 2003; Brown and Petrie, 2006; Weber et al., 2008 Abedi et al. 2011).

Environmental and economic constraints are forcing the farmers to be increasingly precise in determining the rate and time of nitrogen applications. Therefore, forecasts of durum wheat quality and quantity are very important for the modern agriculture.

In this context, the complex simulation models can be useful to fully understand the climate variables determining the harvest, but their direct use as forecast tools remains confined in the research field. Indeed, the simulation models often have strict limitations in operational applications.

The seasonal climate models provide weather data with spatial and temporal scales different compared to those required by the crop model to run, hampering its use as forecasting tool (Stone and Meinke, 2005).

Moreover, technically, the major impediment for the adoption of complex models in farm support is represented by the difficulties in providing reliable and accurate input data, necessary to transfer the model from a specific site to others (Jones et al., 2003; Richter et al. ,2010).

The uncertainty in the spatial distribution of soil properties, initial soil conditions, crop management, and meteorological forcing at field level, leads to simulations with good time coverage but poor spatial coverage (Hansen and Jones, 2000).

Within the crop model, this uncertainty impacts the simulation of two important physiological processes (De Wit and Van Diepen, 2007):

1) simulation of canopy development, which in turn determines the light interception and the potential for photosynthesis;

2) simulation of soil moisture, which in turn determines the evapotranspiration rate and the reduction of photosynthesis due to water stress.

Therefore, the lack of input data, with good spatial resolution and low level of approximation, limits the confidence of model outputs and their spatial representativeness (Stone and Meinke 2005).

For these reasons, in most of the current studies, the forecasts based on crop modeling involve the yield assessment at large scale.

There are few recent papers about modeling applications to durum wheat. These studies deal with the use of crop models in harvest assessment at regional scale. This type of information are more suitable for market and policy implications, rather than for farmers' plans to minimize the harvest uncertainty due to the weather (Rinaldi, 2004; Moriondo et. al, 2007; Rezzoung et. al, 2008; Latiri et. al, 2010; Richter et. al, 2010; Dettori et. al, 2011; Toscano et al. 2012).

The current crop models are subject to even greater restrictions in their adoption as forecasting tools of wheat GPC. They showed discrete performance in yield assessment, but, on the other hand, the results in literature suggested that the simulation of grain protein still represents a challenge.

In most of the wheat models, including CERES-Wheat (Ritchie et al., 1985) SWHEAT (Van Keulen and Selingman, 1987), AFRCWHEAT2 (Porter, 1993), APSIM-N-wheat (McCown et al., 1996; Asseng et al., 2002), and Pan' et al. model (2006), the simulation of GPC is based on N uptake by the plant and the following N distribution from vegetative organs to the grain. The N uptake depends on the soil N availability and crop demand. The demand for nitrogen by the plant is assessed in relationship to the leaf area

expansion, or the accumulation of leaf and non-leaf biomass. Concerning this, in the complex mechanistic models the biomass production is mainly determined by the maximum leaf area index (LAI) and by the solar radiation use efficiency (Feyereisen et al., 2006). However, the major effect of nitrogen shortages on biomass production is under control of green leaf area, rather than of radiation use efficiency (Jamieson and Semenov, 2000).

In this context, studies highlighted poor results in GPC simulation and suggested that the current algorithms for GPC simulation need to be revisited (Otter-Nacke et al., 1986; Asseng et al., 1998; Meinke et al., 1998; Asseng et al., 2002). Therefore, before to use the modeling tool to analyze of the variables affecting the GPC, a diagnostics to trace deficiencies in the model must be carried out and some modifications are required.

Furthermore, most of the current models use crop coefficients concerning to common wheat and thus they do not take into account the higher responsiveness of durum wheat production in meditarranean climate (Cossani et al., 2011).

The genetic differences between wheat cultivars proved to be intrinsic factors in determining the grain protein deposition (Bhatia, 1975; Kramer, 1979; Johnson et al., 1985; Rostami and O'Brein, 1996; jamieson et al., 2004; Cossani et al., 2011). Therefore, further improvements at calibration phase are necessary for a reliable simulation of GPC in durum wheat.

4.3. Crop simulation model CERES

CERES-Wheat (DSSAT-CSM version 4.0) is a deterministic model, designed to simulate the effects of cultivar, crop management, weather and soil on crop growth, development and production (Ritchie and Otter, 1985). CERES operates on a daily time step and the minimum meteorological inputs include: precipitation (mm) (P), solar radiation (MJ/m^2) (R), maximum (TMAX) and minimum (TMIN) air temperatures (°C) (Jones and Kiniry, 1986; Jones et al., 2003). CERES-Wheat simulates eight different development stages (0-7), which can be related to the Zadoks et al. (1974) phenological classification (Eitzinger et al., 2003) (Tab. 4.3.1)

The grain nitrogen content is the result of two independent processes: the dry matter accumulation and N accumulation in the grain (Vos, 1981; Jenner et al., 1991).
Dry matter accumulation is computed as a linear function based on photosynthetically active radiation intercepted by the canopy (fPAR). In turn, fPAR is assessed as an exponential function of LAI. The dry matter allocation is determined by partitioning coefficients, according to phenological stages and environmental stresses. The supply of dry matter for grain filling is derived from direct photosynthesis and re-translocation from pre-stored dry matter (Ritchie et al., 1985). Finally, grain yield is the product of plant population, kernels per plant and grain weight.
Nitrogen accumulation in the grain is simulated on the basis of N uptake by the plant and N translocation into grains. Tissue N content results from the N uptake before and during grain filling, depending on crop and soil properties. Nitrogen translocation into grains starts with the beginning of the grain filling and continues until the end of this phase (Asseng et al, 2002).

The genetic coefficients used in CERES-Wheat describe the growth and development responses of each genotype and its potential productive performance. The number of kernels per plant is determined by G1 (number of grains per ear) and G3 (spike number). G2 (the maximum kernel growth rate) establishes the potential kernel size and weight.

The temperature is the primary variable that determines the phenological development rate. The thermal time of each growth stage is described by specific coefficients which are hereinafter described: P1 (end juvenile to double ridges), P2 (double ridges to end leaf growth), P3 (end leaf growth to end spike growth), P4 (end spike growth to end grain fill lag), P5 (grain filling). These coefficients characterize the response of the different genotypes to climate through the modifying the duration of each growth stage. Furthermore, for each genotype, there are coefficients that characterize the vernalization (P1V), photoperiod response (P1D) and phillochron interval (PHINT).

The model computes the water balance taking into account: effective irrigation, precipitation, surface run-off, drainage, evaporation and transpiration. The soil water balance is based on Ritchie method (Ritchie, 1972; Ritchie et al, 1998). The infiltration is assessed by a modification of the curve number method of USDA soil conservation service (Williams, 1991). The evapotranspiration is established on the basis of the Priestley-Taylor model (Priestley and Taylor, 1972).

The soil nitrogen balance is computed taking into account the contributions of organic matter mineralization and nitrogen fertilizer, on the one hand, and the nitrogen losses due to N leaching and N uptake by the plant (Nain and Kersebaum, 2007).

Tab. 4.3.1 Growth stages in CERES-Wheat and the matching with Zadoks (1974) classification.

CERES-Wheat stages		**Zadoks stages**		
Code	Onset	Code	Period	Description
0 - 1	Germination	00-09	From sowing to emergence	Radicle and coleoptile emerge. The leaves grow just at coleoptiles tip.
	Emergence			
2	Terminal spikelet initiation	10-29	From seedling stage to the end of tillering stage	Growth and unfolding of the leaves. Tillers grow from the main shoot.
3	End of vegetative growth	30-49	From stem elongation to the end of booting stage	Stems grow and the node formation is detectable. Growth and opening of the flag leaf.
4	End of ear growth	50-59	End of heading stage	Fist awns emerge. First spikelet of inflorescence just visible. Fully emergence of ear.
5	Beginning of grain filling	60-69	Anthesis	From beginning to the end of anthesis.
6	End of grain filling	70-89	From milk grain stage to dough grain stage	From caryopsis water ripe to hard dough.
7	Harvest	91-99	End of ripening	From caryopsis hard to the secondary dormancy lost.

5. REMOTELY SENSED DATA DESCRIBING THE VEGETATIVE CANOPY

In the field of remote sensing applications, scientists have developed indices for the qualitatively and quantitatively evaluation of the vegetative cover through spectral measurements (Banner et al., 1995). The following paragraphs provide a description of the main indices related to the plant status.

5.1 Indices describing the crop status

5.1.1 Spectral vegetation indices: Normalized Difference Vegetation Index (NDVI) and Enhanced Vegetation Index (EVI)

NDVI and EVI, defined as vegetation indices, have been designed to provide consistent spatial and temporal monitoring of vegetation conditions. They can be used to distinguish green leaves from many other materials in the landscape.

The green plant tissues absorb blue and red visible light, while reflect in the NIR spectral (Fig. 5.1.1). Therefore both indices are sensitive to the differences between visible red (RED) and near-infrared (NIR) reflectance. The RED reflectance decreases with increasing chlorophyll content and NIR reflectance increases with growing LAI and vegetative coverage (Beck et al., 2007).

NDVI and EVI are based on the simple ratio NIR/RED (SR) (Jordan, 1969) to enhance the contrast between soil and vegetation and to minimize the effects of illumination conditions (Bronge, 2004). The value for both indices has a range limited from -1 to 1.

Data from vegetated areas have positive and high values, due to high NIR and low RED reflectance. In contrast, bare soil and rocks generally show positive but low values, close to zero. Water, clouds, and snow produce negative values.

Blue, RED and NIR reflectances, centered at 469 nm, 645 nm, and 858 nm, respectively, are used to compute the vegetation indices in MODIS products (Satellite Terra NOAA-AVHRR) (Tab. 5.1.1).

The computation of NDVI and EVI follows the equations 1 (Rouse, 1973) and 2, respectively:

(1) NDVI = (NIR − RED) / (NIR + RED)

(2) EVI = G * (NIR − RED) / (NIR + C1 * RED – C2 * Blue + L)

In NDVI, the difference between NIR and RED reflectance is divided by their sum (Eq. 1). This normalization is used to minimize the effects of variable irradiance (illumination) levels. However NDVI is still very sensitive to the noise due to external factors such as, primarily, the soil background, especially in areas with sparse vegetation. Furthermore, NDVI shows scaling problems related to a saturated signals over high biomass conditions (Huete, 1988).

For these reasons, EVI was improved compared to NDVI. EVI uses the blue band to reduce the noise due to atmospheric conditions (e.g. contamination caused by smoke and thin clouds). Moreover it includes the introduction of some coefficients (e.g. G, C1, C2, L) (Eq. 2) to minimize the effects of soil background variation and to maintain the sensitivity over dense vegetation conditions. For this reason, compared to NDVI, EVI shows, for most of the biomes, lower values due to the avoidance of the saturation effect encountered by NDVI (Huet et al., 2002).

Both indices showed a good dynamic range and sensitivity for monitoring and assessing the spatial and temporal variations in amount and condition of vegetation (Huete et al., 2002). However, NDVI is chlorophyll sensitive, while EVI is more responsive to canopy structural variations, including LAI, canopy type, plant physiognomy, and canopy architecture (Gao et al., 2000). Therefore, each index complements the other, in global vegetation studies, improving the detection of the vegetation changes and the extraction of canopy biophysical parameters (Huete et al., 2002).

The vegetation indices have been found to be related to a number of biophysical properties and processes of the plants, including primary production (Schloss et al., 1999), percent vegetation cover (Laidler et al., 2008), green leaf biomass (Masková et al., 2008) and carbon dioxide fluxes (Box et al., 1989). Moreover, several authors used remotely sensed SR and the derivative indices to assess fPAR (Steinmetz et al., 1990; Gallo et al., 1993; Los et al., 2000; Serrano et al., 2000; Lobell et al., 2003; Hilker et al.,

2011) and LAI (Asrar et al., 1984; Benedetti, 1993; Casanova et al., 1998; Haboudane et al., 2004).

Regarding this topic, the reviews of Bronge (2004) and Huete et al. (2002) highlighted some deficiencies of the vegetation indices in describing trend and variability of LAI and fPAR.

Several parameters affect the spectral reflectance from a vegetation canopy. The large variation of the vegetation and background properties involves different reflectance responses. As result, no unique relationship was found between remotely sensed (RS) vegetation indices and the observed LAI and fPAR of the plants (Bronge, 2004). Different values of NDVI or EVI can be observed for similar LAI and fPAR conditions of the canopy (Huete et al., 2002). Therefore, the correlation between the vegetation indices and LAI and fPAR cannot be applicable everywhere and at all times

This highlights that to retrieval the biophysical parameters from NDVI and EVI it is necessary to integrate the two indices with information about each specific biome, stratifying by land cover types and choosing the optimal vegetation index for each stratum (Huete et al., 2002; Bronge, 2004).

With respect to LAI, although the relationships between vegetation indices and LAI have been well-established, the assessment of LAI on the basis of vegetation indices is not straightforward (Bronge, 2004). One of the most serious limitations is that the indices can quickly saturate and become insensitive to variations of LAI for high LAI values (Bronge, 2004). Theoretically, an accurate and reliable estimation of LAI from vegetation indices occurs when the canopy is optically thin enough to allow a significant illumination of the underlying soil (Bronge, 2004).

Similarly, the correlation between vegetation indices and fPAR has been empirical and theoretically shown in several studies and it is linear in most cases. On the other hand this relationship is sensitive to background, atmospheric and bidirectional effects (Bronge, 2004; Hilker et al., 2008). An increase in soil reflectance results in NDVI decrease and fPAR increase.

Furthermore, the positive atmospheric effect at RED wavelength (620 – 670 nm) and the negative effect at NIR wavelength (1230 – 1250 nm) involve a reduction of the ratio NIR/RED and an increase of fPAR (400 – 700 nm) (Bronge, 2004).

Fig. 5.1.1. Spectral reflectance of natural surfaces
(Source: http://Blue Marble Research//wordpress).

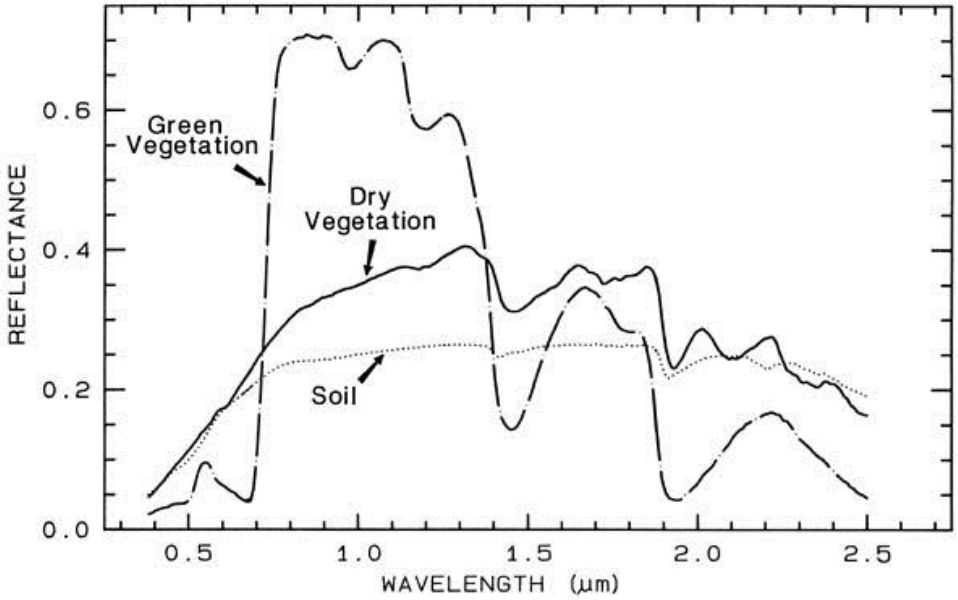

Tab. 5.1.1 MODIS products. (Source: http://modis.gsfc.nasa.gov/).

MODIS product	*Index*	*Temporal Resolution*	*Spatial resolution*
MOD15A2	LAI	8-Day	1 km
MOD15A2	fPAR	8-Day	1 km
MOD13A2	NDVI	16-Day	1 km
MOD13Q1		16-Day	250 m
MOD13A2	EVI	16-Day	1 km
MOD13Q1		16-Day	250 m

5.1.2 Leaf Area Index (LAI) and Fraction of Absorbed Photosynthetically Active Radiation (fPAR).

LAI is a dimensionless ratio (mq / mq) and it defines the number of equivalent layers of leaves relative to a unit of ground area. The amount of leaves in the canopy is determinant factor to establish the light intercepted by the plant and the carbon dioxide and water exchanges, which in turn control the transpiration and the photosynthesis rate (Monteith and Unsworth, 1990).

Ground measurements of LAI are difficult and time consuming to obtain over large areas. However, RS data can provide an effective means to estimate LAI.

In MODIS products (Satellite Terra NOAA-AVHRR) (Tab. 5.1.1), LAI has been estimated on the basis of the correlations found in different biomes, between ground-measures and RS data. LAI MODIS imagery are based on semi-physical algorithms that were developed for the modeling of global LAI (Hilker et al., 2008).

fPAR is expressed as a unitless fraction of the incoming radiation received by the land surface and it provides a measure of potential photosynthesis. fPAR measures the proportion of available radiation in the photosynthetically active wavelengths (400 – 700 nm) that is absorbed by the plant for the photosynthesis. The absorption of light by the chlorophyll has its peak in proximity to 430-480 nm and 663-650 nm (Fig. 5.1.2) (Tucker and Sellers, 1986).

There are many terms related to PAR that require a definition, as shown in table 5.1.2.

fPAR is a function of the leaf surface area (Sellers, 1985). The relationship between fPAR and LAI is near-linear at LAIs < 3 (Myneni and Williams, 1994). Field measurements performed on different crops, such as wheat (Hipps et al., 1983), maize (Gallo et al., 1985), and cotton (Wiegand and Richardsson, 1990), showed that the seasonal behavior of fPAR in relationship to LAI can be expressed by an exponential function based on Beer's law (Baret and Guyot, 1991).

fPAR can be estimated from remotely sensed vegetation indices such as NDVI and EVI (Steinmetz et al., 1990; Gallo et al., 1993; Los et al., 2000; Serrano et al., 2000; Lobell et al., 2003; Hilker et al., 2011). However, even if the relationship between fPAR and vegetation indices is appropriate, as shown above (paragraph 5.1.1), a direct relationship

between vegetation indices and fPAR has limitations that make the application to large areas or in different phenological seasons unsuitable (Bronge, 2004; Hilker et al., 2008). In MODIS products of fPAR (Satellite Terra NOAA-AVHRR) (Tab. 5.1.1), the absorbing biomass is computed on the basis of the RS LAI. The algorithms use photon transport theory to estimate both the radiation regime of the vegetation canopy and the radiant existence, which in turn depends on the architecture of individual plants and entire canopy, the optical properties of vegetation elements and the soil-atmospheric conditions (Myneni et al., 1989; Knyazikhin et al., 1999).

In this context, LAI and fPAR MODIS imagery represent a linkage between various other MODIS products of the same generation (Tan et al., 2005). They are derived by an algorithm that uses MODIS land cover classification (Biome Classification Map), and the surface reflectance products related to canopy transmittance, reflectance and absorptance (Tan et al., 2005; Hilker et al., 2008). In turn, the reflectance algorithms are based on aerosol optical depth products and they derive atmosphere-corrected surface reflectance from calibrated, geo-projected and cloudscreened MODIS radiance measurements (Tan et al., 2005).

LAI and fPAR have many applications for different purposes. They were used to assess the surface photosynthesis, evapotranspiration, and crop net primary production, which in turn are used to estimate terrestrial energy, carbon and water cycle processes, and the biogeochemistry of vegetation (Bronge, 2004).
In particular, fPAR was widely used to assess the gross primary production (GPP) (Hilker et al., 2008; Garbulsky et al., 2011) on the basis of a simple model described by equation 3 (Monteith, 1972; Monteith, 1977):

(3) GPP = RUE * fPARdt

where: fPARdt is the absorbed radiation by green vegetation during the period of study and RUE is the efficiency with which the absorbed radiation is converted into biomass. fPAR can be assessed with a good degree of reliability. On the other hand, RUE varies significantly between plants and ecosystems in relationship to the variation of environmental constraints (Field et al., 1994; Garbulsky et al., 2010). Therefore, a

considerable uncertainty still remains about RUE. High spatial and temporal variability of RUE was observed in relationship to changes in environmental and physiological limitations (Runyon et al., 1994; Gamon et al., 1995; Garbulsky et al., 2010). The main factors contributing to RUE variability include soil nutrients level (Gamon et al., 1997, Ollinger et al., 2008), drought and temperature extremes (Wit, 1965; Wilson and Jamieson, 1985; Landsberg and Waring, 1997; Sims et al., 2006).

Fig. 5.1.2 Typical PAR action spectrum, shown beside absorption spectra for chlorophyll-A, chlorophyll-B, and carotenoids (Whitmarsh and Govindjee, 1999).

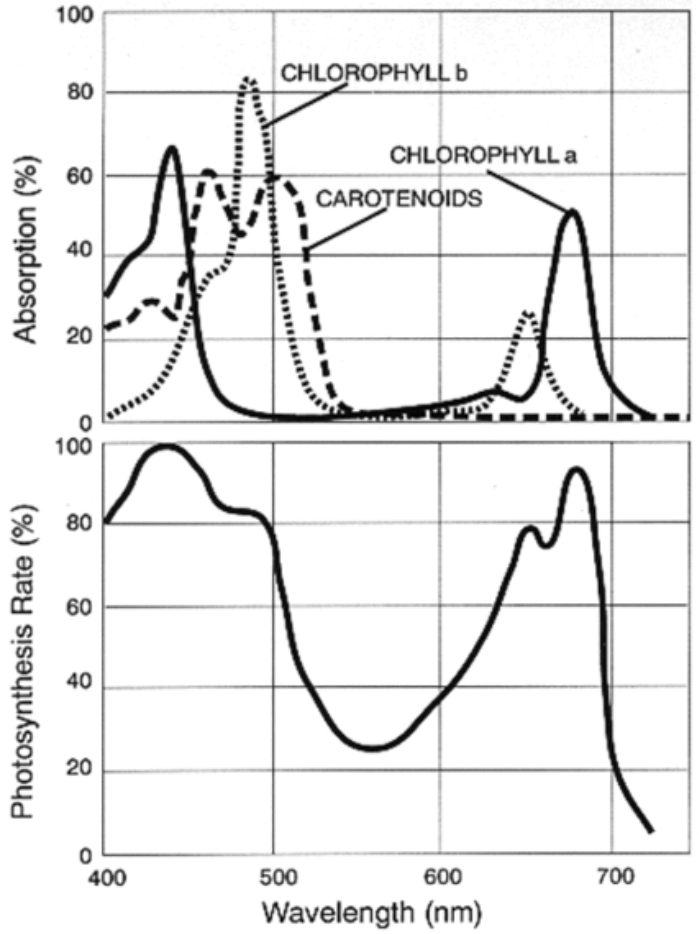

Tab. 5.1.2 Summary of the terminology about PAR

<table>
<tr><th>Index</th><th>Definition</th><th>Computation</th><th>Details</th></tr>
<tr><td>Incident PAR</td><td>Amount of PAR incident at the top of the atmosphere</td><td>It is computed using Earth-Sun geometry and the known solar radiation</td><td>The amount of PAR incident at the top of a vegetation canopy varies seasonally and daily, and with changing latitude and local topography, cloud cover and atmospheric properties.</td></tr>
<tr><td>Intercepted PAR:
IPAR</td><td>Amount of PAR caught by the canopy layers.</td><td>It takes into account the PAR incident at the canopy top and its travel down, through canopy layers, to the ground:
IPAR = PAR above canopy – PAR below canopy</td><td rowspan="2">The difference between IPAR and APAR depends on canopy composition, density and reflectance and on its closure and coverage over the ground. If a canopy has dense coverage and consists of green leaves, IPAR may be a good approximation of APAR, since healthy green leaves do not reflect much PAR.</td></tr>
<tr><td>Absorbed PAR:
APAR</td><td>Amount of PAR actually absorbed by the canopy layers</td><td>It takes into account PAR reflected from the canopy (r) and PAR transmitted through the canopy (t):
APAR = PAR – p – t</td></tr>
<tr><td>Fractional PAR:
fPAR</td><td>Fraction of incident PAR intercepted or absorbed by the canopy.</td><td colspan="2">fIPAR = IPAR / PAR incident
fAPAR =APAR / PAR incident</td></tr>
</table>

5.1.3 MODIS products

Table 5.1.1. shows the MODIS products (Satellite Terra NOAA-AVHRR) that describe the canopy status in relationship to the plant biomass growth and photosynthetic activity.

Compared to the acquired row data, the imagery involve an improved calibration and atmospheric correction. They result in compositing intervals, or time-step, of 16-days (NDVI and EVI) or 8-days (fPAR and LAI). The atmospheric noise is mainly related to clouds, dust and aerosols. The methods to reduce the error in values due to this disturbing factor are based on the maximum value compositing (MVC) over the interval (Holben et al., 1986). In MVC, only the highest value recorded during the time step is retained, resulting in fewer but more reliable imagery.

Despite this, the available data-sets of RS data often contain abrupt temporal changes in values during the time series. When these changes are inconsistent with the relatively gradual manner in which vegetation activity changes in time, they are due mostly to persistent cloud cover or aerosol contamination (Huete et al., 2002; Los et al., 2005).

5.2 Remotely sensed data to monitor wheat production

The RS indices described in the previous paragraph (5.1) were found to be highly related to vigor and condition of the wheat canopy by many authors (Tucker and Holben, 1981; Kumar and Monteith, 1981; Serrano et al, 2000; Tilling et al, 2007).

SR and NDVI showed a strong relationship with the changes in leaf pigment concentration, above ground dry matter accumulation, green leaf biomass and LAI (Yi et al., 2008; Aparicio et al., 2002). Therefore, SR and NDVI proved to be useful tool in monitoring the wheat responses to N fertilization (Serrano et al., 2000; Zhao et al., 2005; Tilling et al., 2007) and to rainfall after mild drought (Tucker and Holben, 1981). The positive correlation between wheat yield and SR or NDVI was shown in many papers (Quarmby et al., 1993; Hamar et al., 1996; Serrano et al., 2000; Ren et al., 2008; Becker-Reshef et al., 2010).

Despite this, as seen in the previous paragraph (5.1), studies highlighted the limits in the assessment of crop LAI on the basis of vegetation indices, such as SR and NDVI.

Although the correlation between NDVI or SR and the wheat growth traits (LAI and above ground biomass) is well-established, it is influenced by factors, such as the plant growth stage or canopy structure (Bellairs et al., 1996). Moreover, the correlation between crop variables and RS indices is affected by the changes in water and nitrogen status.

Aparicio et al. (2000 and 2002) carried out specific studies on durum wheat, based on ground reflectance measurements recorded by field optical instruments. The results showed that NDVI loses its discrimination power for LAI higher than 3 (Aparicio et al., 2002). The relationship between NDVI and wheat LAI resulted to be also affected by the water conditions (Aparicio et al., 2000). In rainfed system significant correlations were found between NDVI and LAI at any crop stage. On the other hand, in irrigated system, significant correlations were found only during the second half of the grain filling stage.

Similarly, Serrano et al. (2000) showed that in wheat the correlation between SR or NDVI and LAI was significantly affected by N supply. As a consequence, the crop LAI

would be over-estimated when an equation obtained under N-deficient conditions is used (Serrano et al., 2000).

These results highlighted the need to verify the usefulness of RS indices in describing the wheat LAI, biomass accumulation and grain harvest. About this, the analysis must be based on the timing of RS data acquisition and the plant phenological development.

Studies suggested that the optimal timing for the wheat yield forecast involves the NDVI at the time of maximum green canopy cover, which generally occurs around one month prior to harvest (Tucker et al., 1980; Mahey et al., 1993; Basnyat et al., 2004).

Ren et al. (2008) showed that, using MODIS NDVI imagery, a good forecast of wheat yield could be obtained about 40 days ahead of harvest time, at booting-heading stage. Becker-Reshef et al. (2010) described a model based on MODIS NDVI imagery able to generate wheat yield assessments six weeks prior to harvest, with an error of 10% compared to the final yield reported by official sources. Quarmby et al. (1993) showed that an early estimation of wheat yield can be made between 50−100 days prior to harvest on the basis of a simple linear regression with MODIS NDVI.

Freeman et al. (2003), carrying out field optical measurements, found a significant correlation between wheat yield and NDVI from flag leaf to anthesis stage, while no correlation during the grain filling stage. Other studies about durum wheat, based on field optical measurements, indicated more predictive value of both NDVI and SR at onset of stem elongation, at half-anthesis stage and at milk-grain stage (Aparicio et al.; 2002; Marti et al., 2007).

Most of the literature on durum wheat is focused on reflectance measurements recorded with field optical instruments (Aparicio et al., 2000; Aparicio et al., 2002; Royo et al., 2003; Babar et al., 2006; Ferrio et al., 2005; Marti et al., 2007). Compared to ordinary wheat, for durum wheat the relationship between yield and RS indices from satellite imagery has been little investigated (Benedetti, 1993; Moriondo et al., 2007; Orlandini et al., 2011).

Therefore, the performance of satellite imagery to capture the high yield variability of durum wheat (Cossani et al., 2011), and the optimal timing to obtain accurate forecasts, are issues yet to be explored.

The use of NDVI in forecasting applications for wheat yield is an issue well addressed in literature. However, the literature is limited regarding the evaluations of the performance of other MODIS indices, such as EVI, LAI and fPAR.

Over different biomes, included croplands with wheat, MODIS LAI and MODIS fPAR showed good correlation with the observed seasonal trends of plant LAI and fPAR, respectively (Fensholt et al., 2004; Yang et al., 2006). In this context, MODIS fPAR required particular attention.

Studies have shown the possibility of obtaining good forecasts of wheat yield through simple models of crop biomass assessment based on fPAR (Serrano et al., 2000; Lobell et al., 2003; Moriondo et al., 2007; Ren et al., 2007; Wu et al., 2009; Ren et al., 2009). Despite this, these studies did not use satellite imagery of fPAR, but were based on fPAR assessment from RS NDVI.

fPAR is related to fundamental processes governing the crop production. The productivity of a crop depends on the ability of plant canopy to intercept the incident radiation (Campillo et al., 2012).

The intercepted solar energy is necessary in the physiological processes related to photosynthesis (light energy absorption by chlorophyll, resulting ATP and NADPH generation, carbon fixation in Calvin cycle and synthesis of vegetal components) which, in turn, determine the plant biomass growth (Campillo et al., 2012).

Wheat fPAR is a function of leaf area (Campillo et al., 2012). When deficiencies in water and nutrient inputs involve a reduction of the leaf growth rate, a decrease of yield occurs as result of an insufficient capture of energy (Gardner et al., 1985).

Studies of wheat confirmed the strict correlations between fPAR and LAI (Hipps et al., 1983), green foliage (Wilson and Jamieson, 1985; O'Connell et al., 2004) biomass accumulation (Green, 1987) and yield (Mitchell et al., 1993; Mearns et al., 1997), as well as between grain yield and plant biomass and LAI (Regan et al., 1992; Kang et al., 2002; Dalirie et al., 2010).

In wheat, a reduction of fPAR led to a lower harvest quantity (Mitchell et al., 1993; Mearns et al., 1997), as well as low values of LAI and biomass were associated with a yield decrease (Regan et al., 1992; Kang et al., 2002; Dalirie et al., 2010).

The radiation fraction absorbed by wheat foliage, increases with the rise of maximum canopy size (Green, 1987). The wheat grain yield is fitted with a quadratic function with the plant dry matter biomass. The yield increased with biomass until a value of 14000 kg/ha biomass and then remained more or less constant (Kang et al., 2002). At small values of LAI (≤ 2), fPAR is a function of both LAI and cloud cover, while at high values of LAI (= 4) fPAR is large and independent from the sky conditions and, hence, from the quality of incident PAR (Hipps et al., 1983).

Green (1987) found that, during the period from stem elongation stage to grain maturity, although the quantity of absorbed radiation increased, the rate of biomass accumulation in wheat remained constant. The author explain this result in relationship to an ontogenetic decline by the crop of the conversion efficiency of absorbed radiation into biomass. However, this result can also suggest that, during the late period of the crop cycle, the physiological processes related to the absorbed solar radiation give its main contribution not to the green biomass growth but to the spike and grain development. About this, studies have shown that the periods most sensitive to the solar radiation are the spike growth stage (approximately from 20-30 days preceding anthesis to one week after anthesis) and the grain filling stage (Willey and Holliday, 1971; Fisher, 1975; Abbate et al., 1997). During these periods the radiation is critical and an its decrease depresses the yield, by reducing the grains number per mq or per spike, the spikes weight per mq and the weight per grain (Willey and Holliday, 1971; Fisher, 1975; Abbate et al., 1997). These results highlighted the relevance of fPAR absorbed or intercepted by the crop during the period when the assimilates are portioned toward the production of the reproductive organs. Abbate et al. (1997) showed that, during the spike growth period, the radiation-use efficiency was not remarkably affected by radiation level. The intercepted PAR was the main factor in determining both quantity and quality of harvest, when wheat was grown in conditions without water or nutrient constraints. The growth rates of the crop and spike were positively and linearly related among them, and both were found linearly related to changes in intercepted PAR (Abbate et al., 1997). Therefore, the grain number per mq, and subsequently, the yield,

were linearly correlated to accumulated intercepted PAR during the period of spike growth (Abbate et al., 1997).

The literature is quite limited on studies that show the performance of EVI, LAI and fPAR, from MODIS products or acquired from other satellite imagery, to forecast GPC of wheat, and especially for durum wheat. Moreover, the literature shows contrasting results about the relationship between GPC of wheat and the RS indices, descriptive of the crop canopy and growth.

Reyniers et al. (2006) found a significant and positive correlation between NDVI close to the harvest time and both GPC and nitrogen content in the straw (R2 = 0.7). Similarly, Basnet et al. (2003) and Xue (2007) showed significant and positive correlations between wheat GPC and NDVI, at flowering (R2 = 0.67) and from heading stage to mid grain filling stage (R2 = 0.4), respectively. Li et al. (2012) realized a estimating model based on the positive correlations found between GPC and NDVI acquired from satellite during four growing stages (standing, anthesis, early filling, mid filling stages) in 2003 and three growing stages (early standing, jointing, early filling stages) in 2004. The authors obtained a good assessment of GPC on the basis of the multi-temporal images combination, with a R2 between estimated and observed data of 0.88 in 2003 and 0.72 in 2004 (Li et la., 2012).

The positive relationship between GPC and NDVI can be explained by the source-limited nature of the protein deposition into the grain (Jenner et al., 1991; Jamieson and Semenov, 2000). GPC depends on the total N content of the crop biomass. GPC showed a positive correlations with total N of wheat leaves at anthesis (Wang et al., 2003; Huang et al., 2004), and at 14 days after anthesis (Li et al., 2005).

Therefore, NDVI can be positively correlated with GPC because the RS index is descriptive of the above ground biomass and plant LAI, and these last are related to the total N available (Huang et al., 2004) for the translocation from the vegetative tissues to the grain.

On the other hand, Orlandini et al. (2011), analyzing the period 1999-2009, found a negative correlation between GPC and NDVI, beginning from mid-May. Moreover, some studies highlighted that NDVI was not able to provide reliable predictions of

wheat GPC, and about N concentration of grain and straw (Freeman et al., 2003; Liu et al., 2006; Xue et al., 2007). The study of Freeman et al. (2003), carried out during 2 years over seven locations, showed a significant correlation between NDVI and grain N uptake, straw N uptake, total N uptake and yield. On the other hand, the authors did not find consistent relationship between NDVI and the N concentrations, of grain and straw, at any growth stage. Similarly, Xue et al. (2007) and Liu et al. (2006) did not find significant correlations between NDVI and grain N or GPC, at any growth stage.

The lack of agreement regarding the relationship between NDVI and GPC highlights the need of further analysis about this issue. Since the RS indices are strongly linked to the plant LAI, an explanation of these contrasting results could be found through a better analysis of the relationship between GPC and LAI.

5.3 Applications in forecasting the crop production

Many studies analyzed with a predictive purposes the relationship between vegetation indices (EVI and NDVI), from MODIS products, and the yield of crops, such as maize (Unganai and Kogan, 1998; Mkhabela et al., 2005), wheat (Ren et al., 2008; Reshef et al, 2010), cotton (Mkhabela and Mkhabela 2000), rice (Dailiang et al., 2011), and soybean (Liu and Kogan 2002). However, the assessment of yield or net primary production, based on the direct relationship with NDVI or EVI, is bonded to the assumption that the incoming radiation and its conversion to dry matter are constant in time and space. This makes the model particularly inadequate in forecasting or monitoring applications. The studies that analyzed the relationship between crop yield and LAI or fPAR, assessed both indices on the basis of RS NDVI or SR, in agreement with the approaches suggested by some authors (Baret and Guyot, 1991; Asrar et al., 1992; Myneni and Williams, 1994; Myneni et al., 1995a; Myneni et al., 1995b; Sellers et al., 1996; Myneni et al., 1997). However, as mentioned in the previous paragraphs, the estimation of LAI and fPAR from RS vegetation indices has some deficiencies.

About this, Fensholt et al. (2004) assessed the performance of the MODIS products, NDVI/EVI and LAI/fPAR, on the basis of the fit with ground measurements performed over different biomes. The seasonal dynamics of LAI and fPAR recorded in situ were captured fairly accurately by MODIS LAI and fPAR. A strong and linear correlation between in situ fPAR and NDVI was found for each vegetation type, as well as between MODIS NDVI and MODIS fPAR (Fensholt et al., 2004). Despite this, the regression coefficient between NDVI and fPAR from satellite imagery differed from that that characterized the in situ data (Fensholt et al., 2004). The discrepancy between MODIS fPAR - MODIS NDVI regression slope, and in situ fPAR - NDVI regression slope, confirmed that fPAR can be retrieved from satellite imagery of NDVI only to a limited extent (Fensholt et al., 2004).

LAI/fPAR MODIS imagery are based on a complex algorithms system, resulting from the linkage among many other MODIS products, and then, in this context, they can be able to partially overcome the deficiencies related to an assessment based on RS

vegetation indices, such as SR, NDVI or EVI. About this, there are very few studies that assess the capability of MODIS LAI and fPAR, in comparison with MODIS NDVI and EVI, in the monitoring of crops production. In literature it is possible to find a similar work performed by Bala and Islam (2009) about potato. Therefore, the performance of LAI/fPAR MODIS imagery, in forecasting wheat harvest, represents an issue that is still little explored. Especially the use of MODIS fPAR with predictive purposes may cover a key role.

MODIS fPAR imagery closely follow the seasonal variations of LAI over different biomes (Tian et al., 2004; Yang et al., 2006). In the same time, they take into account the actual incident PAR and the plant absorption within wavelength range, directly related to plant physiological processes. The light absorbed outside the PAR region may be disadvantageous for the plant because it increases the molecular agitation, causing a rise of leaf temperature. Higher leaf temperatures involve an increase of the required heat dissipation, and hence, an increase of the resulting water losses through transpiration (Taiz and Zeiger, 2010; Campillo et al., 2012).

On the other hand, the harvest assessment through the vegetation indices (SR, NDVI and EVI), assumes the incoming radiation constant, and, is based on RS values that increase with the absorption in the RED (620-670 nm) region. The RED region represents only partially the range of the photosynthetically active wavelengths (400 – 700 nm). For this reason, the vegetation indices are descriptive of the biophysical structure of the canopy coverage and are suitable to classify different vegetation cover, but, in contrast to fPAR, they do not have a direct relationship with the plant physiological processes, underlying the crop growth, development and production.

Furthermore, the use of RS fPAR in forecasting applications can be particular interesting in view of an integration of RS data in a simplified agro-meteorological model. In this context, fPAR supplies information about solar radiation, the weather data rarely available for modeling applications. On the other hand, weather data can decrease the uncertainty, related to RUE, in the GPP assessment, since drought and temperature extremes are determining factors of RUE variability (Wit, 1965; Wilson and Jamieson, 1985; Landsberg and Waring, 1997; Sims et al., 2006).

5.4 Limitations in the use of remotely sensed data and integration with the crop modeling tools

As discussed in the previous paragraphs (4.1 and 4.2) the crop modeling, differently from a statistical approach, allows to capture the interactions between the environmental variables and the key physiological processes of the plant, offering a good temporal coverage. However, the adoption of complex simulation models in operational forecasting applications often has strict limitations that affect the confidence and the spatial representativeness of the output.

On the other hand, as shown in the previous paragraphs (5.1 and 5.2), the relationship between RS indices and crop growth and production is confirmed in many studies.

RS data support the assessment of a number of biophysical properties and physiological processes of the crop. Despite this, the assessment of the quality and quantity of the harvest on the basis of a regression model with RS indices represents an approach that is fundamentally simplistic. Therefore, the integration between RS data and agro-meteorological model is recommended (Quarmby et al., 1993).

Indeed, the use of RS is not perfect to monitor the crop due to the difficulty to establish a stable correlation over the time between RS data and the crop variables. A model based on a correlation found during a growing season, can often not be easily exportable, since the RS value summarizes for each time-step the influences of many and dynamic components of the environment and of the landscape. The change of these components, from year to year, can result in a shift of the range of the RS values not justified by a real change in the range of the yields. About this, for example, the atmospheric perturbations related to the water vapor and aerosol content can drastically affect the RS values range (Moulin et al., 1998). Moreover, the current RS imagery supply a good spatial resolution but a poor temporal coverage due to the methods, based on the MVC, used to eliminating the atmospheric noise in data series. Therefore, the available time-steps for the satellite imagery do not always match the periods of the crop cycle with a key role in the yield determining. For these reasons, RS data can well

support a description of the spatial variability but represent a poor tool for temporal comparisons.

In this context, an integration approach between crop modeling and remote sensing has been developed to overcome the deficiencies that characterize both tools. The integration is mainly based on the ability of RS indices to supply a description of the canopy status and environmental conditions and on the capability of the simulation models to capture the interactions between the plant and the other environment variables. Different types of RS data, acquired at different temporal and spatial scales, can be of great value as input in the development of vegetation models, as well as for the validation of model simulations (Fischer et al., 1997). The use of RS information in the field of crop modeling represents a means to improve the accuracy of predictions under operational conditions (Maas, 1988). RS observations allow to minimize the random error, and their combination with the crop model can result in a simulation less sensitive to field initial conditions, commonly affected by lack of input data (Maas, 1988). For example, the radiometric signal allows the detection of onset of a fast process, such as the beginning of crop growth, or the monitoring of occurrence of accidents (e.g. attack of pathogens) (Moulin et al., 1998), that the model could, respectively, simulate with a certain level of inaccuracy, due to missing input data for the crop management (e.g. sowing date, fertilization plans), or not simulate, due to the lack of the necessary sub-models.

The combination of crop models and remote sensing can be synergistic in various ways. The first area of interest is related to the use of RS data as input into the complex crop models with the aim to overcome the poor accuracy of the available input data, improving the spatial representativeness and reliability of the simulation.

In this context three approaches are possible (Maas et al., 1988; Fischer et al., 1997; Moulin et al., 1998; Pinter et al., 2003):

1. Use the biophysical variables about the crop, assessed on the basis of RS indices, to drive the simulation of the model;
2. Obtain, from RS values, information about the crop simulation environment (e.g. crops classification, sowing or emergence date, soil initial condition, harvest date, etc.),
3. Use the RS data to directly readjust and correct the model final output.

The first approach has been widely addressed. Basically, most of the studies about the coupling of satellite data with crop models are focused on the retrieval of biophysical parameters of the canopy from RS, and on their subsequent assimilation into the complex model. The data-assimilation method allows re-initializing or re-calibrating the model, on the basis of the best fit between the simulated canopy parameter and the one assessed by the RS data, with a general improvement of the model performance (Maas et al., 1988; Fischer et al., 1997; Moulin et al., 1998; Dorigo et al., 2007).

Since LAI represents a key variable that interacts in different ways with the plant physiological processes (Fischer et al., 1997), most of the studies in this field tested different assimilation schemes (e.g. indirectly by adjusting the sowing date, flowering onset, soil moisture etc., or directly with the replacement of the simulated canopy parameter) for the incorporation of RS LAI value in to the model (Clevers et al., 2002; Doraiswamy et al., 2004; Doraiswamy et al., 2005; Jongschaap, 2006; Dente et al., 2008; Yuping et al., 2008; Fang et al., 2008; Fang et al., 2011).

About this, Dente et al. (2008) analyzed different assimilation algorithms to minimize the difference between simulated and RS LAI, and, to determinate the optimal set of input parameters for durum wheat. The study showed that the LAI retrieved from RS imagery can be effectively assimilated into the CERES-Wheat model and lead to an improvement of the accuracy in yield simulation at field level, ranging from 360 kg/ha to 420 kg/ha. The authors highlighted the importance of RS data available during the period of maximum development of the canopy: from steam elongation to heading

stage. The lack of RS data during this period significantly increased the error in yield assessment to 650 kg/ha.

Yuping et al (2008) performed the re-initialization of WOFOST model through the integration with SAVI, a MODIS vegetation index based on the normalized difference between RED and NIR. After integration, the model provided more accurate estimations of above ground dry weight and plant LAI at field level, and assessments of yield at regional scale more consistent with official data of wheat production.

Similarly, Fang et al. (2008) found an improvement of the performance of CERES-Maize model, due to the adjustment of some input parameters (e.g. planting date, planting population, row spacing, and nitrogen amount) on the basis of the best fit between simulated LAI and RS LAI from MODIS imagery. In comparison to the maize yields reported by the statistics at national level, the model provided the best results when the optimization was carried out on the basis of seasonal LAIs, while the assimilation only of the green-up LAIs or the highest LAI has led to a model performance reduction.

Other biophysical parameters were retrieved from remote sensing to improve the model performance, including leaf angle distribution and leaf optical properties (Moulin et al., 1998), fPAR, vegetation height, fractional cover, above ground biomass and net primary production, phenological development, canopy nitrogen content (Jongschaap, 2006), plant water content and evapotraspiration rate (Fischer et al., 1997; Dorigo et al., 2007).

Most of the scientific literature focuses on this first approach. However the re-initialization and re-parameterization processes represent a complex integration procedure and show disadvantages for an operational use. This approach has proven to be a method difficult to be applied to forecast the crop yield at regional scale (De Wit et al., 2007). It necessitates more computer time, compared to the supply of input (second approach) or updating of output (third approach), based on RS information (Maas, 1988).

The literature is relatively limited of studies that describe a harvest forecasting system based on the last two approaches and that find algorithms for the direct spatialization of

model input or output, on the basis of RS imagery. This, of course, still represents a challenge.

Since the models show a high responsiveness in relationship to the set of the environmental initial conditions (e.g. sowing date, planting density, soil water content, e.g.), the second approach can offer the opportunity to improve the model performance. Studies suggested the possibility to improve the simulation reliability, as result of the revisiting of the planting date and seedlings establishment conditions, and of the correcting of soil characteristics, on the basis of RS data (Olioso et al., 1999; Guerif and Duke, 2000; Sehgal et al., 2002; Lobell et al., 2003; Launay and Guerif, 2005; De Wit et al., 2007; Ortiz-Monasterio and Lobell, 2007; Bolten et al., 2010).

About this, Lobell et al. (2003) combined the knowledge of crop phenology from imagery of SR and NDVI to estimate the crop rotations and the wheat sowing date. Similarly, De Wit et al. (2007) used the RS soil moisture index (SWI) to correct the errors in the water balance in WOFOST model, obtaining an improvement of wheat yield simulated at national and regional level.

The third approach has been explored very little, although it offers the opportunity to follow relatively simple procedures for the integration of RS data into the model. It does lend itself more suitable for operational use. Few studies directly compared the satellite reflectance measurements with the model's predictions, analyzing the possibility to integrate RS data in algorithms for the model output adjustment (Faivre et al., 1991; Nouvellon et al., 2001).

This lack of literature can be explained by the fact that, in the past, the attention of the research was focused mostly to improve the description of model process (Fischer et al., 1997). The need for realize an operational application tool is relatively recent issue, in order to support the adaptation measures in response to climate change and weather variability.

Therefore, in recent years, the attention of the scientific community has shifted to addressing the need to develop a simplified application models supported by RS data (Baez-Gonzalez et al., 2002; Lobell et al., 2003; Mo et al., 2005; Prasad 2006;

Moriondo et al., 2007), with the goal of improving the monitoring and forecasting of crop yield fluctuations at farm and sector level.

Lobell et al (2003) used fPAR, assessed from RS NDVI and SR, as input into a simple model that was based on the light-use efficiency of wheat . The authors showed that was possible to obtain accurate yield predictions using only one RS image, acquired at period of peak of crop development.

Moriondo et al. (2007) used the phenological times simulated by the complex model CROPSYST for durum wheat as input in a simple model based on RS data. The model used NDVI to estimate fPAR and crop harvest index, which in turn were used to assess the above ground biomass and the grain yield. The model showed high accuracy in estimating wheat yield at provincial level.

Similarly, Baez-Gonzalez et al. (2002) suggested a simplified model for maize able to account between 76% and 89% of the yields variability using as input RS NDVI and ground measurements about: PAR, LAI, crop development stage and planting date.

In this context, another unexplored approach could be represented by the use of the complex simulation models, such as CERES (Ritchie and Otter, 1985), CROPSYST (Vanevert and Campbell, 1994) or WOFOST (Vandiepen et al., 1989), to study the interactions among the ‘plant-soil-atmosphere’ system and to define the main variables affecting the harvest. These main crop and environmental components could be described by RS indices and, thus, assimilated in a simplified model. Finally, the integration with RS data allows to overcome the lack of ground measurements and improve the spatial resolution of the model output. This results in translating the crop models in tools that can run operationally for supporting applications at farm level.

6 RESEARCH GOAL

6.1 Premises

The Italian industry accounts for almost 25% of world pasta production. In this context durum wheat (*Triticum turgidum* L. var. *durum*) has a main role, in terms of national annual consumption and for the export market, since it is the only species able to provide the raw material for the pasta making. The main Italian production of durum wheat derives from the southern and central regions. In particular, in Tuscany, during the last 50 years, this crop proved its relevance with an increasing trend of harvested quantity, despite the general crisis that the cereal sector is going through (paragraph 1.1).

Thermal and water conditions strongly affect the wheat performance (paragraphs 2 and 3.3). Large fluctuations in the quantity and quality of the harvest were recorded in Mediterranean environment (Borghi et al., 1997; De Vita et al., 2007; Cossani et al., 2011). Compared to ordinary wheat, durum wheat has a higher productive responsiveness to Mediterranean climate, with on average higher yield and grain protein concentration (GPC), as well as less stable final grain size and weight (Cossani et al., 2011). As a consequence, durum wheat shows a larger variability of both yield and GPC. Despite this, most of the studies about the weather impact on the crop are focused on common wheat (paragraphs 2 and 3.3). The assessment of the climate impact on durum wheat, and the identification of the crop development stages susceptible to weather stresses, are issues less addressed in the literature.

The water and thermal conditions do not have a linear effect on the wheat performance, and the direction of their impact is in relationship to the timing, intensity and progress of the drought and heat stress during the crop cycle (paragraphs 2 and 3.3). Several studies analyzed the individual effect on wheat production due to the temperatures trend or water conditions (paragraph 2). Nevertheless, the interactions among these two weather variables and the resulting impact on the crop performance are less investigated.

The interactions between the environmental variables are also more complex and less known in determining GPC of wheat. On one hand, the positive effect on GPC of warm conditions at grain filling stage is well-established, on the other hand, the magnitude and direction of the impact of high temperatures during the other crop stages are still not clear (paragraph 3.3.1). Similarly, the timing of water stress and its interaction with the nitrogen dynamics involve different responses in terms of grain quality (paragraph 3.3.2). Moreover, the impact of temperatures rise and rainfall change on both wheat yield and GPC, is in general non-linear and not univocal, diversifying significantly in relationship to soil types and locations (Ludwig and Asseng, 2006).

In this context, a complex deterministic model represents a useful tool to study the 'soil - atmosphere – plant' system. Differently from a statistical approach, the modeling tools allow describing the interactions between the environmental variables. Capturing the key physiological processes in a simulation model would greatly aid both the interpretation and extrapolation of experimental results. Other than *Triticum aestivum* L., the literature survey on modeling to forecast or assess durum wheat yield in typical Mediterranean areas is quite limited, and, overall any of these studies deals with the issue of GPC simulation for durum wheat (paragraphs 4.1 and 4.2).

The GPC plays a critical role in determining the physical and nutritional characteristics of flour, and then the quality of the derived product (paragraph 3.1). About this, the unpredictability of the climatic conditions makes it difficult to guarantee the quality standards requested by the grain dealers. Therefore, the wheat production in Mediterranean regions suffers from the competition with the imported wheat grain.

In this context, for the farmers the quality has become an ever more important issue, due to the pressure from the marketing strategies of the durum wheat exporting countries. The negative correlation between yield and GPC has been well-established (paragraph 3.2). Therefore, the environmental impacts on GPC are intrinsically linked to the modalities in which the environment variables affect the yield.

Late applications of nitrogen effectively enhance the GPC of wheat, while they do not involve significant changes for the yield (paragraph 1.3). Therefore, the possibility to

obtain forecasts of both yield and GPC, before the beginning of grain filling stage, can be important to ensure the grain quality through a proper management of nitrogen inputs. In the year when high yield can lead to low GPC, the farmer has the opportunity to improve the GPC with late N applications.

However, the direct use of complex crop models as forecasting tools remains confined in the research field, since their operational applications often have strict limitations (paragraph 4.2). The major impediment for the adoption of complex models as farm supporting tools is represented by the difficulties in providing reliable and accurate input data. The uncertainty in the spatial distribution of soil properties, initial soil conditions, crop management, and meteorological forcing at field level leads the models to provide outputs with good time coverage but poor spatial coverage. For these reasons, most of the studies about the use of crop models for predictive purposes involve assessment of yield at large scale (paragraph 4.2).

The current crop simulation models are subject to even greater restrictions in monitoring and forecasting of GPC. The models show discrete performance in the assessment of wheat yield , but the literature suggests that the simulation of GPC still represents a challenge (paragraph 4.2). Some modifications in the model are necessary to use it to analyze the determinants of the grain quality.

The remotely sensed (RS) indices, such as NDVI (Normalized Difference Vegetation Index), EVI (Enhanced Vegetation Index), LAI (Leaf Area Index) and fPAR (Fraction of Absorbed Photosynthetically Active Radiation), provide information about a number of biophysical properties and physiological processes of the crop with a good spatial resolution (paragraphs 5..1 and 5.2).

However, the RS data often provide poor temporal coverage. The assessment of crop harvest with a regression model based on RS data represents an approach that is fundamentally simplistic, since a correlation found during a growing season is not easily exportable to other conditions (paragraph 5.4). The integration between crop modeling and remote sensing provides a solution to overcome the limits of both tools, improving the reliability of the assessments and forecasts of the wheat production. Among the integration approaches, those that offer the opportunity to use relatively

simple procedures have been explored only on a limited basis (paragraph 4.5). A simple integration approach between crop modeling and RS indices allows the translation of the crop model in a operationally running tool.

The use of NDVI in forecasting applications for wheat is an issue well addressed in literature (paragraph 5.3). On the other hand, the literature is limited regarding the use of RS indices, such as EVI, LAI and fPAR in the harvest assessment. Studies comparing the ability of these indices in describing the wheat production have not been carried out (paragraph 5.3). Moreover, most of the studies on durum wheat takes into account reflectance measurements recorded through field optical instruments (paragraph 5.2). Therefore, the performance of satellite imagery and the optimal timing in capturing the yield and GPC variability of durum wheat represent issues yet to be explored. Finally, about the relationship between RS indices and GPC of wheat, the literature shows contrasting results. Some authors found a positive relationship between RS indices and GPC, while other studies showed no significant correlations or negative correlations (paragraph 5.2). Since the RS indices describe the LAI, these results highlight the need to investigate the relationship between LAI and GPC.

6.1 Objectives

In this context, the current study focused on forecasting and monitoring of durum wheat productions in Tuscany region, with the following objectives:

Objective 1. Evaluate the impact of temperature and water conditions on yield and grain quality.

Objective 2. Assess the performance of the complex crop model CERES-Wheat in the simulation of yield and GPC and in determining of key growth stages and of weather variables with greatest effect on the harvest.

Objective 3. Revisit the algorithms adopted by CERES-Wheat for GPC simulation and carry out a diagnosis to trace the model deficiencies.

Objective 4. Set up forecasting indices suitable for operational applications at farm level, and able to provide information about the quantity and quality of the harvest in order to assist with the application of late fertilization.

Objective 5. Assess the improvement in the yield and GPC simulations by crop model due to the integration with RS data, based on a relatively simple procedure for the model output spatialization.

Objective 6. Compare the performance of the satellite imagery (MODIS) related to RS indices (NDVI, EVI, LAI, fPAR) in the monitoring of yield and GPC variability and trace the deficiencies in GPC description.

The study can be divided fundamentally into two research sections:

Section 1) Weather impact on durum wheat harvest and forecasting indices of grain yield and grain protein concentration

Section 2) Performance of remotely sensed indices in monitoring the variability of harvest quantity and quality and integration with crop modeling tools

- The first section is related to the objectives 1, 2, 3, and 4. The section 1 in turn includes two different research lines, one focused on yield and one on GPC.

With the support of CERES-Wheat, the weather impact on crop production was assessed. The crop growth stages and meteorological indices, with a key role in the description and forecast of the harvest, were identified. On this basis, forecasting indices were set up, for both yield and GPC, and their performances were assessed.

The algorithms adopted by CERES-Wheat for the GPC simulation were revisited. Some assumptions about the possible deficiencies of the model to capture the determinants of grain quality have been suggested.

- The second section is related to the objectives 5 and 6. The section 2 in turn includes two different research lines, one focused on yield and one on GPC.

The performances of RS indices in monitoring the crop production were assessed and the correlations with the quality and quantity of the harvest were established. Some assumptions about the capability of RS data in describing the wheat GPC have been suggested.

The best indicators of crop production variability were used to set up spatialization algorithms of yield and GPC. The spatialization algorithms perform the integration of RS data with crop modeling. The capability of RS data in improving the model simulations, resulting from runs without detailed input data, was assessed.

SECTION 1

"Weather impact on durum wheat harvest and forecasting indices of grain yield and grain protein concentration"

Objective 1. Evaluate the impact of temperature and water conditions on yield and grain quality.

Objective 2. Assess the performance of the complex crop model CERES-Wheat in the simulation of yield and GPC and in determining of key growth stages and of weather variables with greatest effect on the harvest.

Objective 3. Revisit the algorithms adopted by CERES-Wheat for GPC simulation and carry out a diagnosis to trace the model deficiencies.

Objective 4. Set up forecasting indices suitable for operational applications at farm level, and able to provide information about the quantity and quality of the harvest in order to assist with the application of late fertilization.

7. MATERIALS AND METHODS SECTION 1

7.1. Study area

The research was carried out in Val d'Orcia (Lat 43.03, Lon 1.66, 250-450 a.s.l.), a large rural area of the Tuscany region (Italy), part of the agricultural hinterland of the Siena Province (Fig. 7.1.1). The valley covers a surface of about 185 km^2 in terrain that is generally featured by rolling hills to a hilly-flat landscape crossed by a river. Durum wheat is one of the main crop traditionally grown and its importance is related to quality productions for the local pasta industry. Val d'Orcia is characterized by a typical Mediterranean climate with an average annual temperature of 13.6 °C and cumulated precipitation of about 715 mm, mostly falling during spring and autumn. In agreement with land use map, cereal crops are grown on 'Typic Ustorthents fine, mixed, calcareous, mesic' soils (USDA classification), moderately deep, weakly alkaline, with a silty-clay-loam texture and a slope from moderate to high (14 – 35 %).

Fig. 7.1.1 Tuscany region (blue), Siena Province (pink) and Val d' Orcia valley (red).

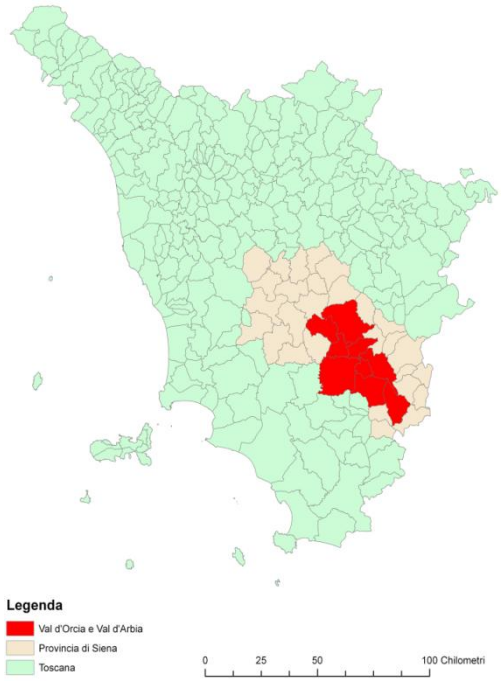

7.2 Weather data and meteorological indices

The mean meteorological daily data for precipitation (mm) (P), maximum (TMAX) and minimum (TMIN) air temperatures (°C) over 56 growing seasons (years 1955-2011) were obtained from six weather stations located in the study area.

The solar radiation (MJ/m^2) (R) was estimated from TMAX and TMIN following the equation (1) (Hargreaveres et al., 1985).

$$(1)\ R = Ra * Ah * \sqrt{TMAX - TMIN} + Bb$$

where: Ra is the daily extra-terrestrial radiation ($J\ m^{-2}\ d^{-1}$), and the values assumed in the study area by the empirical constants Ah ($°C^{-0.5}$) and Bh ($J\ m^{-2}\ d^{-1}$) are 0.18 and −1.76 respectively (Trnka et al., 2005).

Starting from the daily weather data, monthly meteorological indices were computed (Tab. 7.2.1) for all the years from 1955 to 2011, in order to characterize the climate of each growing season and to highlight the water and thermal conditions during the key development stages of wheat.

The months taken into account were March, April and May. During these periods the onset of the main crop growth stages was established, on the basis of both field observations and CERES-Wheat simulations.

In the study area, durum wheat is in tillers growth stage in March, the crop develops and advances from stem elongation to inflorescence emergence during April and reaches the flowering period normally between end of April and beginning of May. During May, the grain filling stage normally occurs, until the grain maturity stage within the first half of June. For further details about the phenological development stages of durum wheat see figure 1.2.1 and table 1.2.1.

Tab. 7.2.1 Meteorological indices. Legend: TMAX = maximum air temperature, TMIN = minimum air temperature, P = precipitation

Indices	*U.M.*	*Description*
MTMAX	C°	monthly mean of TMAX
MTMIN	C°	monthly mean of TMIN
TP	mm	monthly accumulated total P
WD	number of days	Warm Days: monthly sum of days with TMAX above the monthly average TMAX, computed over 56 years
DD	number of days	Drought Days: monthly sum of days with daily P amount below 5 mm

7.3. CERES-Wheat calibration and validation for yield simulation

The complex deterministic model CERES-Wheat (DSSAT-CSM version 4.0) was calibrated and validated for durum wheat (*Triticum turgidum* L. var. *durum*). The model is able to simulate the crop growth, development and production. For further details about CERES-Wheat see the paragraph 4.3.

CERES operates on a daily time step with the following meteorological input: P (mm), TMAX and TMIN (°C), R (MJ/m^2). The model was initialized with the weather database described in paragraph 7.2.

The soil input was supplied in agreement with the soil map. The fields were located over the more common soil type used in Val d'Orcia for the cereal crops production as described in paragraph 7.1. Table 7.3.1 shows the main physical and chemical properties of the soil profile adopted for the model initialization.

Tab. 7.3.1. Soil profile used by CERES-Wheat. Legend: CSC = cation-exchange capacity

Depth (cm)	*Master horizon*	*Clay %*	*Silt %*	*pH*	*CSC cmol/kg*
30	Ap	38	53	8.5	15.5
50	C	43	50	7.6	19.3
150	C	42	50	7.6	18.0

The field input data concerning crop management (e.g. sowing and harvest dates, plants density, fertilization inputs, etc.), wheat phenological stages and harvest (e.g. yield, grain humidity, protein concentration), were supplied by different information sources, for a total of 30 fields over 12 years.

For CERES-Wheat calibration, the data-set from the wheat variety trials carried out by ARSIA (Regional Agency for Development and Innovation in the Agro-forestry Sector), was used. The data were available for 10 years (1998-2009) on one field per year.

For model validation, the data-set from the field monitoring carried out by DIPSA (Department of Plant, Soil and Environmental Sciences - University of Florence) and CAPSI (Siena Provincial Agrarian Consortium), was used. The data were available over three growing seasons (2009-2011), for a total number of 20 fields (9 fields in 2009, 7 fields in 2010, 4 fields in 2011).

In all the fields of the provided data-sets, durum wheat (*Triticum turgidum L.* var. *durum*) cv. *Claudio* was grown. The cultivar *Claudio* is often used in the study area and it is well adapted to the local climate.

The crop was grown in a rainfed system with sowings carried out between the first decade of October and the last decade of January, using 350-450 seeds/m^2, for a final plant density of 250-500 plant/m^2. In agreement with the common cultivation protocol, the primary soil tillage was in autumn (ploughing at 30 cm depth), and, a standard plan was applied to protect the crop from pests and weeds. The amount of applied nitrogen was considerably different among the fields, ranging from 95 to 200 N units (kg/ha), splitted into two or three doses (one fertilization at sowing and two applications during the crop cycle).

CERES-Wheat was calibrated, starting from the default genotype 'Winter-Europe', using the yield and the timing of the crop development. An adjustment of the genetic coefficients was carried out on the basis of the best fit between the simulated and observed data for both yield and the onset of the main phenological stages.

The model accuracy was assessed in order to evaluate the reliability of the output for the following studies. The correlation analysis (set intercept = 0) between simulated and measured yields was performed and the following coefficients were computed: Relative Root-Mean-Squared Error (RRMSE) (Jørgensen et al., 1986) (Eq. 2), Modelling Efficiency (EF) (Nash and Sutcliffe, 1970) (Eq. 3), Coefficient of Residual Mass (CRM) (Loague and Green, 1991) (Eq. 4).

(2) $\text{RRMSE} = \frac{\sqrt{\frac{\sum_{i=1}^{n}(S_i - M_i)^2}{n}}}{\overline{M}} * 100$ (values range 0 / +∞; optimum = 0)

(3) $\text{EF} = 1 - \frac{\sum_{i=1}^{n}(S_i - M_i)^2}{\sum_{i=1}^{n}(M_i - \overline{M})^2}$ (values range −∞ / 1; optimum = 1)

(4) $\text{CRM} = \frac{\sum_{i=1}^{n} M_i - \sum_{i=1}^{n} S_i}{\sum_{i=1}^{n} M_i}$ (values range +∞ / −∞; optimum = 0)

where: *S* and *M* are the simulated and measured data, respectively, and *n* is the total number of observations.

7.4. Calibration and validation of a new routine for GPC simulation with CERES-Wheat

The performance of CERES-Wheat, calibrated and validated as described in the previous paragraph, was assessed for GPC simulation. The correlation analysis between the simulated and observed GPC was performed, using data from ARSIA and DIPSA-CAPSI data-sets. Moreover, RRMSE (Eq. 2), EF (Eq. 3) and CRM (Eq. 4) coefficients were computed. CERES-Wheat output related to grain nitrogen concentration (%) was simply converted in GPC (%), multiplying by a factor of 6.25.

Studies confirmed the role of the genetic differences among wheat species and cultivars, as intrinsic factors capable of affecting grain protein formation in different production conditions (Bhatia, 1975; Kramer, 1979; Johnson et al., 1985; Rostami and O'Brein, 1996; Jamieson et al., 2004). In particular, Cossani et al (2011) highlighted significant differences between ordinary wheat and durum wheat in relationship to the GPC. CERES-Wheat is set for ordinary wheat and it does not take into account the higher qualitative responsiveness of durum wheat. Therefore, a new grain protein routine was performed in order to minimize the errors in the simulation.

The rate and duration of both starch and protein grain accumulation are essentially independent events, controlled by different mechanisms and influenced by different factors (Jenner et al., 1991). The protein deposition in to the grain starts at beginning of grain filling stage, and occurs especially after 2 weeks from the start, during the 'linear phase' and 'maturity phase' of grain development (Vos, 1981).

Under adequate growing conditions, the rate and duration of protein deposition are determined mainly by factors of supply external to the grain. Therefore the GPC is mainly source-limited, depending on the total N content in the crop (Jenner et al., 1991; Jamieson and Semenov, 2000). The proteins are synthesized in the grain starting from amino-acids derived from catabolism of proteins in the vegetative organs (Asseng et al., 2002). Leaves and stems represent the most important reserves of N, with smaller contribution by glumes and roots (Dalling, 1985). Studies on wheat have found a positive relationship between GPC and the total leaf nitrogen in the late period, close to

the beginning of the grain filling stage (anthesis or two weeks after anthesis) (Wang et al., 2003, Huang et al., 2004; Li et al., 2005).

On this basis, for the new routine, the rate and duration of protein deposition in grain were assumed mainly source-limited and leaves and stems were considered as the available N sources.

The above ground biomass per hectare, simulated by CERES-Wheat at beginning of the grain filling stage, was converted in biomass per plant on the basis of a plants density of 500 plants/mq. Only stems and leaves were taken into account, not including the spikes.

Then, the total N available for the translocation in to the grain (TN) was assessed as the above ground biomass (g/plant), multiplied by the simulated nitrogen concentration in the stover (leaves and stems) at beginning of the grain filling stage (Weiss et al., 2006).

The size of the grain nitrogen sink (NS) was assessed equal to the grain weight increase per plant during the grain filling stage (Weiss et al., 2006). Therefore, NS was computed on the basis of the difference between the grain dry matter, simulated by CERES-Wheat, at the end and at beginning of the grain filling stage.

Finally, an additional factor was applied for GPC assessment, since Cossani et al. (2011) showed an average difference of 0.5 in the grain maximum nitrogen concentration between durum wheat (cv. *Claudio*) and common wheat in Mediterranean environment.

The final GPC was assessed following the equation 5.

(5) GPC ={(TN/NS*100)+ 0.5}*6.25

where: TN is the total N available for the translocation into the grain, NS is the size of the grain N sink, 0.5 is the additional factor due to the genetic difference between durum wheat and ordinary wheat, 6.25 is the conversion factor from nitrogen to protein.

The performance of the new routine was assessed, through the correlation analysis between simulated and observed data and the computation of RRMSE (Eq. 2), EF (Eq. 3) and CRM (Eq. 4) coefficients. The performances of the original and the new routine were compared, assessing the improvements due to the modified algorithm (Eq. 5) for GPC simulation.

7.5 Field trials

The field trials were set up over two growing seasons, 2009-2010 and 2010-2011, respectively, for a total number of 11 and 13 farms.

The ground data collected during the trials were used in the following analysis to validate the forecasting indices of yield and GPC.

In this context, the aim of the study was to validate the performance of operational tools in real cropping systems, for the forecast or description of durum wheat productions.

Therefore, the field trials represented a complex and heterogeneous environment to assess the capability of these tools to capture the main variables determining the harvest variability.

The field measurements were part of a farm production monitoring, rather than of an experimental design. The collected data were the result of the interactions among many environmental and agronomic variables (e.g. micro-climate conditions, field specific soil fertility, soil stoniness and hydrological properties, previous crop and rotation plans, plot exposure, elevation and slope, crop management, weed diffusion, damages due to strong wind, pathogenic attacks, wild pig invasions, etc.), which, in turn were characterized by temporal and spatial variability.

The fields crop management did not follow an experimental standard protocol. Different sowing date, plant density and fertilization plans were applied according with the agronomic practices commonly used by each farm. Moreover, the land plots differed for exposure, elevation and slope. The land plots were selected on the basis of three requirements: cultivation of durum wheat cv. *Claudio*, size enough large and central position in relationship to the pixel of MODIS imagery grid at 250 m spatial resolution.

The crop phenological monitoring was carried out in according with the BBCH-scale. Surveys were performed each 14 days through widely observations over each field.

From April to harvest, each 14 days, three plants samples were collected, each from an area of 1 m^2, following an diagonal scheme crossing the field (Fig.7.5.1). The dry weight of the above ground biomass was measured after oven drying (105 C° per 144

h), dividing leaves, culm, and ear. The number of plants per sample was counted to compute the average dry weight per plant.

At the end of the crop vegetative growth stage (at ear emergence, during the second half of April), five plants samples were collected, each from an area of 1 m^2, following an X scheme in each field (Fig.7.5.1). The plant LAI was measured with the support of an electronic planimeter (Delta-T, Dias II image analysis system, UK).

At grain maturity (during the first half of June), ten plants samples were collected, each from an area of 1 m^2, following an X scheme, with two repetitions, in each field (PHM) (Fig.7.5.1). The quality and quantity of the harvest were measured. Simultaneously, the production from the whole field was monitored with the measure of the same qualitative and quantitative harvest components (WHM). Therefore, two parallel data-sets were obtained. They were called punctual harvest measurements (PHM) and wide harvest measurements (WHM), respectively.

PHM were completed for 11 and 13 fields, in 2010 and 2011, respectively. For WHM, it was possible to collect yield data only for 9 and 6 fields, respectively in 2010 and 2011, and qualitative data for 8 and 9 fields, in 2010 and 2011 respectively.

In PHM, the yield (kg d.m./ha) was recorded through a precision mini-combine able to thresh an ear by separating the grain from the chaff. The percentage humidity of grain was assessed on the basis of the weight loss by sub-samples, after oven drying (105 C◦ per 144 h). In WHM the yield was recorded after the standard threshing operations over the field and the following storage, drying and weighing at local agrarian consortium (CAPSI).

In both PHM and WHM data-set, grain sub-samples were analyzed with the Infratec System 1241 Grain Analyzer. The average protein (GPC) and gluten concentrations (%), specific weight (Whl) and color, were measured.

All the data from PHM and WHM were checked, in order to assess the reliability and the representativeness of the measurements. Simple linear regression analyses were performed between the harvest components (grain yield, GPC, gluten concentration, kernel specific weight, color) and the crop growth variables (LAI, aerial biomass

weight, number of culms). The data subjected to exclusion because inconsistency or anomalous errors were detected.

Fig. 7.5.1 Sampling scheme. Legend: B = surveys about above ground biomass weight: three sampling areas of 1 m^2 each (diagonal scheme); L = surveys about plant LAI: five sampling areas of 1 m^2 each (X scheme); H = surveys about the quality and quantity of the harvest: ten sampling areas of 1 m^2 each (X scheme with two repetitions).

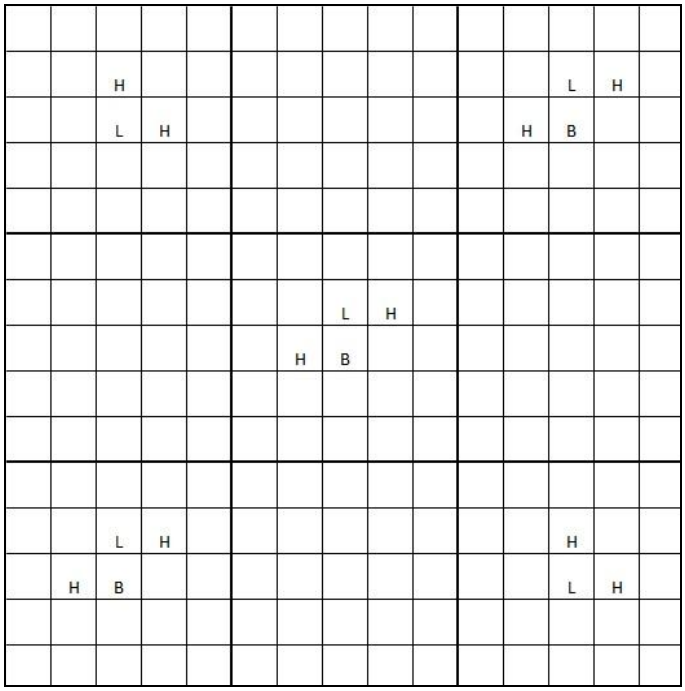

7.6 Long-term analysis: climate impact and LAI influence on harvest

The CERES-Wheat model, calibrated and validated as described in paragraph 7.3, was used to perform a long-term analysis over 56 growing seasons (years 1955-2011) in order to assess the main weather impacts during the key crop stages and the plant LAI influence on wheat harvest.

CERES-Wheat supported the study of the interactions in the 'plant-soil-atmosphere' system over many years. It allows to discern the weather impacts from the confounding influence of the technology development, contrary to an analysis based on historical crop production series.

The analysis of the crop responses to the weather conditions was carried out. Thanks to the support of crop modeling tools, the analysis was not influenced by typical weather patterns characterizing few growing seasons, contrary to a study based on field experiment data.

This proposed method represents an unexplored approach to set up a forecasting index of the crop production. It involves the use of a complex simulation model, such as CERES, to identify the main crop and weather variables that determine the quantity and quality of the harvest. Then, the identified variables are assimilated in a simplified forecasting index suitable for operational applications (paragraphs 7.7. and 7.8).

The model run over the years 1955-2011 using the meteorological database described in paragraph 7.2., and the soil profile described in table 7.3.1

The crop management was set up, for all the years, according with the protocol widespread in Val d' Orcia. A total N amount of 140 kg/ha, splitted in three times (26 N units at sowing, 57 N units at 80 days after sowing and 57 N units at 130 days after sowing) was included. The sowing date was simulated automatically by CERES at optimum soil condition (soil temperatures between 2-37 °C and soil water content between 40-100%) within the more common sowing window adopted by the local farms. Therefore, the sowings were simulated from the first decade of November to the last decade of December, excluding the earlier (in October) and later (in January)

periods. The model set the harvest time automatically when the grain maturity was reached.

The yields (kg d.m./ha) simulated by CERES-Wheat were directly taken into account, while the GPC were assessed over the 56 growing seasons following the new routine described by the equation 5 in paragraph 7.4.

The correlation analysis was performed between the monthly meteorological indices (Tab. 7.2.1) and both yield and GPC.

Similarly, the correlation analysis was carried out between plant LAI, simulated at the end of the vegetative growth stage, and the harvest components (yield and GPC).

The relationships was assessed as significant at $P \leq 0.05$, at $P \leq 0.01$ and at $P \leq 0.001$.

The trends of the meteorological indices and crop harvest (yield and GPC) were analyzed over the years 1955-2011.

7.7. Multiple regression analysis to set up forecasting indices for yield and GPC

A multiple regression analyses were performed using the simulated data over the years 1955-2011 (paragraph 7.6), in order to set up forecasting indices on the basis of the main crop and weather variables able to provide an early assessment of the harvest.

Two multiple regression models were set up, taking into account as dependent variable yield and GPC, respectively.

The monthly meteorological index, resulting with higher correlation with the harvest components (yield and GPC) (paragraph 7.6), was selected as independent variable in the multiple regression models. Only the meteorological indices of March and April were taken into account, with the aim to provide information about the harvest before the grain filling stage.

CERES simulated for the years 1955-2011 the shift from the vegetative growth stage to the reproductive phase between mid-April and end April. In this period the simulations showed the maximum values of LAI reached by the crop (paragraph 7.6).

Many studies have shown that LAI covers a critical role in determining wheat production. LAI was found strictly related to crop fPAR (Hipps et al., 1983, Gardner et al., 1985, Green, 1987), which in turn significantly affects the biomass growth and yield (Gardner et al., 1985; Wilson and Jamieson, 1985; Green, 1987; Regan et al., 1992, Mitchell et al., 1993; Mearns et al., 1997; Kang et al., 2002; O'Connell et al., 2004; Dalirie et al., 2010).

Then, the LAI value reached at the end of the plant vegetative growth (LAI_{april}) was selected as second independent variable. Previously, the existence of a significant correlation between LAI_{april} and the harvest components (yield and GPC) were established, as well as the absence of autocorrelation with the other independent variable.

A stepwise multiple linear regression analysis was performed with the support of SPSS (version 18) statistical software. The multi regression model described by the equation 6 was detected.

$$(6)\ Y = \beta_0 + \beta_1 * X_1 + \beta_2 * X_2$$

where: Y is the dependent variable (yield or GPC), β_0 the intercept value, and β_1 and β_2 the regression coefficients of the predictor variables X_1, the meteorological index (climate component), and X_2, the LAI_{april} (crop component), respectively.

7.8. The forecasting indices validation

The performances of the multiple regression models (paragraph 7.7) were assessed as forecasting tools of durum wheat harvest.

The equation 6 was validated with ground measured data. On this basis, it was evaluated the capability of the meteorological index and LAI_{april} to summarize the impact on the harvest, due to the combined effects and interactions among many environmental variables.

The meteorological indices computed over the growing seasons 2009-2010 and 2010-2011(paragraph 7.2), and the measured LAI_{april} during the field trials (paragraph 7.5), were implemented in the equation 6 in place of X_1 and X_2, respectively.

The yield and GPC assessed by the multiple regression models were compared with the observed data through a linear regression analysis. Moreover, the following coefficients were computed: RRMSE (Eq. 2), EF (Eq. 3) and CRM (Eq. 4).

For GPC, it was necessary to assess the performance of the forecasting index in relationship to different values ranges measured for plant LAI at field level.

About this, the validation of the multi regression model (Eq. 6) was performed separately for fields having LAI value within the intermediate range 0.9 - 1.8 (ILAI group), and for fields with LAI values below 0.7 or above 2 (ELAI group).

The correlation analysis between GPC and yield was carried out separately for ILAI and ELAI, in order to understand the non-linear relationship between GPC and LAI_{april}.

8 RESULTS AND DISCUSSION SECTION 1

8.1. CERES-Wheat calibration and validation for durum wheat yield

The CERES-Wheat model calibrated and validated to simulate durum wheat production showed highly significant correlation ($P \leq 0.001$) between observed and simulated yield ($R^2 = 0.7$; set intercept = 0) (Fig. 8.1.1).

The results showed a moderate general error (RRMSE RRMSE = 20 %), a model efficiency close to the optimum (EF = 0.7) and a weak error for under-estimation (CRM = 0.07). The results showed the good capability of CERES in the simulation of durum wheat yield.

Fig. 8.1.1 Liner regression between grain yield simulated by CERES-Wheat and observed in ARSIA (Δ) and CAPSI-DIPSA (□) data-sets, used for model calibration and validation, respectively.

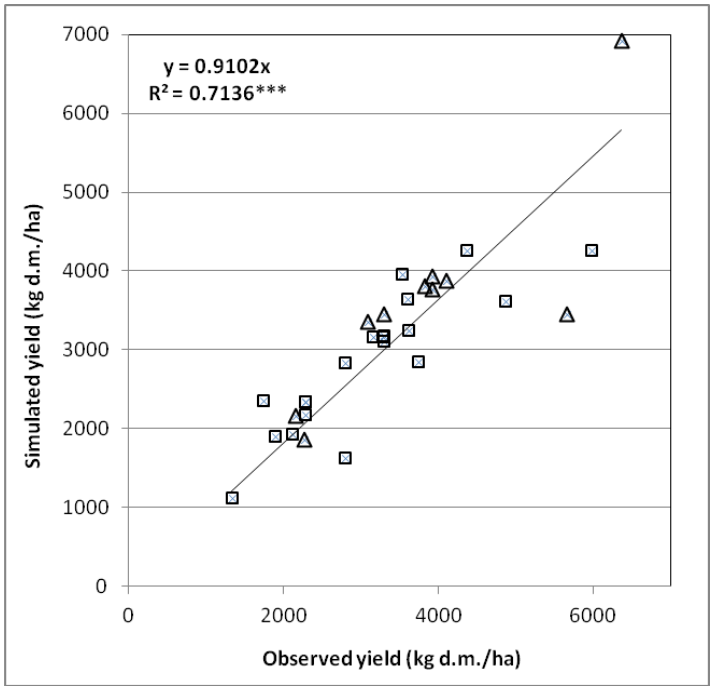

8.2. Calibration and validation of a new routine for GPC simulation with CERES-Wheat

Table 8.2.1 shows the performances of the original CERES-Wheat routine and the new routine in GPC simulation. Both routines showed highly significant correlation ($P \leq 0.001$) between the observed and simulated data (Fig. 8.2.1 and 8.2.2).

However, compared to the CERES-Wheat routine, the new grain protein routine led to an increase of R^2 from 0.3 to 0.4, a reduction of RRMSE of 10.75 %, an improvement of EF of 4.39 % and a decrease of CRM of 64.79 %.

Despite the significant R^2 and the EF close to the optimum, CERES-Wheat showed a high general error (RRMSE), in part due to the solid error of under-estimation (CRM).

The results showed that the new routine was able to take into account the higher responsiveness of durum wheat compared to ordinary wheat in term of GPC (Cossani et al., 2011). The improvements were mainly due to the considerable reduction of general error and under-estimation error.

Finally, compared to the yield, CERES-Wheat showed lower reliability in the simulation of the spatial and temporal variability of GPC. Indeed, despite the EF close to the optimum, in both routines the model showed a R^2 lower than that shown for the yield. These results are in agreement with the scientific literature on the current complex simulation models. The studies highlight that the crop models were able to provide reliable information on wheat harvest quantity, while less accurate assessment of harvest quality (Otter-Nacke et al., 1986; Asseng et al., 1998; Meinke et al., 1998; Asseng et al., 2002).

Tab. 8.2.1 Performance of the original CERES-Wheat routine and the new routine in GPC simulation.

	R^2	*RRMSE*	*EF*	*CRM*
CERES routine	0.35 **	26.33	0.93	0.23
New routine	0.42 **	15.58	0.98	0.08

Fig. 8.2.1 Liner regression between GPC simulated by CERES-Wheat and those observed.

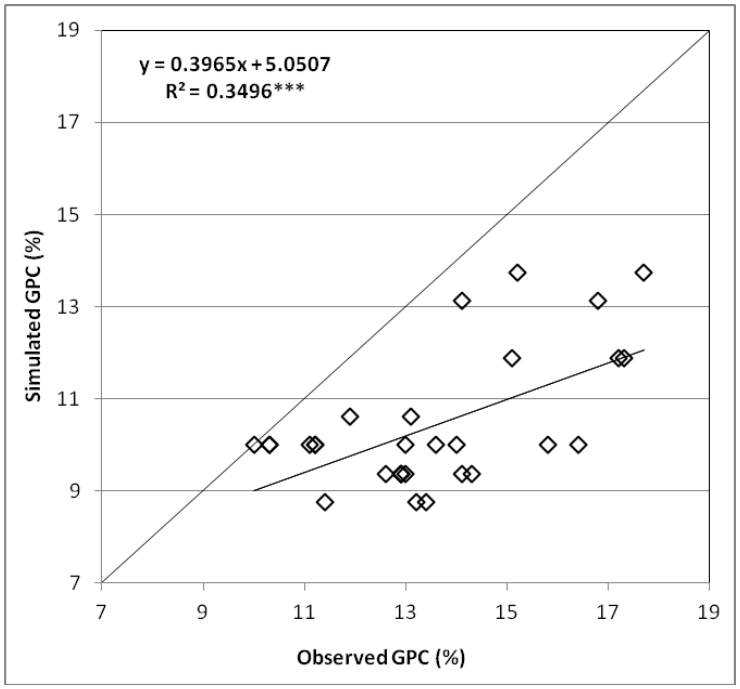

Fig. 8.2.2 Liner regression between GPC simulated by the new routine and those observed.

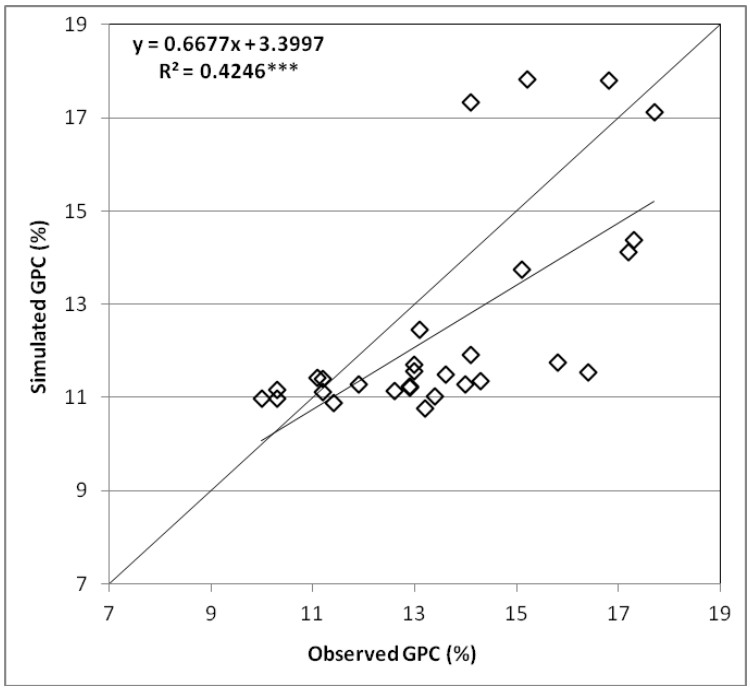

8.3 Field trials: GPC and yield

The correlation analysis over 14 observations that were common to PHM and WHM showed a significant correlation ($P \leq 0.05$) between the yield measurements (Fig. 8.3.1). Despite this, the value of R^2 was low ($R^2 = 0.3$). PHM data over-estimated the yield compared to WHM data.

Fig. 8.3.1 Liner regression between yield from PHM and WHM data-set.

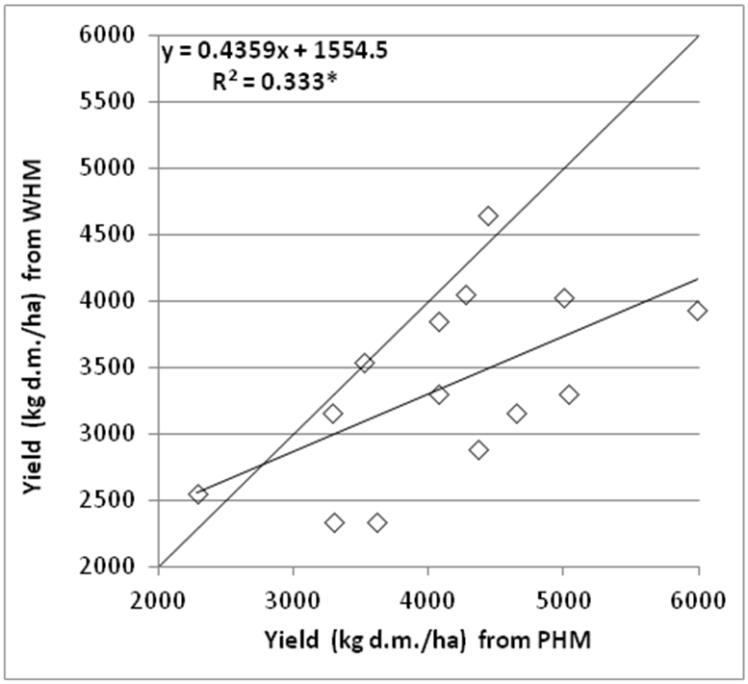

- This result can indicate grain losses during the traditional harvest practices over the whole field supported by common threshing machine, with the higher accuracy of PHM data resulting from a more careful harvest.
- On the other hand, a high spatial variability of grain yield within the same field could be at the basis of the disagreement between PHM and WHM. The differences between two data-sets can indicate a high deviation of each sampled sub-plot from the average of the whole field.

The correlation analysis over 14 GPC observations that were common to PHM and WHM, showed better results, compared to yield. Higher significant correlation ($P \leq 0.001$,) and R^2 value ($R^2 = 0.7$) were found between the two type of measurements (Fig. 8.3.2).

Fig. 8.3.2 Liner regression between GPC from PHM and WHM data-set.

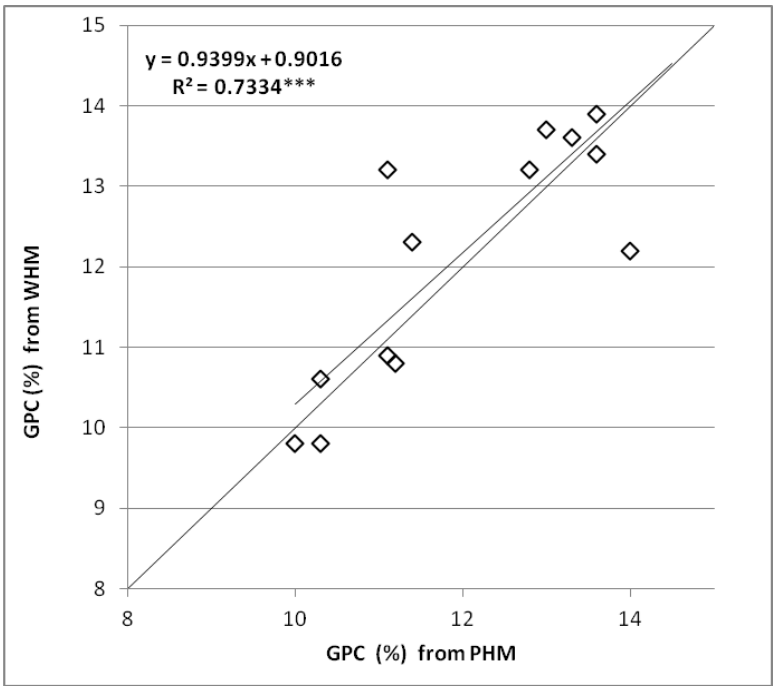

- The agreement between punctual and wide measurements can suggest a less intra-field spatial variability of GPC compared to yield. The yields may have been more affected by the micro-local environment (e.g. response of the single plant genotype to the site-specific soil fertility and micro-climate conditions), while the GPC may has been more determined by the macro-local environment.
- On the other hand, these results can suggest that GPC data simply were not affected by the measurement errors due to careless harvest during of the wide surveys. Indeed, the quality properties of the grain do not change even if the production is affected by grain losses.

However, this topic deserves further studies. If the first hypothesis is true, the GPC of durum wheat may be characterized by a higher predictability, compared to the yield. This can make easier the forecast of the harvest quality through simple models.

Both PHM and WHM showed on average lower GPC and higher yield in 2010 compared to 2011 (Fig. 8.3.3 and 8.3.4). These results pointed out the inverse tendency between the annual harvest quantity and quality for durum wheat grown in the study area. This result is in agreement with the scientific literature on wheat. The negative correlation between yield and GPC is well-established by many studies (Spiertz, 1977; Johnson et al., 1985; Fischer et al., 1993; Feil, 1997; Novaro et. at, 1997; Rharrabti et al., 2001a; Rharrabti et al., 2001b). The inverse relationship between the two harvest components is emphasized more in durum wheat compared to common wheat (Cossani et al., 2011). In durum wheat an increase of grain weight is accompanied by a higher pronounced decrease of N percentage of the grain (Cossani et al., 2011).

PHM data-set confirmed the highly significant and negative correlation ($P \leq 0.001$) between yield and GPC ($R^2 = 0.6$) (Fig. 8.3.5). No significant correlation was found on WHM data. This discrepancy with the results shown in the scientific literature confirmed the possible presence of anomalies or inaccuracies about the yield data in WHM data-set.

On the basis of these results, PHW data were assessed more reliable and consistent, compared to WHM. For this reason PHW data-set was used in the following studies.

Fig. 8.3.3 Annual average of yield recorded by PHM and WHM.

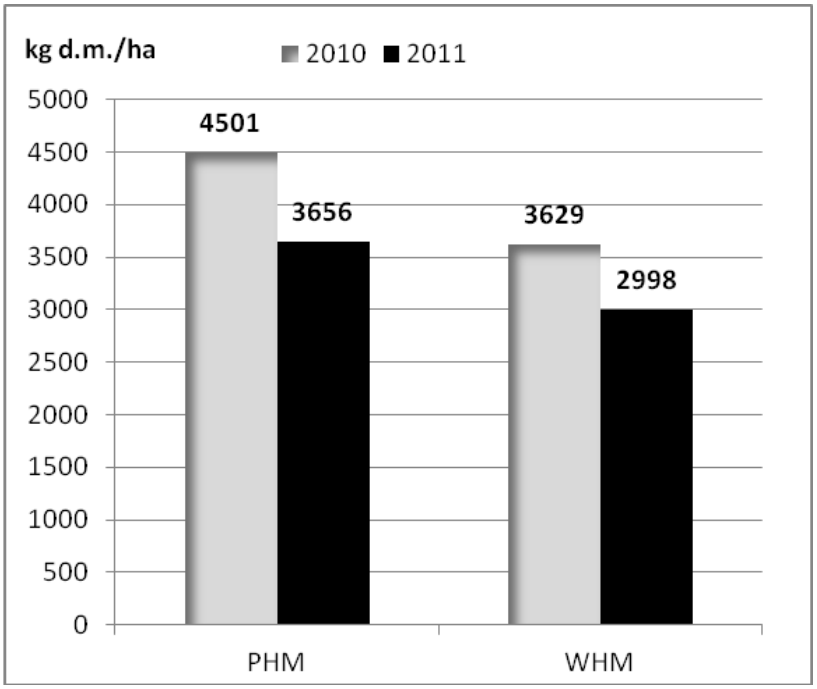

Fig. 8.3.4 Annual average of GPC recorded by PHM and WHM.

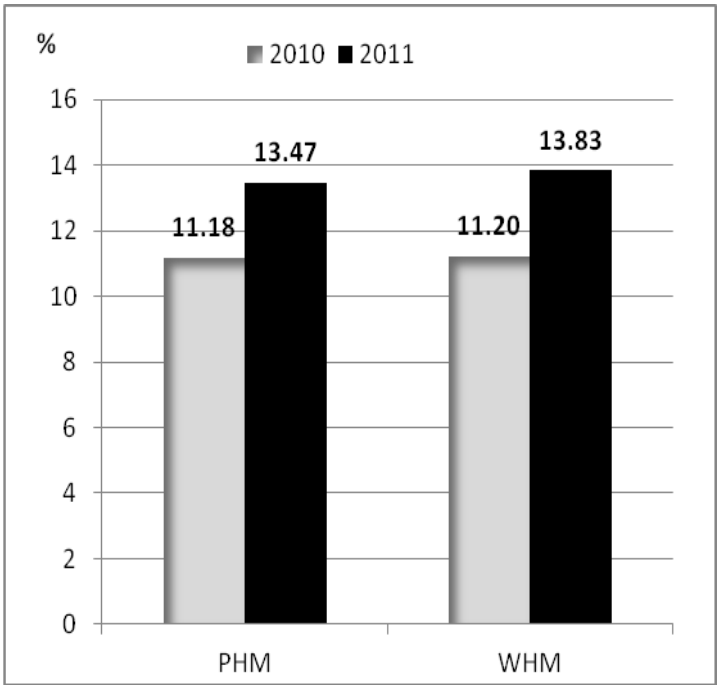

Fig. 8.3.5 Liner regression between GPC and yield of PHM data-set.

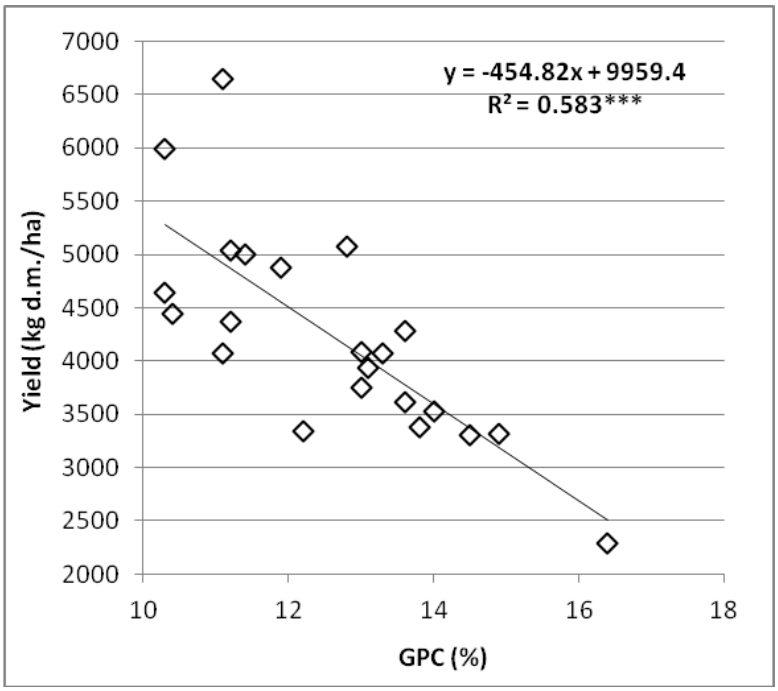

8.4 Field trials: other grain quality parameters

Contrarily to expectations, no correlations between the grain specific weight and yield, as well as between grain specific weight and GPC, were found in both PHM and WHM. These results suggest that the collected data of grain specific weight are not consistent. Therefore, harvest component was not taken into account for the following analysis.

PHM and WHM showed a similar average of grain gluten concentration, with lower value in 2010 compared to 2011 (Fig. 8.4.1). In WHM, the gluten averaged 65.28 % of the total grain protein, with a minimum and maximum, of 51 % and 74% of GPC respectively. Similarly, in PHM, the gluten averaged 68.63 % of GPC, with values ranging within 59–77 %.

Both PHM and WHM showed highly significant correlation ($P \leq 0.001$) with $R^2 = 0.97$ (Fig. 8.4.2) between GPC and gluten concentration. Since there was close agreement between the two variables, including the gluten concentration for the following studies was considered needless.

As expected, PHM showed highly significant correlations ($P \leq 0.001$) between grain color and GPC ($R^2 = 0.56$), and between grain color and gluten concentration ($R^2 = 0.60$). No correlation was found in WHM due to the presence of anomalies or inaccuracies in the data-set.

On the basis of these results, the PHW data were assessed more reliable and consistent for the following studies compared to WHM.

Fig. 8.4.1 Annual average of grain gluten concentration recorded by PHM and WHM

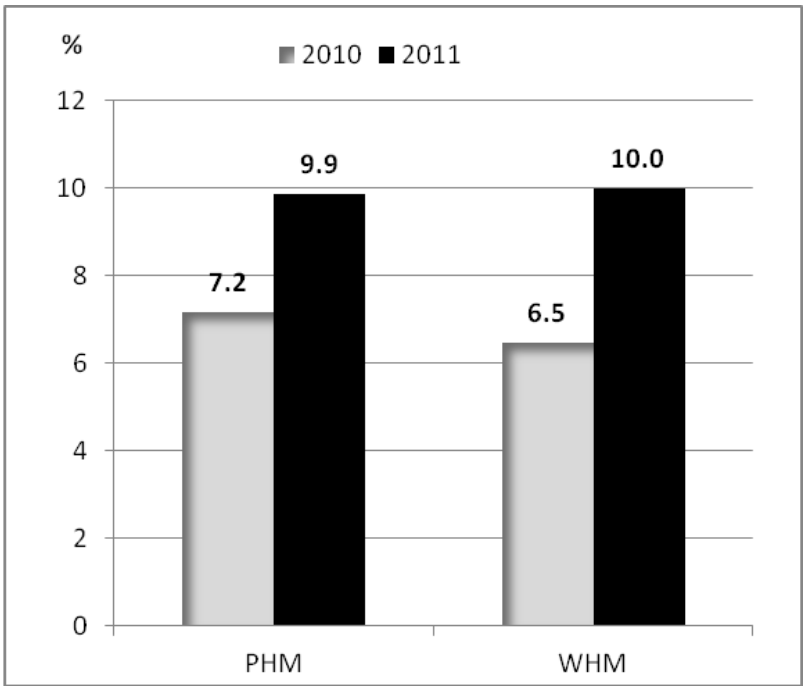

Fig. 8.4.2 Liner regression between GPC and grain gluten concentration of PHM data-set.

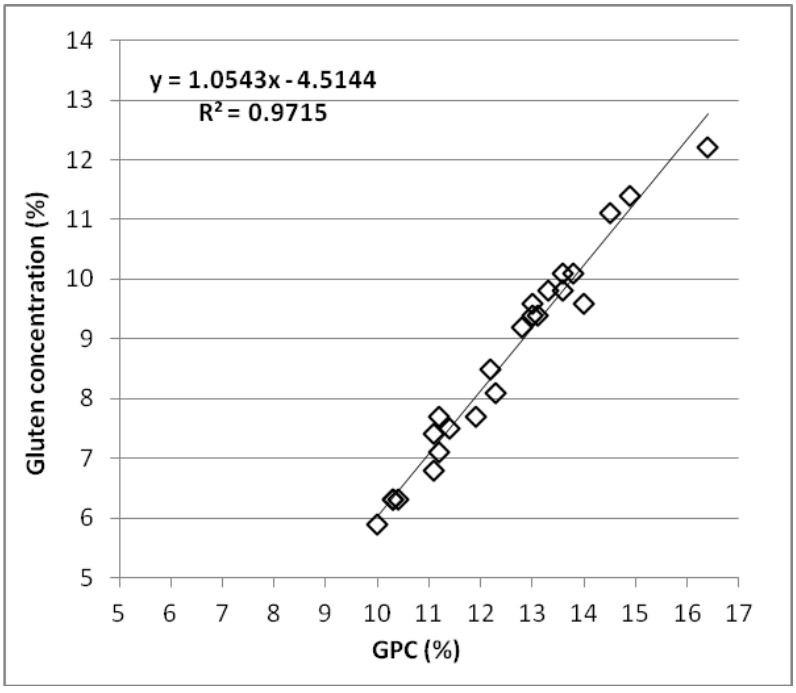

8.5 Field trials: harvest and the crop growth parameters

In PHM, both yield and GPC were found significantly correlated with LAI in April ($P \leq 0.01$), showing a positive and negative relationship, respectively. The yield showed positive correlations with the leaves weight in April and May ($P \leq 0.01$), as well as with the total aerial biomass in May and June ($P \leq 0.01$). Negative correlations were found between GPC and leaves weight in April and May ($P \leq 0.05$), as well as with the total aerial biomass in May ($P \leq 0.01$).

These results showed that the crop LAI and leaves weight can provide early information about the final harvest, beginning in April, for both grain yield and GPC. On the other hand, the total aerial biomass was able to describe the harvest in the later period of the crop cycle, beginning in May.

Regarding WHM, no correlations were found between the harvest components (yield and GPC) and plant LAI or biomass.

About this, it is necessary to take into account that in PHM the measurements on plant LAI and biomass, and the final surveys on harvest, followed a similar X scheme of sampling (Fig. 7.5.1). Therefore, in PHM the data on crop growth and harvest were collected in close sub-plots and, thus, in field areas quite homogeneous. The fact that no correlations between the punctual growth measurements and the wide harvest measurements were found suggests a large variability of LAI and biomass within the same field.

In WHM, highly significant correlations were found between the number of culms in May and both yield ($P \leq 0.01$) and GPC ($P \leq 0.001$). However, no correlations were found between yield or GPC and the number of culms in PHM. These results can suggest that it was not possible to recognize a significant influence of the plant density on the site-specific harvest over a relatively small sample of plants. The impact of the plant density became noticeable in the large-scale measurements related to the total harvested quantity in each field.

8.6 Long-term study: climate impact and LAI influence on harvest

The trends simulated for yield and GPC, as well as the trends recorded for the monthly meteorological indices were not significant over the 56 years (data not shown).
Table 8.6.1 shows the results about the effect of plant LAI and weather conditions on durum wheat harvest. On the basis of the long-term analysis with CERES-Wheat, the crop performance resulted significantly affected by weather conditions and influenced by crop leaf development.

Tab. 8.6.1 Correlations between harvest (grain yield and GPC) and meteorological indices and plant LAI. Legend: positive (+), negative (−), no significant (n.s.), significant at $P \leq 0.05$ (*), significant at $P \leq 0.01$ (**), significant at $P \leq 0.001$ (***).

Weather variable	***GPC***			***Yield***		
	March	*April*	*May*	*March*	*April*	*May*
MTMAX (°C)	n.s.	n.s.	+*	ns	ns	ns
MTMIN (°C)	− **	− *	n.s.	ns	ns	− *
TP (mm)	− ***	− *	−*	+ ***	ns	+ *
WD (warm days)	n.s.	n.s.	+ *	ns	ns	− *
DD (drought days)	+ ***	+ *	+**	− ***	ns	− *
Crop variable	*April*			*April*		
LAI	+ ***			+ ***		

8.6.1. Weather impacts on yield

March and May were found to be the critical periods influencing the yield. The crop development stages of 'tillering' and 'grain filling' occur in March and May respectively. The weather conditions in April, corresponding to the period 'from stem elongation to ear emergence', did not show significant correlation with yield.

- The crop yield was positively affected by the rainfall in March, underlining highly significant correlations with TP and DD (Tab. 8.6.1).

These results showed the relevance of water availability for the crop during the early growth stage. During this period the leaves grow, lengthening the sheaths, the number of tillers, and the final plant density are established (Miller, 1992). The number of potential spikelets per spike are also set (Miller, 1992). Therefore, since the survival of numerical components of wheat grain per m^2, such as tillers and spikelets, is positively related with the final yield (Slafer and Whitechurch, 2001; Gonzalez et al., 2005; Fischer, 2011), a favorable water supply at tillering stage can promote the harvest quantity.

The negative impact on wheat yield due to water stress during the seedling stage was shown by different studies (Zhang et al., 1998; Guttieri et al., 2001; Zhang et al., 2004; Dalirie et al., 2010; Li at al., 2010). The lack of rainfall over this period was pointed out as the major cropping risk to wheat producers in Mediterranean environment (Dalirie et al., 2010).

As a consequence of drought conditions at early development stages, wheat shows smaller leaf area growth, with a reduction of the upper leaves size and of the leaf area index (Zhang et al., 1998; Guttieri et al., 2001). On the other hand, the water availability at tillering stage supports early vigour of the seedling, that has a key role in determining the crop performance.

The plants with larger leaves and higher number of tillers reach higher growth rates and green area index, involving a large degree of ground cover and high light interception (Regan et al. 1992). High values of LAI support the plant ability to accumulate green biomass through the photosynthesis, and higher availability of stored nutrients for the grain filling stage (Regan et al., 1992).

Therefore, favorable water supply at tillering stage results in higher yield (Regan et al., 1992). On the other hand, water stress over this period involves the inability of wheat to produce adequate dry matter (Regan et al., 1992) and it causes lower grain weight, less grains per spike, and, thus, lower yield (Zhang et al., 1998; Guttieri et al., 2001).

- Significant correlations between yield and MTMIN and WD, on one hand, and with DD and TP, on the other hand, were found in May (Tab. 8.6.1),

The grain filling stage was pointed out as another critical period for durum wheat. During this period the crop production was negatively affected by drought and warm conditions.

At grain filling stage, the nutrients move from vegetative organs to grains, and, the final kernel mass is determined (Miller, 1992). In particular, the starches, that represents between 60% and 75% of the final dry weight (Hurkman et al., 2003), are synthesized and accumulated in grain from soluble carbohydrates stored in stems, spikes and leaves (Spiertz and Van De Haar, 1978; Van Herwaarden et al., 1998).

The starch translocation and deposition in the grain appear to be particular sensitive to adverse environmental conditions (Campbell et al., 1981; Bhullar and Jenner, 1985; Garcia del Moral et al., 1995; Fernandez-Figares et al., 2000; Rharrabti et al., 2001a). Drought and warm conditions, during the grain development, result in yield decrease.

High temperatures, in accordance with the thermal time concept, shorten the duration of grain filling phase, reducing the available period for the deposition of nutrients in to the grain. Therefore, warm conditions during this stage result in smaller kernel weight and lower yield (Wardlaw et al., 1980; Al-Khatib and Paulsen, 1984; Slafer and Rawson, 1994; Stone et al., 1994; Wheeler et al., 1996).

Similarly, water stress imposed during the grain filling stage reduces the grain weight, which in turn leads to a significant decrease of yield (Kobata et al., 1992; Zhang et al., 1998; Eitzinger et al., 2003).

Despite this, at grain filling stage, the correlations between the meteorological indices and GPC did not show high values of R^2. This.

On one hand, these results suggest a smaller contribution to the yield of the weather effects during grain filling stage, compared to the weather impacts during the previous periods. For example, some studies pointed out that water deficit conditions during grain filling stage limit the production less severely compared to weather stresses that occur during the other crop stages (Zhang et al., 2004; Zhang and Oweis, 1999; Li et al., 2010).

On the other hand, the lack of highly significant correlations can be explained by the fact that an increase of temperatures and water deficit has also a positive influence on the grain filling processes underlying the final crop performance.

Higher temperatures shorten the duration of the grain filling stage, but on the other hand, they promote the grain growth rate. In fact, there is a positive correlation between temperature and the increase of grain weight (Sofield et al., 1977; Angus et al., 1981; Hunt et al., 1991; Jenner, 1991; Wardlaw and Moncur, 1995).

However, the net final result of the warm conditions was negative for the yield, since the increase of the grain growth rate was not able to compensate the negative impact due to the shorter grain filling period.

Similarly, a mild water stress can promote the biosynthesis and accumulation of starch in the grain, involving higher grain weight and yield, compared to a favorable water supply and a severe water deficit (Zhao et al., 2009). Moreover, the negative impact of the water stress can be conditioned by the contributory presence of thermal stress. After the first 14 days from anthesis, the drought conditions can be not able to negatively affect the yield, unless they are associated with high temperatures (Gooding et al., 2003). Therefore, water deficit during the grain filling stage does not always involve a yield decrease, since the significance of its impact depends on the intensity of the water stress and the concurrent presence of thermal stress.

- In April, the durum wheat did not show significant correlations with the meteorological indices (Tab. 8.6.1).

These results can be explained by the fact that during the vegetative growing season the combined effect due to the concurrent presence of both thermal and water stresses can lead to opposite results than those due to the individual impacts of these weather constraints. The simultaneous occurrence of both high temperatures and water deficit can potentially improve the final harvest (Van Ittersum et al., 2003; Xiao et al., 2008). In fact, warm and drought conditions during the crop cycle involve an early flowering, shifting the grain filling stage in a period less warm and drought (Van Ittersum et al., 2003; Xiao et al., 2008).

8.6.2. Weather impacts on GPC

The weather conditions at all crop stages significantly affected the final GPC.

- The significant correlations between GPC and TP and DD, found in March, April and May (Tab. 8.6.1), pointed out that the grain quality was severely influenced by the amount and distribution of the rainfall. Low precipitation, from early growth stage to the grain filling stage, had a positive effect on GPC.
- The negative correlation in March and April between GPC and MTMIN showed that cold conditions during the vegetative growth stages, from tillering to ear emergence, were able to promote the GPC.
- On the other hand, the grain protein accumulation was furthered by warm temperatures during the grain filling stage, on the basis of the positive relationship with MTMAX and WD) (Tab. 8.6.1).

In general, weather conditions that adversely affect the yield are able to enhance the GPC on the basis of the well-established negative relationship between yield and GPC (Spiertz, 1977; Johnson et al., 1985; Fischer et al., 1993; Feil, 1997; Novaro et. at, 1997; Rharrabti et al., 2001a; Rharrabti et al., 2001b).

During the grain filling stage, warm and water deficit conditions involve a general decrease of the photosynthesis activity, grain growth rate, and the grain filling duration. However, these weather stresses affect the starch accumulation in the grain more than that of the protein, resulting in a relatively increase of GPC (Bhullar and Jenner, 1985; Garcia del Moral et al., 1995; Fernandez-Figares et al., 2000; Troccoli et al., 2000; Rharrabti et al., 2001a; Zhao et al., 2009).

Similarly, drought and cold weather during the growing season can negatively affect the yield, and then positively the GPC. Many studies found a reduction of rainfall during the wheat growing season associated to an improvement of GPC, since the water stress tends to reduce the kernel size and weight, involving a relative increase of GPC (Troccoli et al., 2000; Rharrabti et al., 2003a; Rharrabti et al., 2003b; Ludwig and Asseng, 2006; Rharrabti et al., 2003b; Erekul and Köhn, 2006; Orlandini et al., 2011).

- The more significant correlations between GPC and rainfall were found in March. The results pointed out the key role of drought conditions at tillering stage to improve the GPC.

As viewed in the previous paragraph (8.6.1), the water availability during this period has a key role in determining the crop yield. Water deficit at tillering stage involves lower leaf area growth, which in turn results in lower light interception and biomass accumulation, and, finally, in a yield decrease (Regan et al., 1992; Zhang et al., 1998; Guttieri et al., 2001). Therefore, on the basis of the inverse relationship between GPC and yield, the water conditions during the early period have an important impact also on GPC.

- Unlike to grain filling stage, during the vegetative growth period the GPC was supported by low temperatures.

The scientific literature showed clear results about the temperature effect on GPC during the grain filling stage. Despite this, studies of the impact of temperature during the pre-anthesis period, show inconclusive results, especially when long-term analyses are taken into account. On one hand, a positive impact on GPC of a temperature rise over the wheat growth cycle was found (Erekul and Köhn, 2006; Campbell et al.; 1981). On the other hand, Orlandini et al. (2011) did not find significant correlation between GPC and the average monthly temperature. Similarly, Smith and Gooding (1996) and Garrido-Lestache et al. (2005) showed that the temperatures in pre-anthesis period were not able to explain the GPC temporal or spatial variability. Ludwig and Asseng (2006) suggested that higher temperatures could involve both an increase and a decrease of GPC. The authors showed that under wet conditions, higher temperatures increased GPC, but at a lower rainfall regime, the warmer climate was able to reduce GPC.

Therefore, the literature shows disagreement among the results about temperature impact on GPC. This can be explained on the basis of the different directions of the temperature effect on crop growth and yield.

On the one hand, higher temperatures cause the shortening of all crop stages (Batts et al, 1998a; Batts et al, 1998b; Lawlor and Mitchell, 2000), resulting in smaller period

available for the plant growth, and then in lower yield. Therefore, when this latter is the prevailing effect, the rise of temperature results in an increase of GPC.

On the other hand, a temperature rise involves an increase of the biomass growth rate (Lawlor and Mitchell, 2000). This effect of temperature on photosynthesis activity of wheat is smaller at values below 5 °C, and it rises with the temperature until an optimum around 25 °C (Lawlor and Mitchell, 2000). Therefore, low minimum temperatures during the key periods for the plant biomass development, such as tillering and steam elongation stages, can hinder the crop growth rate. Therefore, cold conditions cause a lower accumulation of green biomass. On the basis of mechanics similar to that previously described, the reduction of the crop capacity to produce adequate leaf area or dry matter result in lower quantitative performance at harvest. Therefore, when this is the prevailing effect, a decrease of temperature results in an increase of GPC.

8.6.3. LAI effect on yield and GPC

The long-term study supported by CERES-Wheat showed positive and highly significant correlations ($P \leq 0.001$) between LAI in April, at the end of the vegetative growth stage, and both yield and GPC.

The significance of the correlation between crop LAI and harvest was clearly expected in relationship to the simulation dynamics adopted by CERES, as well as by the other complex models. CERES takes into account that LAI ris a key parameter to describe and explain the crop growth and productivity. The amount of leaves in the canopy is a factor in determining the quantity of intercepted light and absorbed carbon dioxide, which in turn control the photosynthesis rate (Monteith and Unsworth, 1990).

- LAI and yield: a positive correlation was found between LAI in April and yield.

CERES-Wheat computed the dry matter accumulation as a linear function based on photosynthetically active radiation intercepted by the canopy (fPAR). fPAR is assessed as an exponential function of LAI. The simulated yield depends on the supply of dry matter for grain filling, from direct photosynthesis or re-translocation of pre-stored dry matter in vegetative tissues (Ritchie et al., 1985).

This simulation dynamic is in agreement with the results from the field data analysis (paragraph 8.5). The observed data showed a positive and highly significant ($P \leq 0.01$) correlation between yield and LAI in April, the leaves weight in April and May ($P \leq 0.01$) and the total aerial biomass in May and June.

The basis used by CERES to simulate the yield is confirmed also in studies that analyzed the LAI effect on yield in an indirect way, through the relationship between yield and RS vegetation indices.

The RS vegetation indices are based on the ratio between NIR/RED. RED reflectance decreases with increasing contents of chlorophyll, and NIR reflectance increases with rising LAI and vegetative coverage (Beck et al., 2007). Therefore, the vegetation indices provide a description of the canopy LAI (Asrar et al., 1984; Benedetti, 1993; Haboudane et al., 2004; Casanova et al., 1998). In particular, in wheat, they were found strongly related to above ground dry matter accumulation, green leaf biomass and LAI

(Tucker and Holben, 1981; Serrano et al, 2000; Zhao et al., 2005; Tilling et al, 2007; Yi et al., 2008; Aparicio et al., 2002).

The positive correlation between vegetation indices and wheat yield was confirmed in many research papers (Quarmby et al., 1993; Hamar et al., 1996; Serrano et al., 2000; Ren et al., 2008; Becker-Reshef et al. 2010). In agreement with our results, the optimal timing to assess the wheat yield was the period of maximum green canopy cover, which generally occurs about 40 days before grain maturity, at the end of the vegetative growth stage (Tucker et al., 1980; Mahey et al., 1993; Quarmby et al., 1993; Aparicio et al.; 2002; Freeman et al., 2003; Basnyat et al., 2004; Marti et al., 2007; Ren et al., 2008; Becker-Reshef et al., 2010).

- LAI and GPC: a positive correlation was found between LAI in April and GPC.

In most of the complex crop models, including CERES-Wheat, the crop GPC is based on N uptake by the plant, which in turn is estimated on the basis of soil N availability and crop demand. The crop demand is determined in relationship to the leaf biomass or leaf area expansion. Therefore, the major influence of nitrogen shortages on production is through control of green leaf area (Jamieson and Semenov, 2000).

This simulation dynamic is based on the assumption that the rate and duration of protein deposition are determined mainly by factors of supply external to the grain. Therefore, GPC is mainly source-limited and depends on the total N content of the vegetative biomass (Jenner et al., 1991; Jamieson and Semenov, 2000). Studies confirmed that wheat leaves are the main source of amino-acidis for grain protein synthesis (Dalling, 1985) and a positive relationship was found between GPC and the total leaf N at anthesis (Wang et al, 2003, Huang et al., 2004; Li et al., 2005).

Nevertheless, these results are not in agreement with those from the correlation analysis on the field data (paragraph 8.5). The observed data showed a negative relationship between GPC and LAI in April ($P \leq 0.01$), leaves weight in April and May ($P \leq 0.05$) and the total aerial biomass in May ($P \leq 0.01$).

High LAI values can improve the N availability for the protein deposition in the grain and, then, promote the GPC. However, on the other hand, the positive relationship between crop LAI and yield was definitive. Therefore, on the basis of the well-

established negative correlation between yield and GPC (Spiertz, 1977; Johnson et al., 1985; Fischer et al., 1993; Feil, 1997; Novaro et. at, 1997; Rharrabti et al., 2001a; Rharrabti et al., 2001b), high LAI values, promoting the yield, can involve a GPC decrease.

Generally, the complex simulation models are able to provide a good simulation of yield, but not as much of GPC. This suggests that the current algorithms for GPC simulation need to be revisited and that a diagnostics to trace the deficiencies of the models must be carried out (Otter-Nacke et al., 1986; Asseng et al., 1998; Meinke et al., 1998; Asseng et al., 2002).

Therefore, the disagreement between the results from the analysis of field data and CERES-Wheat analysis can be explained by a deficiency of the model in fully capturing the interaction between LAI, GPC and yield. The results suggest that CERES-Wheat has failed to simulate the impact of yield variations on GPC.

The assumption about the failure of LAI in promoting GPC is supported by the contrasting results, shown in literature, about the relationship between wheat GPC and RS indices. The positive and significant correlation between LAI described by RS data and GPC was not fully confirmed.

Some authors found a positive relationship between RS indices and GPC (Basnet et al., 2003; Reyniers et al., 2006; Xue, 2007; Li et al., 2012). Despite this, Orlandini et al. (2011) highlighted a negative relationship between NDVI and GPC. Similarly, other studies have shown that RS indices were not able to provide a significant correlation with GPC and, then, a reliable prediction of the grain quality (Freeman et al., 2003; Liu et al., 2006, Xue et al., 2007).

8.7. Forecasting index for yield

The multiple regression model, obtained from the long-term analysis (1956-2011), indicated the following equation 1 to assess the yield:

(1) $Y = 8622.546 – 200.57 * DD_{march} + 122.299 * LAI_{april}$

where: Y is the grain yield, DD_{march} the number of days in March with precipitation below 5 mm and LAI_{april} the plant LAI at the end of the vegetative growth.

Highly significant correlation was found between the yield assessed through the equation 1 and the yield simulated by CERES-Wheat over 56 growing seasons, with a R^2 of 0.4 ($P \leq 0.001$).

Then, the performance of the multiple regression model as a forecasting index of durum wheat yield was assessed through the validation with the ground measurements from the field trials. DD, recorded in March, and the crop LAI, measured at second half of April, were used to simulate the harvest in 2010 and 2011 through the equation 1. The estimated yields showed highly significant correlation with those observed, with R^2 of 0.58 ($P \leq 0.001$) (Fig. 8.7.1).

The table 8.7.1 summaries the forecasting index performance in comparison with that resulting from CERES-Wheat at calibration and validation step (paragraph 8.1).

The lower performance of the forecasting index compared to CERES, is mainly due to the higher error of over-estimation (Tab. 8.7.1, Fig. 8.7.7).

Since the aim of the forecasting index is to provide early indications of the harvest quantity, it did not take into account the impact of weather during the grain filling stage. Water and heat stresses at grain filling stage significantly decrease the wheat yield (Sofield et al. 1977, Al-Khatib and Paulsen 1984; Kobata et al., 1992; Stone et al., 1994; Zhang et al., 1998; Eitzinger et al., 2003). Therefore, the forecasting index assessed higher yield compared to those observed as result of not including this key growth stage.

Fig. 8.7.1 Liner regression between observed and forecasted yield.

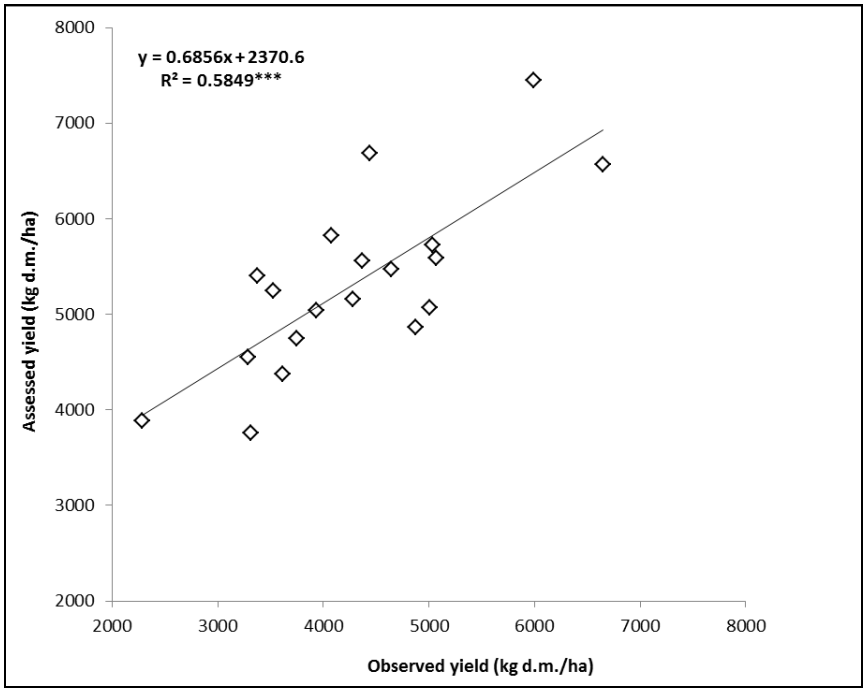

However, the forecasting index was able to provide predictive information on yield trend beginning in April, on the basis of few input data compared to those required by CERES. An assessment of yield in this period represents a useful input for farm decisions pertaining to late fertilization.

The results showed that CERES-Wheat was an efficient tool to analysis the 'soil-plant-atmosphere' system. The complex model identified the main crop and weather variables that affect durum wheat yield. These variables were used to set up an efficient forecasting index. The rainfall during the tillering stage represented the main weather constraint for the harvest quantity, and, LAI at the end of the vegetative growth stage was best able to indicate the yield variability between the fields.

Tab. 8.7.1 Performance of the forecasting index in yield assessment in comparison with CERES-Wheat performance at calibration and validation step.

Coefficient	*CERES-Wheat*	*Forecasting index*
R^2	0.7	0.6
RRMSE	20 %	28 %
EF	0.7	- 0.5
CRM	0.07	- 0.24

8.8. Forecasting index for GPC

The multiple regression model, obtained from the long-term analysis, indicated the following equation 2 to assess GPC:

(2) $Y = -9.064 + 0.607 * DD_{march} + * 6.317\ LAI_{april}$

where: Y is the GPC, DD_{march} the number of days in March with precipitation amount below 5 mm and LAI_{april} the crop LAI at the end of the vegetative growth.

Highly significant correlation was found between GPC assessed through the Eq. 2 and GPC simulated by CERES-Wheat over 56 years, with a R^2 of 0.5 ($P \leq 0.001$).

The performance of the multiple regression model as a forecasting index of grain quality was assessed through the validation with ground measurements from the field trials. DD, recorded in March, and the crop LAI, measured at second half of April, were used to assess the GPC in 2010 and 2011 through the equation 2.

The resulting correlation between GPC assessed through the forecasting index and those observed, was significant, with R^2 of 0.58 ($P \leq 0.01$) (Fig. 8.8.1).

Nevertheless, from the analysis of these results and the field measurements, it was possible to divide the observed data into two groups on the basis of the corresponding measurements of plant LAI. A group of fields were detected with average LAI_{april} within the intermediate range 0.9 - 1.8 (ILAI), as well as a group of fields with extreme LAI_{april}, below 0.7 or above 2 (ELAI), (Fig. 8.8.1 and 8.8.2).

Fig. 8.8.1 Liner regression between observed and forecasted GPC. Legend: (○) = GPC of fields with $LAI_{april} \leq 0.7$ or ≥ 2 (ELAI group), (Δ) = GPC of fields with LAI_{april} within the range 1.8-0.9 (ILAI group).

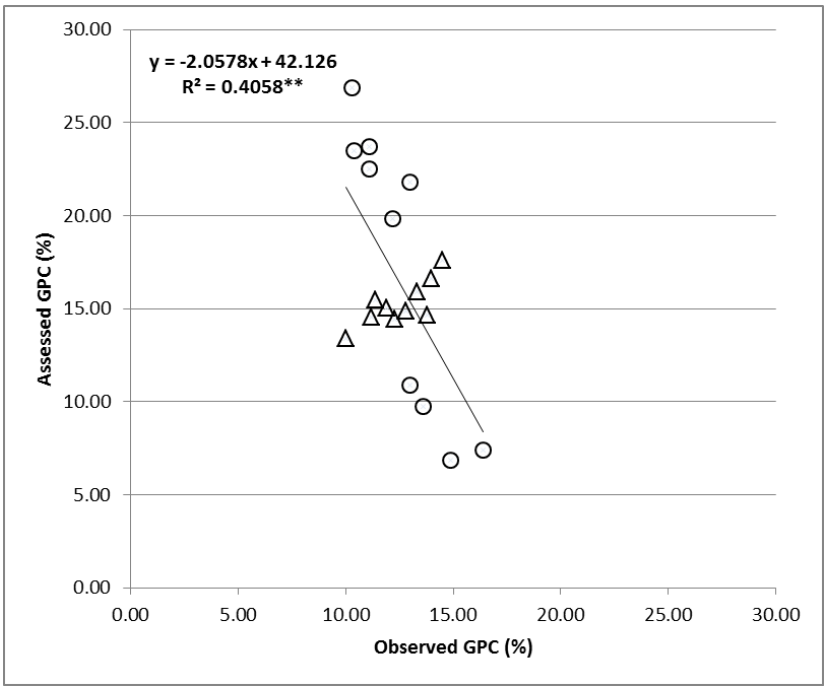

Fig. 8.8.2 LAI_{april} of the fields in the ELAI group (○) ($LAI \leq 0.7$ and $LAI \geq 2$) and in the ILAI group (Δ) ($1.8 \geq LAI \geq 0.9$).

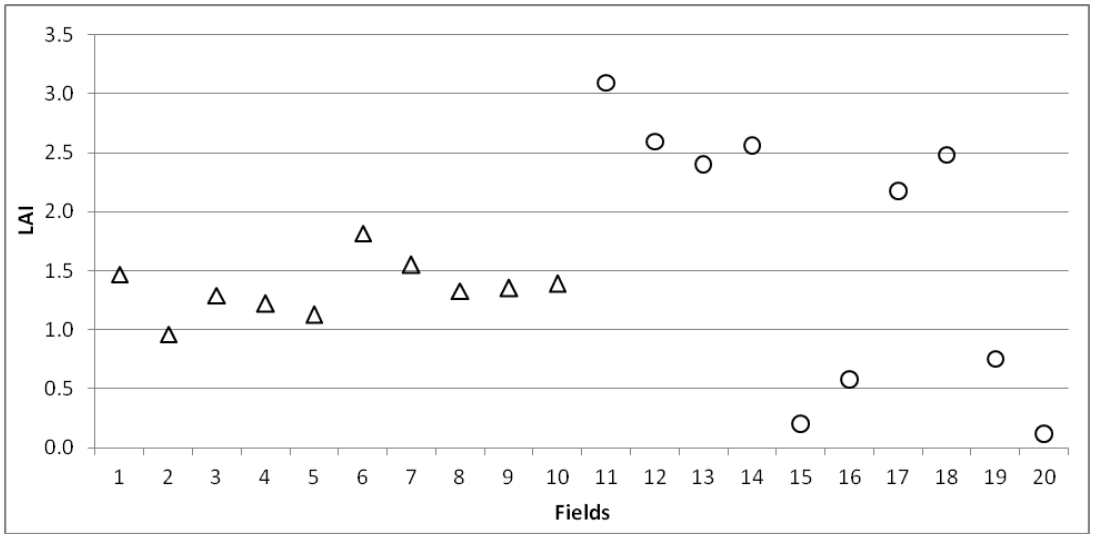

Ten fields fell in ILAI and ten fields in ELAI, respectively. The field data from different growing seasons had a heterogeneous distribution among the LAI groups. This result showed that the crop LAI was importantly affected not only by seasonally weather but also by different crop management of each farm during the same year.

The forecasting index validation was carried out separately on ILAI and ELAI data-sets. The performances of the multiple regression model (Eq. 2) differed in relationship to the values range of LAI.

In ILAI, the assessed GPC showed significant and positive correlation with those observed ($R^2 = 0.6$, $P \leq 0.01$) (Fig. 8.8.3). However, in ELAI, a highly significant and negative correlation ($R^2 = 0.8$, $P \leq 0.001$) was found between the assessed and observed GPC (Fig. 8.8.4).

These results showed that for the ILAI group, the forecasting index was able to capture the spatial and temporal variability of GPC, among the seasons and the fields. In this case, the forecasting index, beginning in April, provided early information about the harvest quality. On the other hand, the forecasting index was completely unable to catch the GPC variability in ELAI fields. The results suggest that at crop LAI outside an intermediate range, the GPC cannot be forecasted on the basis of the relationships described by CERES-Wheat, between GPC and the rainfall distribution in March and LAI in April.

The table 8.8.1 summaries the forecasting index performance for the ILAI group in comparison with that shown by CERES-Wheat at calibration and validation step of the new routine of GPC simulation (paragraph 8.2). The forecasting index showed higher capacity to capture the spatial and temporal variability of GPC, with higher R^2 value. However, the forecasting index involved a higher general error (RRMSE) and a lower model efficiency (EF) that can be ascribed mainly to the over-estimation error (CRM).

Tab. 8.8.1 Performance of the forecasting index in GPC assessment, in comparison with CERES-Wheat performance at calibration and validation step.

Coefficient	*CERES-Wheat New routine*	*Forecasting index*
R^2	0.42	0.60
RRMSE	15.58 %	22.85 %
EF	0.98	- 3.49
CRM	0.08	- 0.22

As studies confirmed, the environmental variables during the grain development stage impact the protein deposition into the grain. In general, relatively cold weather and favorable water supply during the grain filling stage negatively affect the GPC (Neales et al., 1963; Troccoli et al, 2000; Gooding et al, 2003; Zhao 2009). Therefore, the over-estimation error can be mainly due to the fact that the predictive capability of the forecasting index does not include the weather condition after anthesis. Despite this, the index has proved be able to account for the grain protein accumulation during the grain filling stage, simulating the relative differences in the GPC trends at harvest.

However, the forecasting index was validated only for fields with LAI values within an intermediate range.

Fig. 8.8.3 Liner regression between the forecasted GPC and those observed in the ILAI group.

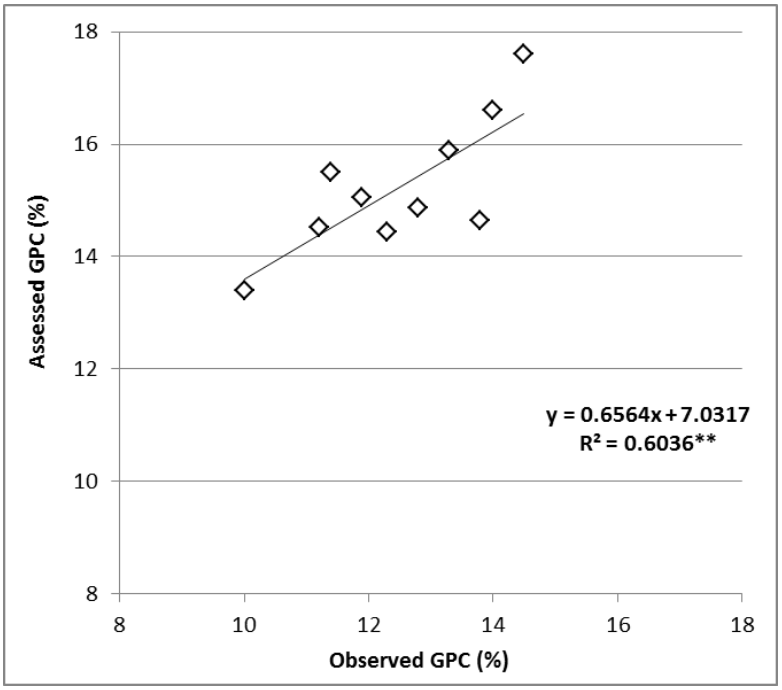

Fig. 8.8.4 Liner regression between the forecasted GPC and those observed in the ELAI group

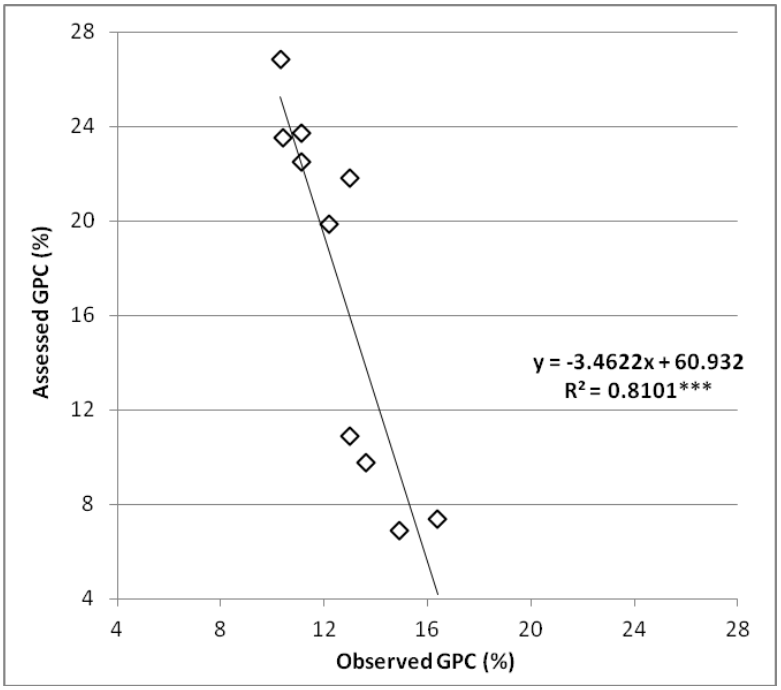

8.9. Model deficiencies in GPC simulation

The literature on crop modeling shows poor results in GPC assessment, suggesting that the current simulation algorithms need to be revisited (Otter-Nacke et al., 1986; Asseng et al., 1998; Meinke et al., 1998; Asseng et al., 2002). In this context, the study carried out a diagnostics of CERES-Wheat, tracing the deficiencies of the model. The results highlighted an important aspect.

CERES-Wheat described a positive impact of crop LAI on both GPC and yield (paragraph 8.7). For the yield this relationship was confirmed by the validation of the forecasting index with field data. On the other hand, the forecasting index of GPC showed good performance only for the fields in which the crop had an intermediate values of LAI (ILAI). In this case, the increasing values of LAI involved a GPC increase.

However, at increasing or decreasing LAI outside the intermediate range (ELAI), the forecasted GPC did not fit with those observed. In this case, CERES-Wheat was not able to identify the main crop and weather components that contribute to spatial and temporal variability of GPC.

The correlation analysis between the observed GPC and yield did not show significant results for the ILAI group, while significant and negative correlation was found in ELAI ($R^2 = 0.6$, $P \leq 0.01$) (Fig. 8.9.1).

These results suggest that the failure of the forecasting index in describing GPC can be due to a deficiency of CERES-Wheat in fully capturing the interactions between LAI, yield and GPC.

Fig. 8.9.1 Liner regression between the observed GPC and yield in the ELAI group.

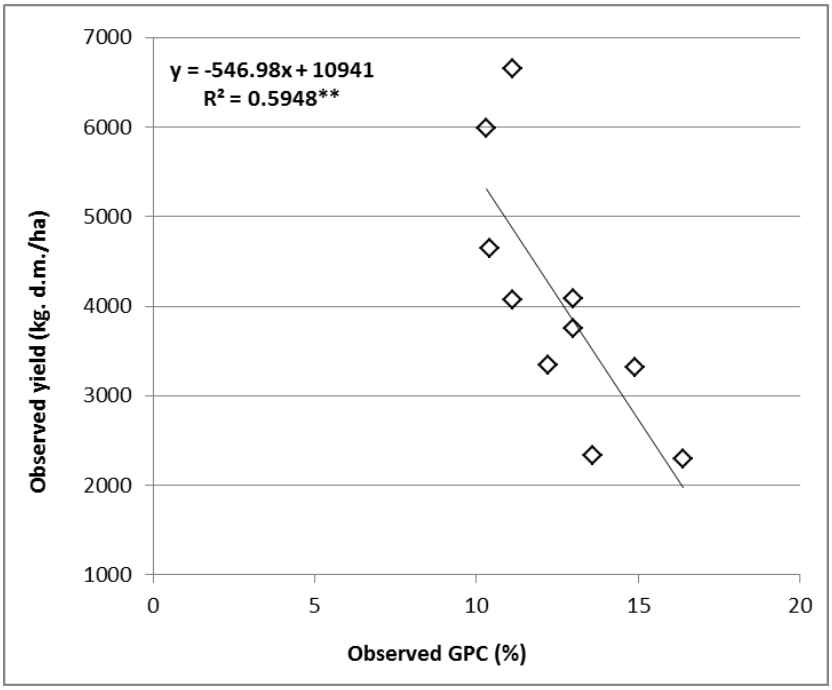

- Within an intermediate range (ILAI), a LAI increase was accompanied by a corresponding increase of GPC, while the yield not significantly affect the GPC.

This conclusion is in agreement with the common assumptions of the crop simulation models, in which the N uptake depends on the leaf area expansion and the grain protein deposition increases with the total N content of the leaves (Dalling, 1985; Jenner et al., 1991; Jamieson and Semenov, 2000). On the other hand, the crop models simulate the yield on the basis of the pre-stored dry matter in vegetative tissues, which in turn increases with fPAR, that is an exponential function of LAI (Ritchie et al., 1985). Therefore, CERES-Wheat simulated at increasing values of LAI an increase of both GPC and yield. These basic assumptions, adopted by CERES-Wheat, disagree with the inverse relationship between yield and GPC, well confirmed in scientific literature of wheat (Spiertz, 1977; Johnson et al., 1985; Fischer et al., 1993; Feil, 1997; Novaro et. at, 1997; Rharrabti et al., 2001a; Rharrabti et al., 2001b). In particular, concerning this point, in durum wheat the yield impact on GPC is emphasized more, compared to common wheat (Cossani et al., 2011). In durum wheat, an increase of grain weight is

accompanied by a higher pronounced decrease of grain N percentage (Cossani et al., 2011).

The dilution of protein by non-nitrogen compounds in the grain seemed to be the primary cause for the negative association between harvest quantity and quality (Pleijel et al., 1999). Rharrabti et al. (2001a) suggested also that, since the protein synthesis uses more photosynthate compared to those necessary for the carbohydrates synthesis (Penning De Vries et al., 1974), an increase of protein synthesis into the grain can lead to a decrease of photosynthate available for the carbohydrates production. Moreover, the starch accumulation in the grain appears to be more sensitive to adverse environmental conditions than the nitrogenous compounds translocation and protein synthesis. Therefore, water or thermal stresses affect the starch deposition more than that of the protein, resulting in a relatively increase of GPC and reduction of yield (Campbell et al., 1981; Bhullar and Jenner, 1985; Garcia del Moral et al., 1995; Fernandez-Figares et al., 2000; Rharrabti et al., 2001a; Erekul and Köhn, 2006; Zhao et al., 2009; Orlandini et al., 2011).

- Out of the intermediate range (ELAI), towards extreme LAI values, the impact of the inverse relationship between yield and GPC overrides the positive effects on GPC of N supply from the plant tissues.

Higher LAI values promoted the yield, so that the benefits for the grain protein accumulation, related to the greater N supply from biomass, were minimized. Following a similar and opposite mechanism, lower LAI values, being a disadvantage for grain yield, were able to support the GPC, despite the lower N available for the grain protein deposition.

Finally, LAI affected GPC in opposite way, depending on its range of values. CERES-Wheat was not able to fully capture the relationship between GPC and LAI, and to simulate the interaction between yield and GPC in durum wheat.

These results can explain the disagreement shown in literature on the capability of RS indices, descriptive of crop LAI, to monitor and forecast the wheat GPC.

Studies describe a positive correlation between GPC and RS LAI (Basnet et al., 2003; Reyniers et al., 2006; Xue, 2007; Li et al., 2012) that, however, is not confirmed by

other authors (Freeman et al., 2003; Liu et al., 2006, Xue et al., 2007; Orlandini et al., 2011).

In this context, understand and define the interactions between GPC, LAI and yield, represents an important step to appropriately use both RS data and crop modeling in developing operational applications to support the quality of the production of durum wheat .

SECTION 2

"Performance of remotely sensed indices in monitoring the variability of harvest quantity and quality and integration with crop modeling tools"

Objective 5. Assess the improvement in the yield and GPC simulations by crop model due to the integration with RS data, based on a relatively simple procedure for the model output spatialization.

Objective 6. Compare the performance of the satellite imagery (MODIS) related to RS indices (NDVI, EVI, LAI, fPAR) in the monitoring of yield and GPC variability and trace the deficiencies in GPC description.

9. MATERIALS AND METHODS SECTION 2

9.1. Study area

The study was carried out in Val d'Orcia (Lat 43.03, Lon 1.66, 250−450 a.s.l.). For more details see paragraph 7.1. in section 1.

9.2. Weather data

The mean meteorological daily data for precipitation (mm) (P), maximum (TMAX) and minimum (TMIN) air temperatures (°C) over the growing seasons 2009-2010 and 2010-2011 were supplied from six ground weather stations located in the study area.
The solar radiation (MJ/m^2) (R) was estimated from TMAX and TMIN following the equation (1) (Hargreaveres et al., 1985).

$$(1)\ R = Ra * Ah * \sqrt{TMAX - TMIN} + Bb$$

where: Ra is the daily extra-terrestrial radiation (J m^{-2} d^{-1}), and the values assumed in the study area by the empirical constants Ah (°C$^{-0.5}$) and Bh (J m^{-2} d^{-1}) are 0.18 and −1.76, respectively (Trnka et al., 2005).

9.3. CERES-Wheat calibration and validation

CERES-Wheat was calibrated, starting from the default genotype 'Winter-Europe', in relationship to the best fit between the observed and simulated data for the crop yield and onset of the main phenological stages, as described in paragraph 7.3, section 1.
The field input data concerning crop management, wheat phenological timing, and harvest were supplied by different information sources (ARSIA and CAPSI-DIPSA data-sets), for a total of 30 fields over 12 years. In all the fields, durum wheat (*Triticum turgidum* L. var. *durum*) cv. *Claudio* was grown. For further details about the model input see paragraph 7.3, section 1.

The performances of the crop simulation model, used in the present study, were assessed in the previous section 1 (paragraphs 8.1 and 8.2).
The reliability of the simulations about yield and GPC was assessed through the correlation analysis between simulated and measured data and the computation of the following coefficients: Relative Root-Mean-Squared Error (RRMSE) (Jørgensen et al., 1986) (Eq. 2), Modelling Efficiency (EF) (Nash and Sutcliffe, 1970) (Eq. 3), Coefficient of Residual Mass (CRM) (Loague and Green, 1991) (Eq. 4).

(2) $\mathrm{RRMSE} = \frac{\sqrt{\frac{\sum_{i=1}^{n} (S_i - M_i)^2}{n}}}{\overline{M}} * 100$ (values range 0 / +∞; optimum = 0)

(3) $\mathrm{EF} = 1 - \frac{\sum_{i=1}^{n} (S_i - M_i)^2}{\sum_{i=1}^{n} (M_i - \overline{M})^2}$ (values range −∞ / 1; optimum = 1)

(4) $\mathrm{CRM} = \frac{\sum_{i=1}^{n} M_i - \sum_{i=1}^{n} S_i}{\sum_{i=1}^{n} M_i}$ (values range +∞ / −∞; optimum = 0)

where: *S* and *M* are the simulated and measured data, respectively, and *n* is the total number of observations.

The table 9.3.1 shows the performance of CERES-Wheat in simulation of durum wheat production. The model proved discrete performance in estimation of yield. The model showed a moderate general error (RRMSE), a model efficiency close to the optimum (EF) and a weak error for under-estimation (CRM). On the other hand, compared to yield, CERES-Whet was less efficient tool for GPC simulation, showing a higher general error (RRMSE), in part due to the solid error of under-estimation (CRM).

Tab. 9.3.1. CERES-Wheat performances in simulation of yield and GPC (the original CERES-Wheat routine) of durum wheat. Legend: *** = significant at $P \leq 0.001$.

Coefficient	*Yield*	*Sig.*	*GPC*	*Sig.*
R^2	0.7	***	0.35	***
RRMSE	20 %		26 %	
EF	0.7		0.93	
CRM	0.07		0.23	

9.4. Field trials

The field trials were set up during two growing seasons, 2009-2010 and 2010-2011, for a total number of 11 and 13 fields (PHM), respectively.

In this context, the aim of the trials was to validate the performance of operational tools in real cropping systems, for the description of durum wheat harvests. The field data were used in the following analysis to assess the spatialization algorithms of GPC and yield. The field trials represented a complex and heterogeneous environment. The capability of set tools to capture the harvest spatial and temporal variability was assessed.

The land plots differed for crop management, exposure, elevation and slope. The fields were selected on the basis of three requirements: cultivation of durum wheat cv. *Claudio*, size enough large and central position, in relationship to the pixel of MODIS imagery grid at 250 m spatial resolution.

Crop phenological observations, measurements about plant LAI and monitoring on the quality and quantity of the harvest were carried out. For further details about growing environments, samplings and surveys see paragraph 7.5, section 1.

9.5. CERES-Wheat run without detailed input data

CERES-Wheat, calibrated and validated for durum wheat, was run over the growing seasons 2009-2010 and 2010-2011 with different meteorological data by year, but the same input data for crop management and soil profile.

Since the input data were not able to discriminate the different micro-climate, soil-specific, and crop management conditions of each field, one output value of yield (kg d.m./ha) and GPC (%) has been resulted per year.

The capacity of the model, running without detailed input data, to provide information about the average trend of yield and GPC was assessed on the basis of the observed data during the field trials. The model outputs were compared with the average values of yield and GPC observed in 2010 and 2011 harvests.

CERES-Wheat was initialized with the daily meteorological data-set described in paragraph 9.2. The soil input data was supplied in agreement with the typical soil characterizing the cereal crops arable lands in the study area. Land use map shows that the cereal crops in Val d' Orcia are grown on 'Typic Ustorthents fine, mixed, calcareous, mesic' soils (USDA classification), moderately deep, weakly alkaline, with a silty-clay-loam texture and a slope from moderate to high (14 – 35 %). The physical and chemical properties of the used soil profile are described in Table 9.5.1.

Tab. 9.5.1. Soil profile used by the CERES-Wheat model. Legend: CSC = cation-exchange capacity

Depth (cm)	*Master horizon*	*Clay %*	*Silt %*	*pH*	*CSC cmol/kg*
30	Ap	38	53	8.5	15.5
50	C	43	50	7.6	19.3
150	C	42	50	7.6	18.0

The input data for crop management were set up, for both growing seasons, according with the protocol widespread in Val d' Orcia. It included a total nitrogen amount of 140 kg/ha, splitted in three times (26 N units at sowing, 57 N units at 80 days after sowing and 57 N units at 130 days after sowing).

The sowing date was simulated automatically by CERES-Wheat at optimum soil conditions (soil temperatures between 2-37 °C and soil water content between 40-100%), within the more common sowing window adopted by the local farms. Therefore, the sowing window was established from the first decade of November to the last decade of December, excluding the earlier (in October) and later (in January) periods. The model set the harvest time automatically when the grain maturity was reached.

The model output (GPC and yield) was spatialized over the land plots of the field trials through the algorithms described in the following paragraphs.

9.6. Remotely sensed data acquisition and processing

MODIS imagery (Satellite Terra NOAA-AVHRR) on the study area were acquired from the website: http://reverb.echo.nasa.gov/reverb. The MODIS products that were taken into account are shown in table 9.6.1. The RS indices describe the canopy status in relationship to the plant biomass growth (NDVI, EVI, LAI, fPAR) and photosynthetic activity (fPAR). For more details about RS indices see the paragraph 5.1.

The imagery were processed thanks to a specific program and with the support of the softwares: Python, MODIS Reprojection Tool and MODIS Reprojection Tool Swath, downloaded from the following links, respectively:

- http://www.python.org
- https://lpdaac.usgs.gov/tools/modis_reprojection_tool
- https://lpdaac.usgs.gov/tools/modis_reprojection_tool_swath

The pixel values related to the land plots of the field trials were extracted for the two growing seasons (2009-2010 and 2010-2011), from 13 October (286 JD) of the sowing year, to 12 July (193 JD), of the harvest year.

The average RS value of the study area was computed per each time-step. Therefore, the average trend of each RS index, during each growing season, was analyzed. The trends shown by the indices were compared. The periods of the crop cycle that involved the maximum values were identified. Furthermore, the abrupt temporal changes in value were detected. The abrupt changes in value were considered anomalies due to persistent cloud cover when they proved be not consistent with the relatively gradual manner in which crop activity changes in time.

Tab. 9.6.1. MODIS products (Source: http://modis.gsfc.nasa.gov/).

MODIS product	*Index*	*Temporal Resolution*	*Spatial resolution*
MOD15A2	LAI	8-Day	1 km
MOD15A2	fAPAR	8-Day	1 km
MOD13A2	NDVI	16-Day	1 km
MOD13Q1		16-Day	250 m
MOD13A2	EVI	16-Day	1 km
MOD13Q1		16-Day	250 m

9.7. Correlations between RS indices and the harvest

The correlation analysis between wheat harvest (yield and GPC) and RS indices were performed. The period from 2 February (33 JD) to 10 June (161 JD) was studied, in 2010 and 2011.

The values of single imagery at each time-step were taken into account, as well as the values from the imagery combination on multi-time-steps. In this latter case, the maximum value recorded over the reference period was considered with the aim to reduce the influence of the abrupt temporal changes in values, characterizing the single time-step. The maximum value was computed over the entire period from 33 to 161 JD, as well as on combinations of bi-time-steps and three-time-steps.

The timing of RS imagery was analyzed in relationship to the wheat phenological development. Therefore, the correlations with RS data were not computed on the basis of the imagery acquisition calendar, but on the basis of the onset of the growth stages. Thus, the analysis took into account the differences in the phenological development between the fields and the years.

The RS index that showed higher correlation with the harvest at the optimal timing, was integrated with CERES-Wheat output, as described in the following paragraphs.

9.8. Calibration and validation of spatialization algorithm for yield

On the basis of the results from the previous paragraph 9.7, fPAR at beginning of grain filling was used to develop a spatialization algorithm.

The performance of fPAR was assessed in describing the yield spatial variability, and then, the yield deviation from the annual average. The annual average of yield was represented by CERES-Wheat output. A linear regression analysis was carried out between the yield deviation of each field from the yield annual average (Yd) and the fPAR deviation of each field from the fPAR annual average (X_1).

The analysis was performed using the field trials data of the growing season 2009-2010. The resulting linear regression model is described by the equation 5.

(5) $Yd = (\beta_1 * X_1 + \beta_0)$

where: Yd is the yield deviation (dependent variable), X_1 the fPAR deviation (predictor variable), and β_0 and β_1 the intercept value and the regression coefficient, respectively.

The model of the equation 5 was implemented in a spatialization algorithm for CERES output. The algorithm was calibrated on 11 fields of season 2009-2010, following equation 6.

(6) $Y = OUT \pm Yd \pm FC$

where: Y is the yield (dependent variable), OUT is the yield simulated by CERES-Wheat, FC is the correction factor for the average error of under- or over- estimation.

FC was calculated on the basis of the equation 7. The positive (+) or negative (−) sign of FC depends on the error for under- or over-estimation described by CRM (Eq. 4). CRM was computed on the basis of the yield simulated through the equation 6 with FC equal zero.

(7) $$\mathrm{FC} = \pm \left[\mathrm{Yi} * \left(\frac{\sum_{i=1}^{n} \mathrm{S} - \sum_{i=1}^{n} \mathrm{M}}{\sum_{i=1}^{n} \mathrm{S}} \right) \right]$$

where: Yi is the yield assessed following the equation 6 with FC equal zero, *S* is the simulated data following the equation 6 with FC equal zero, *M* is the measured data, and *n* the total number of observations.

The spatialization algorithm (Eq. 6) was validated on 13 fields of season 2010-2011.

The yield simulated by CERES-Wheat (OUT) was the only value of the equation 6 that was replaced. The same model for Yd assessment (Eq.5) and the same FC value (Eq. 7), calibrated in the previous year, were used.

The performance of the spatialization algorithm (Eq. 6) was assessed at both calibration and validation step through the linear regression analysis between observed and simulated yield and with the computation of the following coefficients: RRMSE (Eq. 2), EF (Eq. 3), CRM (Eq. 4).

9.9. Calibration and validation of spatialization algorithm for GPC

From the previous analysis (paragraph 9.7) no correlations between RS indices and GPC were found with a sufficient R^2 value to set up a spatialization algorithm, or to be explained consistency from an agronomic point of view.

Therefore, a further correlation analysis, led by the pervious results, was performed.

The study focused on fPAR, since it was found the RS index more correlated to the yield (paragraph 9.8).

Non-linear relationship was found between GPC and LAI in the previous study of section 1. Therefore, the field data were divided in four quartiles, on the basis of the maximum fPAR value reached during the crop cycle by each field.

Then, the linear regression between GPC and fPAR was computed separately for the fields within the I and IV quartiles, and the fields within the II and III quartiles. The correlation analysis was carried out between GPC and fPAR with the same modalities described in paragraph 9.7.

The fields in I and IV quartiles were associated to extreme LAI values, outside an intermediate range. The fields in II and III quartiles were associated to intermediate LAI values. Only the field data of I and IV quartiles showed significant correlations with fPAR. At flag leaf and booting stage, fPAR showed a R^2 value sufficient to describe the GPC variability. Therefore, fPAR was used in the spatialization algorithm.

The spatialization algorithm was set up on 12 fields belonging to I and IV quartiles without distinguishing between the years. Since the reduction of observed data from 24 to 12, a leave-one-out cross validation was applied to assess the performance of the algorithm. The cross-validation was performed with leaving out one sample at time. In this leave-one-out cross validation, a calibration of the algorithm was built using *n-1* observations, and the observation left out was used for the validation (Li et al., 2012). Given a set of *n* observations ($n = 12$), this process was repeated *n* times, so that each observation had been left once, obtaining 12 different spatialization algorithms.

Similarly, as described for the yield (paragraph 9.8), the capability of fPAR to describe the GPC variability between the fields was assessed. The correlation analysis was

carried out between the GPC deviation of each field from the GPC annual average (Yd) and the fPAR deviation of each field from the fPAR annual average (X_1). The annual average of GPC was represented by CERES-Wheat output. The resulting linear regression model (Eq. 5) was implemented in the algorithm for GPC spatialization. The algorithm was described by the equation 8.

(8) $Y = OUT \pm (\beta_1 * X_1 + \beta_0) \pm FC$

where: Y is GPC (dependent variable), OUT is GPC simulated by CERES, ($\beta_1 * X_1 + \beta_0$) the regression model to assess Yd (Eq. 5). The algorithm included the correction factor FC for the under- or over-estimation error, computed following the equation 7.
The algorithm (Eq. 8) was calibrated and validated during the crossing-validation.
Each resulting algorithm was described through the linear regression analysis between observed and simulated data at calibration (*n-1*). Moreover, the following coefficients were computed: RRMSE (Eq. 2), EF (Eq. 3), CRM (Eq. 4). The performance of each algorithm was compared with that shown by CERES-Wheat running without detailed input data (paragraph 9.5) over the same combination of observations (*n-1*).
The standard deviations, resulting from the validation of each algorithm, were used to assess the average performance of the algorithm, through the correlation analysis between observed and simulated data and the computation of the following coefficients: RRMSE (Eq. 2), EF (Eq. 3), CRM (Eq. 4). The best performance was associated to the algorithm that showed at validation the lower standard deviation.

10. RESULTS AND DISCUSSION SECTION 2

10.1. Trend of RS indices for durum wheat canopy

In both growing seasons, NDVI, EVI, LAI and fPAR showed the maximum values between the time-steps at 113 JD (7 April - 23 April) and at 145 JD (9 May - 25 May) (Fig. 10.1.1 and 10.1.2). During this period, the durum wheat grown in the study area shifts from the vegetative growth phase to the reproductive one, through the following development stages: flag leaf and booting stage, ear emergence and anthesis stages, beginning-mid of grain filling stage.

During this period (113 JD – 145 JD), an abrupt change of values for NDVI and EVI was detected at 113 JD in 2010 (Fig. 10.1.1). The maximum peaks of both NDVI and EVI occurred at 129 JD (23 April - 09 May) in 2010, and at 113 JD (7 April - 23 April) in 2011 (Fig. 10.1.1). The time-steps at 129 JD and 113 JD corresponded approximately to the periods from ear emergence stage to anthesis, and from flag leaf stage to ear emergence stage, respectively. However, since the abrupt decrease of values observed at 113 JD in 2010, it is reasonable to assume that, without this interference due to atmospheric noise, in 2010 the maximum values of NDVI and EVI were reached by the canopy during the previous time-step, at 113 JD (Tab. 10.1.1).

During the period of the maximum values (113 JD – 145 JD), abrupt changes of fPAR and LAI were observed in 2010, at 121 JD (23 April - 01 May) and 129 JD (01 May - 09 May), and in 2011, at 113 JD (15 April - 23 April) and 129 JD (01 May - 09 May) (Fig. 10.1.2). The results pointed out that RS LAI and fPAR trends were more affected by abrupt values changes, compared to NDVI and EVI, because the shorter time-step used for the maximum value compositing (MVC). Overlapping the two growing seasons data-sets, only the time-steps at 137 JD (09 May – 17 May) and at 145 JD (17 May – 25 may) were not affected by atmospheric noise (Tab. 10.1.1). These time-steps covered approximately the late period from anthesis to beginning-mid of grain filling stage.

The maximum peaks occurred for both indices at 113 JD (15 April - 23 April) in 2010, and at 121 JD (23 April - 01 May) in 2011 (Fig. 10.1.2). These two time-steps corresponded approximately to the period from flag leaf stage to anthesis. Since the abrupt decrease of values was recorded at 113 JD in 2011, it is reasonable to assume that, without this interference due to atmospheric noise, the maximum values of LAI and fPAR in 2011 were reached by the canopy during the previous time-step, at 113 JD (Tab. 10.1.1).

Fig. 10.1.1 Average trends of NDVI and EVI recorded for the fields during two growing seasons 2009-2010 and 2010-2011.

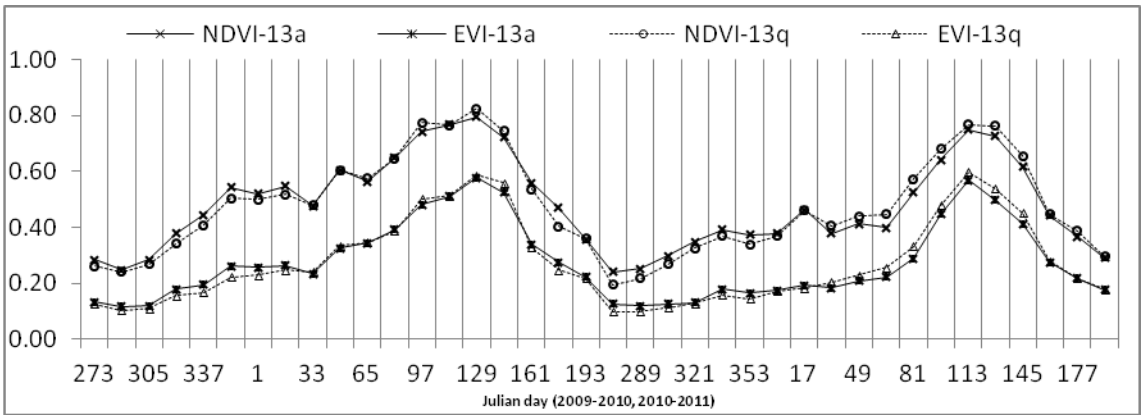

Fig. 10.1.2 Average trends of fPAR and LAI recorded for the fields during two growing seasons 2009-2010 and 2010-2011.

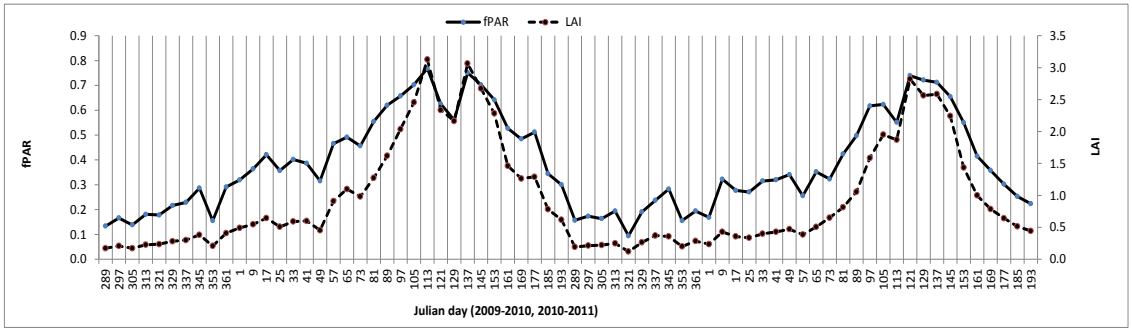

Tab. 10.1.1 Time-steps of RS indices affected by abrupt change of value and time-steps corresponding to the maximum value.

Time-step	***NDVI / EVI***		*Time-step*	***fPAR / LAI***	
	2010	*2011*		*2010*	*2011*
113	abrupt change	maximum	113	maximum	abrupt change
129	maximum	_	121	abrupt change	maximum
145	_	_	129	abrupt change	abrupt change
			137	_	_
			145	_	_

In conclusion, the results suggest that at 113 JD, durum wheat reached the maximum values of NDVI, EVI, LAI and fPAR. This time-step corresponded to the end of the vegetative growth period indicated by the flag leaf stage. Despite this, the data analysis not always showed this period corresponding to the maximum peaks, because the values decreases due to the persistent cloud cover during the time-step.

The MODIS-13A and MODIS-13Q imagery, with 1 km and 250 m of spatial resolution, respectively, did not show significant differences in the average values (Fig. 10.1.1). This result suggests that the monitored fields were in a landscape that did not affect the average trend of the RS data, despite the presence of mixed pixels. This can be due to the quite homogeneous land use in the study area, mainly covered by farmlands dedicated to durum wheat production.

NDVI and EVI followed a similar trends during the two seasons (Fig. 10.1.1). EVI can be assessed by an exponential function of NDVI (Fig. 10.1.3) and it showed lower values compared to NDVI. As shown in literature, NDVI loses its discrimination power for durum wheat canopy at LAI higher than 3 (Aparicio et al., 2002) and the lower values of EVI proved the avoidance of the saturation effects encountered by NDVI (Huet et al., 2002; Huete et al., 1988).

fPAR tacked close the trend of LAI (Fig. 10.1.2). fPAR can be assessed by a logarithmical function of LAI (Fig. 10.1.4). The fPAR values approached more those of LAI during the period in which the wheat canopy showed the maximum values of RS data (113 JD – 145 JD). These results are in agreement with those from Hipps et al. (1983) study. The authors showed that, in wheat, fPAR is mainly determined by LAI when high LAI values are reached.

Fig. 10.1.3 Correlation between average values of EVI and NDVI recorded for the study area during two growing seasons.

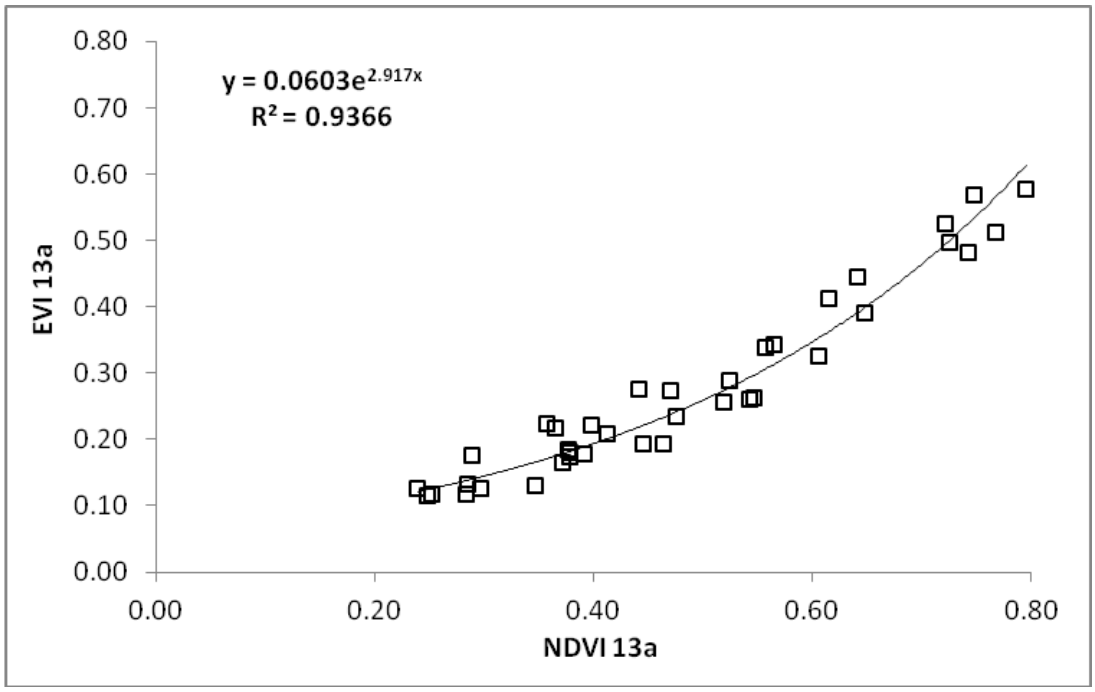

Fig. 10.1.4 Correlation between average values of fPAR and LAI recorded for the study area during two growing seasons.

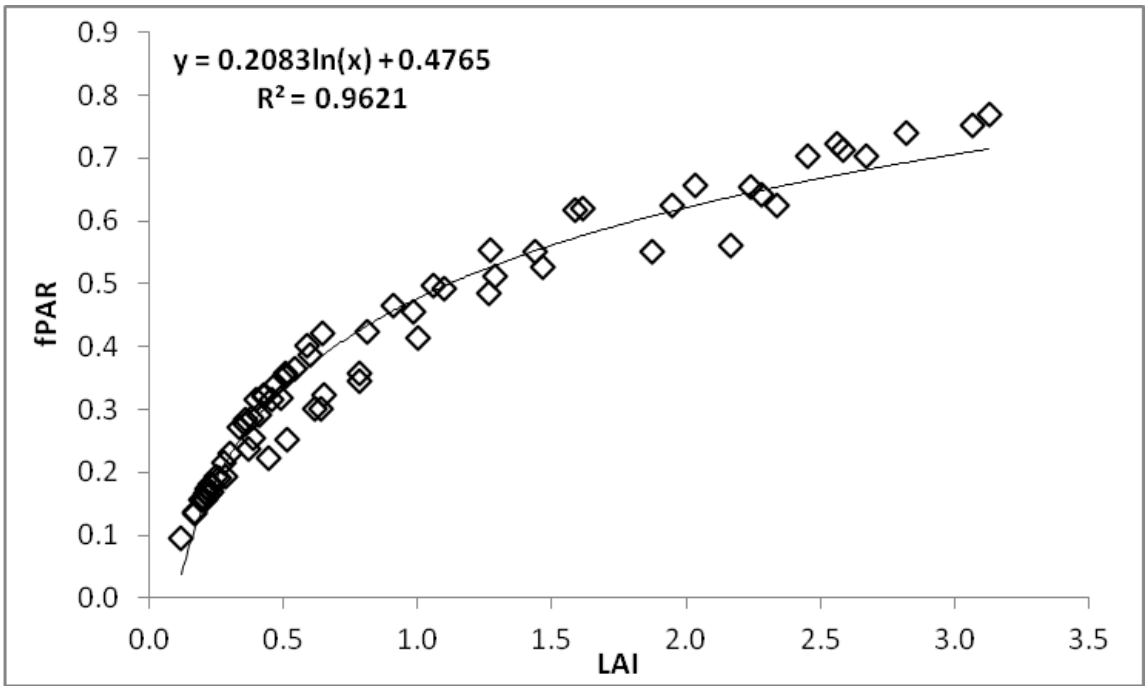

10.2. CERES-Wheat simulation

CERES-Wheat showed an over-estimation error compared to the observed average annual yield. The model simulated 27 % and 25 % more than the observed data, in 2010 and 2011 harvest, respectively. On the other hand, the model showed an under-estimation error compared to the observed average annual GPC, simulating 16% and 26% less than the observed data, in 2010 and 2011 harvest, respectively.

However, the simulation of harvest components (yield and GPC) was in agreement with the average trend observed for the two growing seasons, and CERES-Wheat described higher yield and lower GPC in 2010, compared to 2011 (Fig. 10.2.1 and 10.2.2.).

The results show that, although CERES-Wheat represents a tool less efficient in the simulation of GPC compared to yield (paragraph 9.3), it was able to provide also for GPC information about the average trend over the two growing seasons.

Fig. 10.2.1 Observed and simulated average data for yield, in 2010 and 2011 harvest.

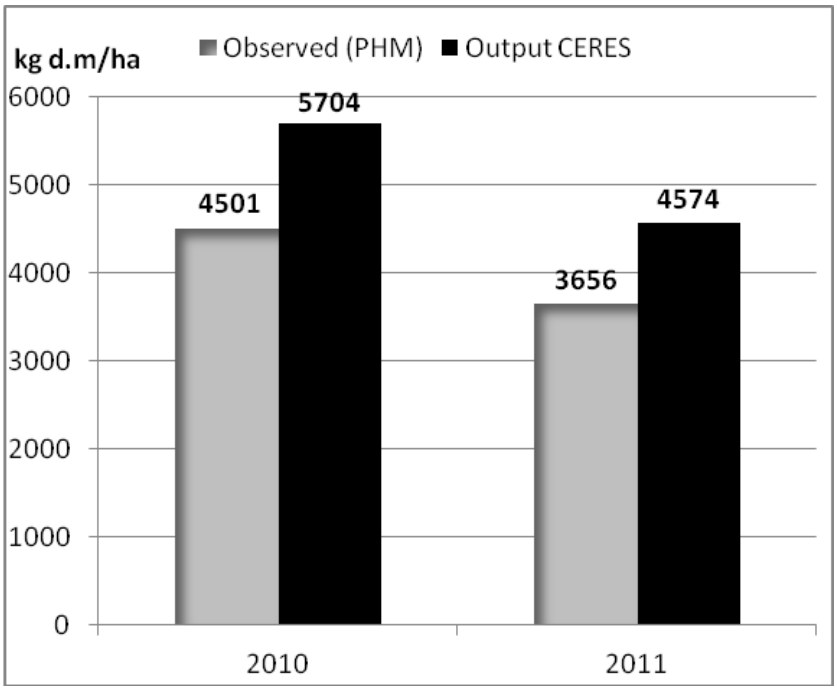

Fig. 10.2.2 Observed and simulated average data for GPC, in 2010 and 2011 harvest.

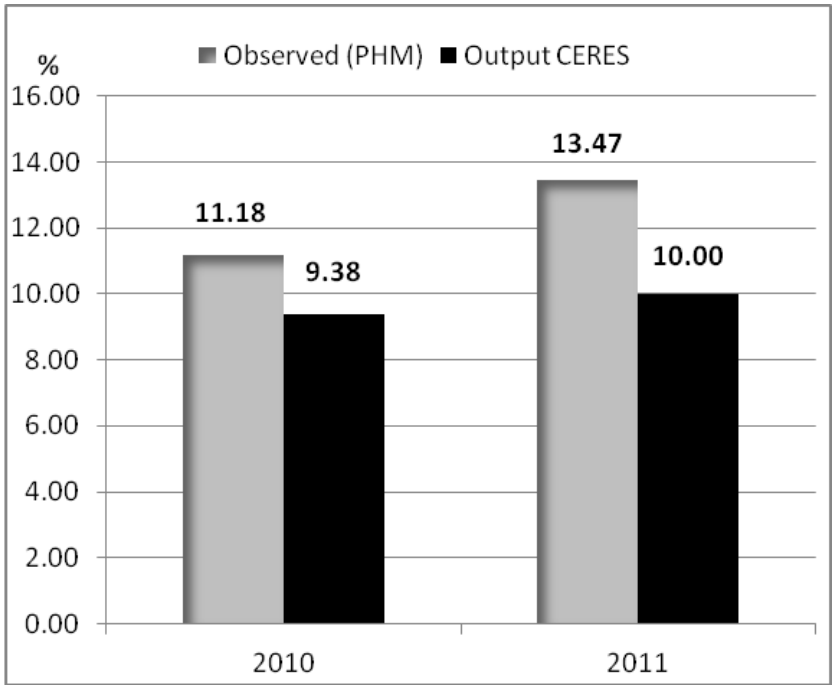

10.3. Relationship between remotely sensed indices and yield

All RS indices (NDVI, EVI, LAI and fPAR) showed correlations with yield. Significant and positive correlations were found during the late period of the crop cycle, from the flag leaf stage to the grain filling stage (Tab. 10.3.1). For most of the fields, this period corresponded to the time-steps covering the days from 97 JD (07 April) to 145 JD (25 May), except for few fields showing plants phenologically earlier or later than average. As seen in the previous paragraph, within the period from 97 JD to 145 JD the average maximum values of all RS indices were reached (tab. 10.1.1).

These results were confirmed in the scientific literature. The positive correlation was well-established between wheat yield and the RS indices, based on the simple ratio NIR/RED. (Quarmby et al., 1993; Hamar et al., 1996; Serrano et al., 2000; Ren et al., 2008; Becker-Reshef et al., 2010). Studies of soft wheat (*Triticum aestivum* L.) analyzed the optimal timing of RS data acquisition for the yield assessment. The authors indicated the time of maximum green canopy cover as the best period, which generally occurred around 30-40 days prior to harvest (from ear emergence to anthesis stage) (Tucker et al., 1980; Mahey et al., 1993; Quarmby et al., 1993; Freeman et al., 2003; Basnyat et al., 2004; Ren et al., 2008; Becker-Reshef et al., 2010).

Similarly, low values of LAI and biomass were associated with a yield decrease (Regan et al., 1992; Kang et al., 2002; Dalirie et al., 2010). Also a reduction of fPAR involved for wheat a lower yield (Mitchell et al., 1993; Mearns et al., 1997). In particular, it has been proved that a solar radiation decrease depresses the yield when it occurs the in the late period, during the spike development (booting stage) and grain filling phase (Willey and Holliday, 1971; Fisher, 1975; Abbate et al., 1997).

The MODIS-15A imagery at lower spatial resolution did not show correlations with yield when the MODIS-13Q showed correlations significant at $P \leq 0.05$. However, the MODIS-15A imagery agreed with the imagery at higher spatial resolution when these latter showed higher significant correlations, at $P \leq 0.01$.

The yields were correlated with both EVI-13Q and EVI-13A during the time-steps corresponding to the period from anthesis to beginning of grain filling stage (Tab. 10.3.1). On the other hand, only EVI-13Q showed significant correlations during the pre-anthesis period (Tab. 10.3.1). Similarly, both NDVI-13Q and NDVI-13A were correlated with yields during the period from anthesis to beginning of grain filling stage. On the other hand only NDVI-13Q showed significant correlations during the pre-anthesis period and during the late period of grain maturity (Tab. 10.3.1).

LAI and fPAR were found correlated with yields during the time-steps covering the period from flag leaf stage to the beginning-mid of grain filling stage. At beginning-mid of grain filling stage, fPAR and LAI showed the higher significant correlations, with R^2 values of 0.7 (Fig. 10.3.1) and 0.6, respectively (Fig. 10.3.2). Therefore, the optimal time for the yield assessment occurred for most of fields between 137 JD and 145 JD, with few exceptions for fields showing plants phenologically earlier or later than average. However, taking into account that this time-step was less affected by the persistent cloud cover in both growing seasons (Tab. 10.1.1), it is reasonable to assume that a good indication about the harvest could be obtained also from previous periods in the season when the RS data are not affected by atmospheric noise.

Also for NDVI and EVI the beginning of grain filling stage was the period higher correlated with yields. However, these indices, at both spatial scales, were not able to provide information about harvest as LAI and fPAR proved able to do. Indeed, NDVI and EVI showed low R^2 values and, thus, poor performance in describing yield variability (Tab. 10.3.1).

In conclusion, among the MODIS products that were taken into account, MODIS LAI and fPAR were best able to monitor and forecast the durum wheat production, despite their lower spatial resolutions compared to MODIS-13Q imagery. In particular, fPAR showed the higher significant correlation with yield (Fig. 10.3.1) and for this reason was selected to set the spatialization algorithm of yield.

The capability of MODIS fPAR imagery to describe the durum wheat yield is a issue that merits a special attention. The higher significant correlation shown by fPAR, compared to the other RS indices, can be explained by taking into account that the index values are related to plant photosynthesis activity, which in turn governs the crop performance.

fPAR takes into account the wavelength range directly related to photosynthesis (400 – 700 nm), while the vegetation indices, such as NDVI and EVI, take into account only partially (RED region: 620-670 nm) the wavelength range at the basis of the plant physiological processes. For these reasons, the vegetation indices describe the biophysical structure of the canopy coverage but they do not have a direct relationship with the plant photosynthesis.

On the other hand, fPAR supplies information not only about the crop canopy growth status, providing a description of the plant biomass accumulation or LAI expansion, but it also includes an important weather variable represented by the solar radiation. The intercepted solar radiation has a direct impact on the physiological processes underlying the crop growth and production. A reduction of leaf growth involves a reduction of yield due to insufficient energy capture (Gardner et al., 1985; Campillo et al., 2012).

In this context, the integration between fPAR and crop modeling tools can be particular interesting, taking into account that the solar radiation represents the main weather data rarely available for the crop models initialization.

Tab. 10.3.1 Correlations between durum wheat yield and RS indices

Index	R^2	*Sig.*	*Phenological stage*
EVI-13Q	0.280	**	From anthesis to beginning of grain filling
	0.160	*	From flag leaf stage to anthesis
EVI-13A	0.256	**	From anthesis to the beginning of grain filling
NDVI-13Q	0.352	**	From anthesis to the beginning of grain filling
	0.255	**	From ear emergence to anthesis
	0.233	*	From middle grain filling to grain maturity
NDVI-13A	0.286	**	From anthesis to the beginning of grain filling
LAI	0.646	***	Beginning of grain filling
	0.157	*	From flag leaf to ear emergence
fPAR	0.703	***	Beginning of grain filling
	0.245	*	Flag leaf to ear emergence
	0.176	*	Anthesis

Fig. 10.3.1 Linear regression between durum wheat yield observed during two growing seasons and the related MODIS fPAR acquired at beginning of grain filling.

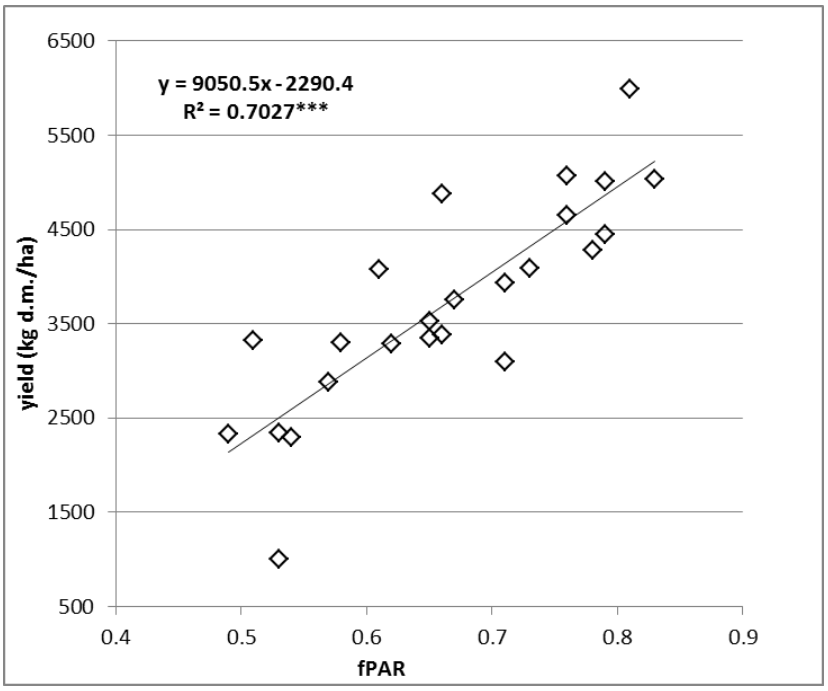

Fig. 10.3.2 Linear regression between durum wheat yield observed during two growing seasons and the related MODIS LAI acquired at beginning of grain filling.

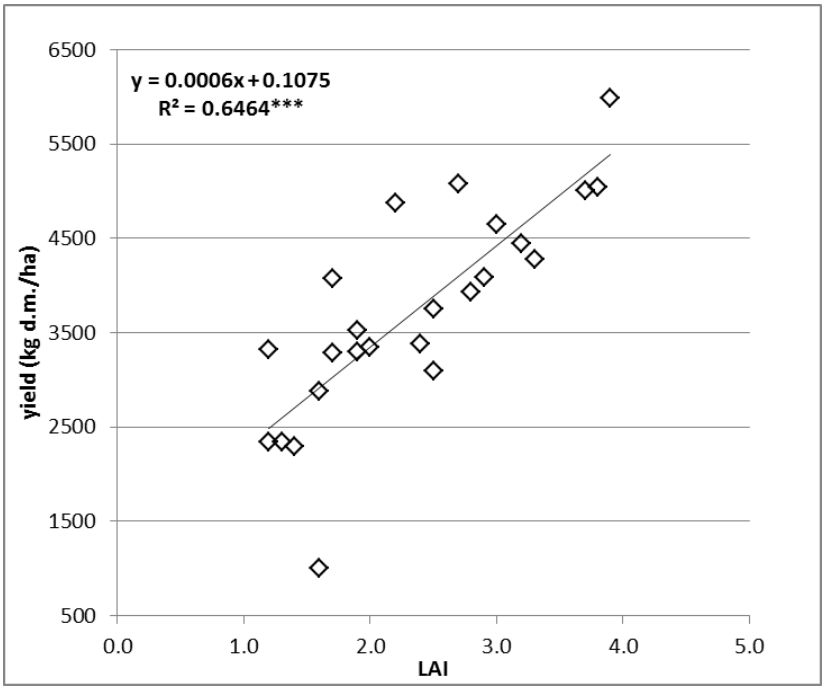

10.4. Spatialization algorithm for yield

fPAR data showed the higher significant correlation with GPC (R^2 = 0.7) (Tab. 10.3.1) at beginning of the grain filling stage. This period was assessed as the optimal time to obtain information about the crop, during which in both growing seasons the fPAR was not affected by abrupt changes in value (Tab. 10.1.1).

fPAR at beginning of the grain filling stage was used in the spatialization algorithm to simulate the yield spatial variability. Highly significant correlation (R^2 = 0.7) was found between Yd (yield deviation of each field from the yield annual average) and fPARd (fPAR deviation of each field from the fPAR annual average) in 2009-2010 growing season (Fig. 10.4.1). Equation 1 describes the assessment of Yd on the basis of fPARd.

(1) Yd = 11228 * fPARd + 9E-13

Fig. 10.4.1 Linear regression between the deviations from the annual average of yield (Yd) and fPAR (fPARd).

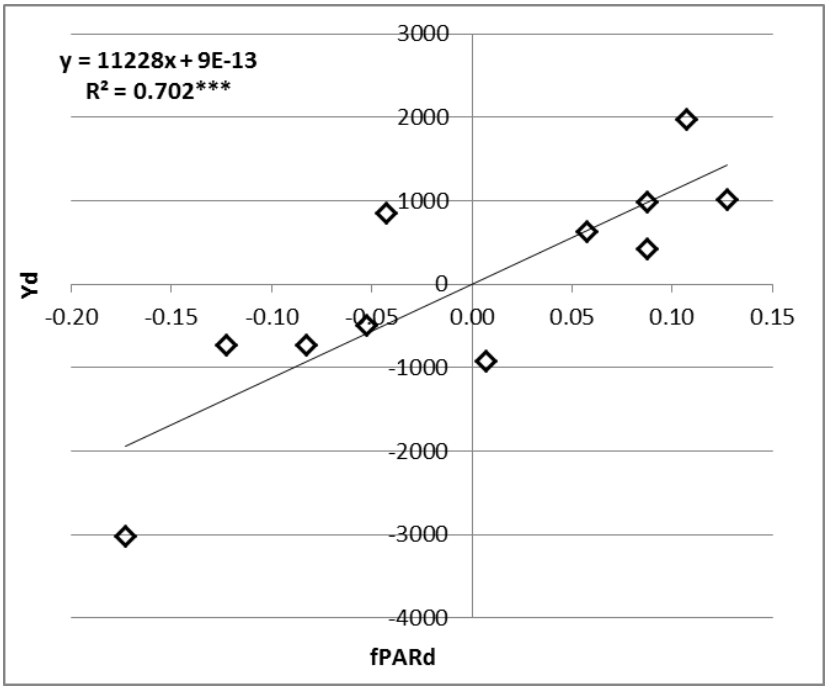

The equation 1 was implemented in the algorithm described by the equation 2.

(2) Yi = 5904 ± (11228 * fPARd + 9E-13)

Where: 5904 is the average yield (kg d.m./ha) simulate by CERES-Wheat for 2010 harvest.

The performance of equation 2 in simulation of yield spatial variability are shown in table. 10.4.1. Despite the highly significant correlation between assessed and observed data ($P \leq 0.001$, Fig. 10.4.2), the yield estimation based on CERES output and fPARd involved a considerable general error (RRMSE) mainly due to the major error indicated by CRM.

Therefore, the spatialization algorithm was corrected for the over-estimation error according to the equation 3.

(3) Y = 5904 ± (11228 * fPARd + 9E-13) – (Yi * 0.295)

Compared to equation 2, the performance in yield assessment was considerably improved with equation 3 (Tab. 10.4.1). The highly significant correlation between the assessed and observed yield (Fig. 10.4.3) was accompanied by a consistent reduction of general error (RRMSE) and an improvement of model efficiency (EF).

Tab. 10.4.1. CERES-Wheat performance and spatialization algorithm performance, at calibration (Eq. 4 and Eq. 5) and validation (Eq. 6) step.

Coefficient	*Eq. 2*	*Eq. 3*	*Eq. 4*	*CERES-Wheat*
R^2	0.70	0.70	0.74	0.7
RRMSE	45.44 %	19.3 %	14 %	20 %
EF	- 0.9	0.6	0.6	0.7
CRM	- 0.4	0.0	0.0	0.07

The spatialization algorithm was validate replacing in equation 3 the average yield simulated by CERES-Wheat for 2011 harvest (4574 kg d.m./ha) as shown in equation 4.

(4) Yi = 4574 ± (11228 * fPARd + 9E-13)

The good performance of the algorithm was confirmed by a highly significant correlation between assessed and observed yields ($P \leq 0.001$, Fig. 10.4.4), an unchanged model efficiency (EF), low general error (RRMSE) and an CRM value close to zero (Tab. 10.4.1)**.**

The results showed that the algorithm (Eq. 3 and 4) was able to simulate the yield spatial variability with a good accuracy, on the basis of the fPAR variability and CERES-Wheat output.

The good spatial coverage supplied by MODIS fPAR imagery has allowed to associate to each field a yield value close to that observed, improving the simulation in absence of model input data with suitable spatial resolution and accuracy (Tab. 10.4.1).

The integration between MODIS fPAR and CERES-Wheat led to an improvement of the yield assessment and allowed to use the complex simulation model as operationally running tool.

Fig. 10.4.2 Linear regression between observed yield in 2010 and those assessed following the Eq. 4

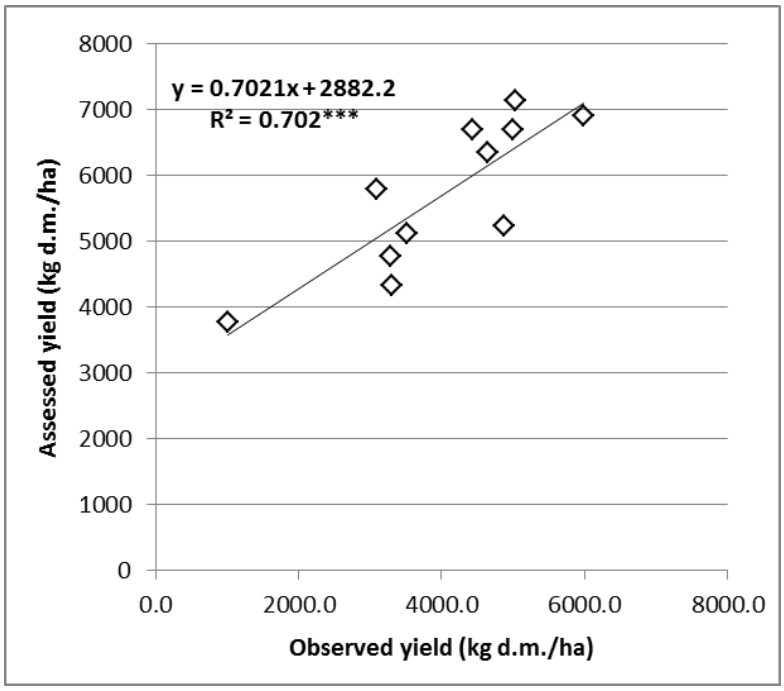

Fig. 10.4.3 Linear regression between observed yield in 2010 and those assessed following the Eq. 5

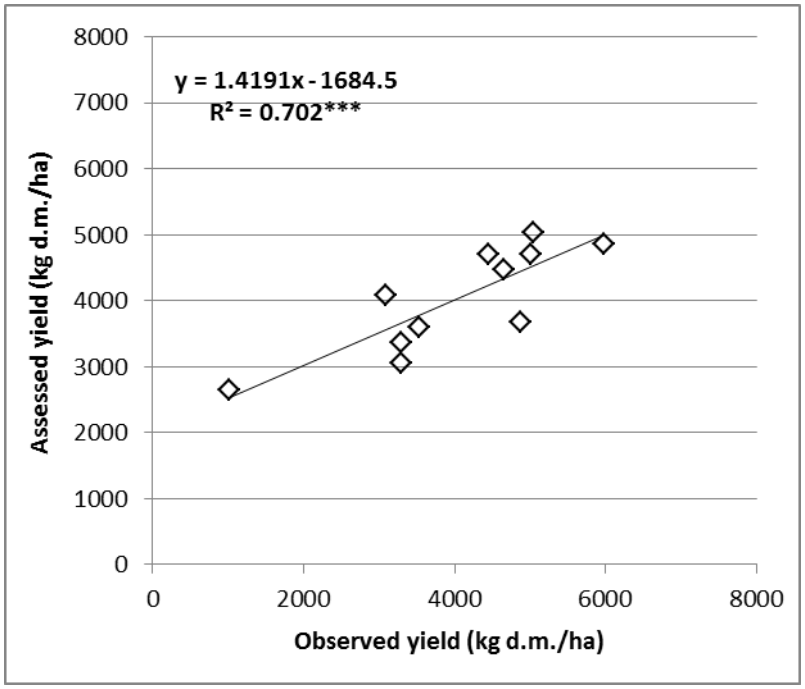

Fig. 10.4.4 Linear regression between observed yield in 2011 and those assessed following the Eq. 6.

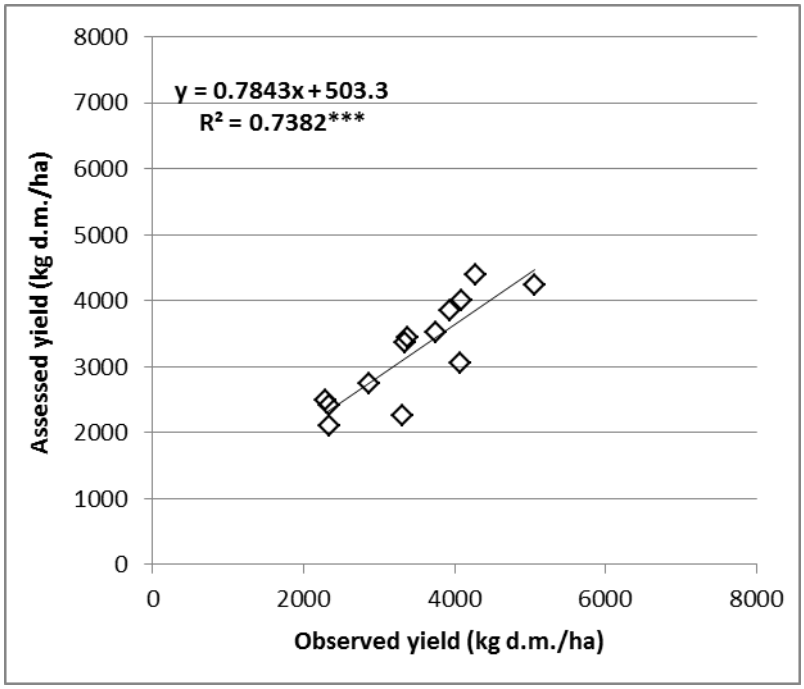

10.5. Relationship between remotely sensed indices and grain protein concentration

Significant and negative correlations were found between GPC and all RS indices (NDVI, EVI, LAI and fPAR) during the crop cycle, from the early period of seedling and tillering stage to grain maturity stage (Tab. 10.5.1 and 10.5.2).

These results are in contrast with those shown in literature. Studies on wheat showed a positive correlation between grain quality and the RS indices derived from the simple ratio NIR/RED (Basnet et al., 2003, Reyniers et al., 2006; Xue, 2007; Li et al., 2012).

These studies support the assumption that the protein deposition into the grain is source-limited, and then, is mainly determined by the total N content in the plant biomass (Jenner et al., 1991; Jamieson and Semenov, 2000). In agreement with this assumption, studies showed a positive correlation between GPC of wheat and the total leaf nitrogen (Wang et al., 2003; Huang et al., 2004; Li et al., 2005), and between this latter and the canopy LAI (Huang et al., 2004). Also the complex simulation models simulate the GPC on the basis of the source-limited assumption, including a positive relationship between LAI and GPC. In most of the crop models, such as CERES-Wheat (Ritchie et al., 1985), SWHEAT (Van Keulen and Selingman, 1987), AFRCWHEAT2 (Porter, 1993), APSIM-Nwheat (McCown et al., 1996; Asseng et al., 2002), and Pan' et al. model (2006), the wheat GPC depends on N uptake by the plant, which in turn is positively related to the nitrogen crop demand. Finally, the nitrogen crop demand is established on the basis of the leaf biomass or plant LAI.

On the other hand, the negative relationship between crop LAI and GPC is in agreement with the results of the previous study in section 1. The correlation analysis on fiend trials data highlighted a negative relationship between LAI and GPC (paragraph 8.5) and the deficiencies of CERES-Wheat in GPC simulation has been attributed to the model inability to fully capture the non- linear interactions between LAI, yield and GPC (paragraph 8.9). The negative correlation between GPC and RS indices supports the hypothesis that a GPC decrease can result from a LAI increase.

Tab. 10.5.1 Correlations between durum wheat GPC and both EVI and NDVI

Index	R^2	*Sig.*	*Phenological stage*
EVI-13Q	0.167	*	Tillering I (I half of February)
	0.381	**	Tillering I (II half of February)
	0.297	**	Tillering I (I half of March)
	0.416	***	From anthesis to beginning of grain filling
	0.294	**	From middle grain filling to grain maturity
	0.436	***	From anthesis to grain maturity
EVI-13A	0.457	***	Tillering I (I half of February)
	0.516	***	Tillering I (II half of February)
	0.537	***	Tillering I (February)
	0.402	***	Tillering I (I half of March)
	0.380	**	From flag leaf stage to anthesis
	0.270	**	From anthesis to beginning of grain filling
	0.462	***	From flag leaf stage to middle grain filling
	0.243	*	From middle grain filling to grain maturity
	0.276	**	From anthesis to grain maturity
NDVI-13Q	0.273	**	Tillering I (I half of February)
	0.427	***	Tillering I (II half of February)
	0.446	***	Tillering I (February)
	0.295	**	Tillering I (I half of March)
	0.447	***	Tillering I (February and March)
	0.177	*	From flag leaf stage to anthesis
	0.419	***	From anthesis to beginning of grain filling
	0.327	**	From middle grain filling to grain maturity
	0.420	***	From beginning of grain filling to grain maturity
NDVI-13A	0.470	***	Tillering I (I half of February)
	0.544	***	Tillering I (II half of February)
	0.257	**	Tillering I (I half of March)
	0.211	*	Tillering II (II half of March)
	0.321	**	From flag leaf stage to anthesis
	0.316	**	From anthesis to beginning of grain filling
	0.359	**	From flag leaf stage to beginning of grain filling
	0.320	**	From middle grain filling to grain maturity
	0.328	**	From beginning of grain filling to grain maturity

Tab. 10.5.2 Correlations between durum wheat GPC and both LAI and fPAR

Index	R^2	*Sig.*	*Phenological stage*
LAI	0.459	***	Tillering I (I half of February)
	0.350	**	Tillering I (II half of February)
	0.260	**	Tillering I (February)
	0.463	***	Tillering I (I half of March)
	0.267	**	Tillering II (II half of March)
	0.269	**	Tillering II (March)
	0.227	*	Stem elongation
	0.251	*	Beginning of grain filling
	0.298	**	Middle grain filling
	0.366	**	From beginning to middle of grain filling
	0.239	*	From end grain filling to grain maturity
fPAR	0.5753	***	Tillering I (I half of February)
	0.303	**	Tillering I (II half of February)
	0.405	***	Tillering I (February)
	0.544	***	Tillering I (I half of March)
	0.357	**	Tillering II (II half of March)
	0.306	**	From end tillering to stem elongation
	0.267	**	Beginning of grain filling
	0.323	**	Middle grain filling
	0.401	***	From beginning to middle of grain filling
	0.303	**	From end grain filling to grain maturity

The LAI increase can be able to promote the yield so that the benefits, related to the greater N supply from the leaf biomass, are minimized by the inverse relationship between yield and GPC.

This assumption explains the negative correlation between NDVI and durum wheat GPC that was found by some authors (Orlandini et al., 2011). Similarly, the impact of a yield rise on GPC can explain the lack of significant correlation between NDVI and GPC, shown in some studies (Freeman et al., 2003; Liu et al., 2006, Xue et al., 2007). The interaction between yield and GPC represents a confounding factor in the study of the relationship between LAI, or RS indices describing LAI, and wheat grain quality.

EVI and NDVI, at both spatial resolution, as well as LAI and fPAR, showed significant correlations during the early period of crop development, in February and March (Tab. 10.5.1 and 10.5.2). Also during the following periods, from flag leaf stage to grain maturity, correlations were found between GPC and RS data.

Despite this, the higher R^2 values were associated for all indices at the first phase of tillering, in February (Fig. 10.5.1), with the only exception of EVI-13Q. EVI imagery at higher spatial resolution instead showed higher R^2 during the period from anthesis to beginning of grain filling stage (Fig. 10.5.2).

These results can be explained by taking into account the fact that canopy coverage at seedling and tillering stages is mainly influenced by the sowing date. The later sowings tend to result in lower soil cover at beginning of the growing season compared to the fields that are sown earlier. Some authors highlighted the influence of the sowing date on final GPC (Ciaffi et al., 1996; Singh and Jain, 2000; Ehdaie and Waines, 2001). About this, the sowing date is able to influence the onset of grain filling stage, shifting this key development phase in early or late summer. The different weather conditions that occur during this period affect the rate of the grain protein deposition in relationship to that of starch (Bhullar and Jenner, 1985; Garcia del Moral et al., 1995; Fernandez-Figares et al., 2000; Rharrabti et al., 2001a; Zhao et al., 2009).

In this context, low values of RS data at tillering stage can indicate a late sowing, which in turn may be associated with a onset of the grain filling stage in a late period. Warmer and more drought conditions, characterizing the late summer, involve higher GPC.

Indeed, water deficit or heat stress tend to shorten the duration of the grain filling stage, affecting the starch deposition more than the protein synthesis. This results in a relative increase of GPC (Campbell et al., 1981; Bhullar and Jenner, 1985; Garcia del Moral et al., 1995; Fernandez-Figares et al., 2000; Rharrabti et al., 2001a; Zhao et al., 2009).

However, the noise due to the presence of mixed pixel must be taken into account. Indeed, at beginning of the crop growing season, the pixel value of each field can be determined most by landscape components associated to other type of vegetation (e.g. trees and shrubs border, weed, etc.), than by the arable field, in which the crop coverage still represents a minimal percentage. In this case, the statistical relevance that was found would not be accompanied by meaningful information for crop analysis.

Therefore, it was not possible to establish the optimal timing for RS data acquisition to obtain information about the GPC.

Fig. 10.5.1 Linear regression between GPC and fPAR at seedling stage.

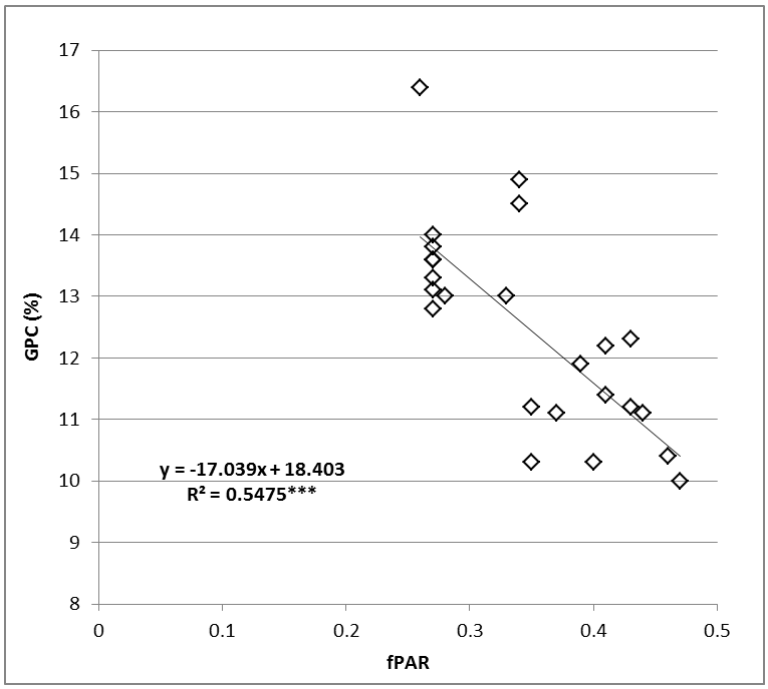

Fig. 10.5.2 Linear regression between GPC and EVI-13Q from anthesis to the beginning of grain filling stage.

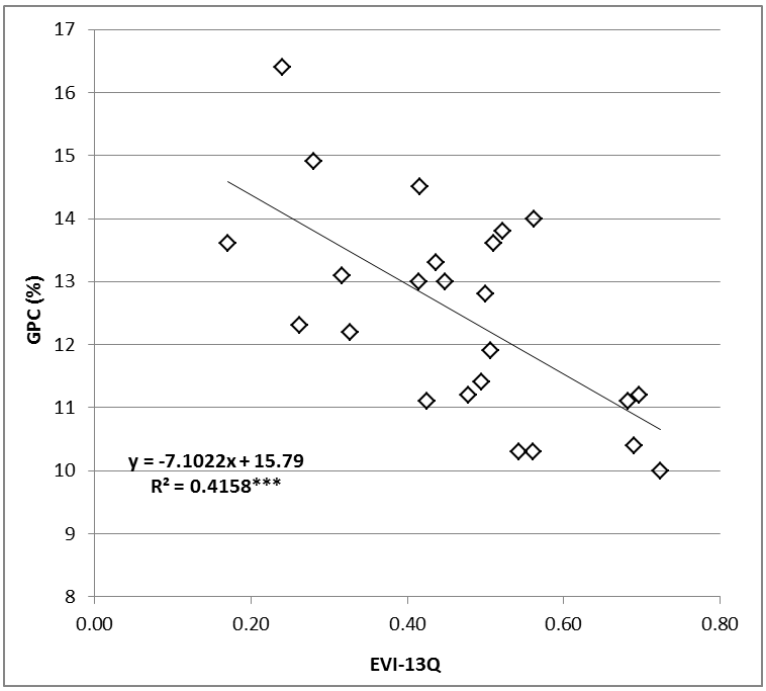

10.6. Spatialization algorithm for grain protein concentration

10.6.1. Analysis of fPAR values range

fPAR at early tillering stage showed the higher correlation with GPC (R^2 = 0.57) (Tab. 10.5.2). The performance of fPAR in describing GPC variability was. However, the significance of the correlation with GPC was not sufficient to calibrate and validate the spatialization algorithm for CERES output over the two growing seasons, as was made for the yield. This result confirmed the doubts about the meaningfulness of the correlation, suggesting the presence of some deficiencies in adapting the analysis process used with the yield (paragraphs 10.3 and 10.4) to GPC.

Therefore, the data were analyzed with a different approach. The previous study (paragraph 8.8 and 8.9, section 1) highlighted the role of the values range of LAI in determining the relationship with GPC. Within an intermediate range, LAI was positively related to GPC, while, beyond the middle range, LAI was negatively correlated with GPC.

This assumption was confirmed by the correlation analysis between GPC and fPAR, carried out separately per quartiles, I and IV quartile, on one hand, and II and III quartile, on the other. The fields in I and IV quartiles showed highly significant and negative correlations between GPC and fPAR during the crop vegetative growth, in particular at tillering and booting stage. (Tab. 10.6.1.). On the other hand, no correlations were found for fields in II and III quartiles.

Since fPAR is strictly related to LAI (Tian et al., 2004; Yang et al., 2006; Hipps et al., 1983), these results showed that, within an intermediate range, increases of LAI are not associated with a GPC decrease, because the negative impact of yield on GPC is compensated by the benefits due to the higher N availability from leaf biomass. However, the positive impact of a LAI rise within the middle range was not able to significantly increase the GPC. On the other hand extreme values of LAI significantly affected the grain quality. When LAI increases beyond the middle range, the resulting rise in yield depresses the GPC, overriding the positive impact of a higher amount of available N for the translocation into the grain.

The optimal timing to obtain information about crop GPC for fields in I and IV quartiles corresponded to the flag leaf and booting stage. During this period the highest negative correlation (R^2 = 0.9) between GPC and fPAR was found (Fig. 10.6.1).

Tab. 10.6.1 Correlations between GPC recorded in fields of I and IV quartiles and fPAR

Index	R^2	*Sig.*	*Phenological stage*
fPAR	0.764	***	Tillering I (I half of February)
	0.670	***	Tillering I (I half of March)
	0.647	***	Tillering II (II half of March)
	0.909	**	Flag leaf – booting stage

Fig. 10.6.1 Linear regression between GPC and fPAR during the flag leaf and booting stage.

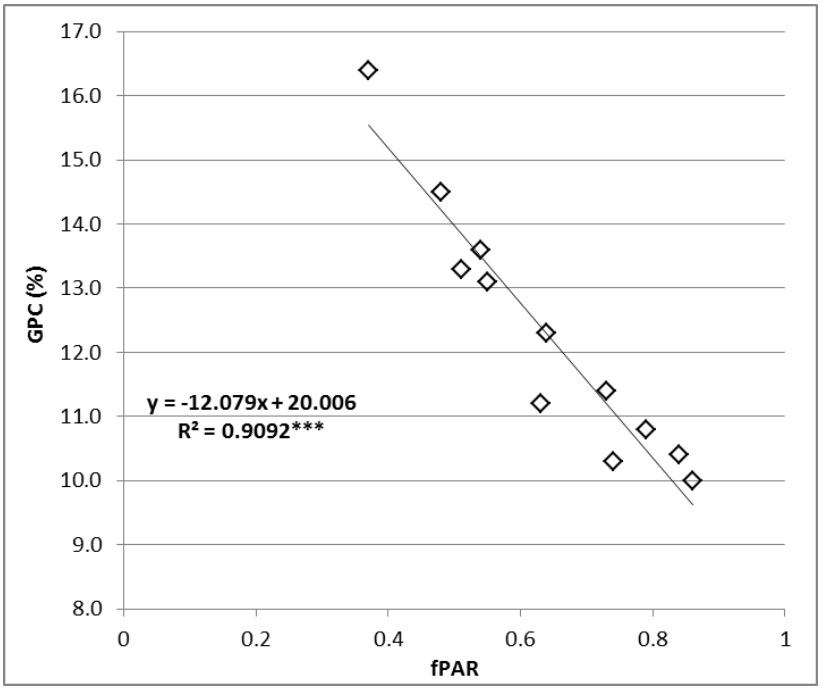

The identified optimal time occurred in most of fields between 106 JD and 113 JD, with few exceptions for fields showing plants phenologically earlier or later than average. During this time-step, in 2010 fPAR on average reached the maximum value, while in 2011 the index was affected by an abrupt change of value (Tab. 10.1.1). The abrupt change was due to a persistent cloud cover during the acquisition time-step. This type of atmospheric noise represents one of the main limits in assessment of yield on the basis of the direct relationship between RS data and harvest. A correlation found during a growing season can be not valid for the next, mainly because the atmospheric conditions can occurs differently, resulting in a different regression model for the yield assessment.

However, assuming that an homogeneous cloud cover affects in the same way the reflectance responses of fields that are in the same study area, the resulting relative decrease of RS values can be assumed of similar intensity for all the fields. Therefore, the relative differences among canopies belonging to different fields are preserved. In this context, RS values still are able to provide information about the yield deviation of each field from the average.

Moreover, the choice of fPAR, instead to the other indices, to describe the spatial and temporal variability of the harvest, offers some advantages.

The value of fPAR is a function of both LAI and the quality of incident PAR, and this latter in turn is conditioned by sky conditions (Hipps et al., 1983). Therefore, on one hand, fPAR, being strictly related to wheat LAI (Hipps et al., 1983), green foliage (Wilson and Jamieson, 1985; O'Connell et al., 2004), and biomass accumulation (Green, 1987), is able to provide information on the amount of dry matter and nutrients stored in the plant tissues and then available for the translocation and deposition into the grain.

On the other hand, fPAR describes the impact of the solar radiation on the crop. fPAR value is determined in relationship to the available energy for the photosynthetic process. The literature on wheat showed that during the period when the assimilates are portioned toward the production of the reproductive organs (spikes, spikelets and grains), a decrease of radiation depresses the crop yield. The spike development phase,

that occurs approximately from 20-30 days before the anthesis (flag leaf and booting stage) to one week after anthesis, and the grain filling stage were shown as the more critical periods (Willey and Holliday, 1971; Fisher, 1975; Abbate et al., 1997).

A decrease of solar radiation during this period involved a significant reduction of grains number per mq or per spike, spikes weight per mq and weight per grain. Taking into account the well-established inverse relationship between GPC and yield, this can explain the high and negative correlation that was found between GPC and fPAR value at flag leaf and booting stage. This can explain the higher correlation that was found between fPAR and GPC at flag leaf and booting stage, compared to those detected during the tillering stage.

Finally, the decrease of RS values, due to persistent cloud cover, does not represent an element of noise anymore, that limits the GPC assessment from RS data, but an added value. Thanks to the abrupt changes in values, fPAR supplies the description and quantification of a weather variable of major importance in determining of the harvest.

10.6.2. Spatialization algotithm for GPC

The performances in describing the GPC variability of 12 different algorithms, resulting from the cross-validation, in comparison with CERES-Wheat, are shown in table 10.6.2. All the algorithms was correlated with GPC at $P \leq 0.001$, while most of the correlations shown by CERES-Wheat output were significant at $P \leq 0.01$, with one exception significant at $P \leq 0.001$ (Tab. 10.6.2).

The spatialization algorithms have showed on average a $R^2 = 0.89$, a model efficiency close to the optimum (EF = 0.68), a low RRMSE, ranging between 7.29 % and 8.9 %, and, thanks to the adoption of FC, a null CRM. On the other hand, CERES-Wheat showed on average a $R^2 = 0.57$ and EF = – 1.72, a higher RRMSE, ranging between 21.52 % and 25.75 %, and an important error of under-estimation described by CRM = 0.21.

The adoption of the algorithm was able to accurately simulate the spatial and temporal GPC variability, starting from CERES-Wheat output. The algorithm improved significantly the model performance in case of lack of detailed input data.

On the basis of the standard deviations, resulting from the cross validation, the general algorithm showed the following performance: highly significant R^2 ($P \leq 0.001$) equal to 0.84, RRMSE of 9.84, EF of 0.65 and CRM equal to zero.

The II algorithm in table 10.6.2 was chosen for the best performance at validation. It is described by the following equations 1, 2 and 3.

Tab. 10.6.2 Performances in GPC simulation of the spatialization algorithms, in comparison with the CERES-Wheat output. Legend: St.dev. = Standard deviation at validation

Algorithm N°	***CERES-Wheat Output***					***Algorithm***				
	R^2	*RRMSE*	*EF*	*CRM*	*St.dev.*	R^2	*RRMSE*	*EF*	*CRM*	*St.dev.*
I	0.62 **	25.12	-1.48	0.21	8.56	0.89 ***	8.9	0.69	0	0.21
II	0.53 **	25.65	-1.96	0.22	0.86	0.88 ***	8.69	0.66	0	**0.01**
III	0.53 **	25.64	-1.92	0.22	1.05	0.88 ***	8.7	0.66	0	3.68
IV	0.52 **	25.64	-2.09	0.22	0.39	0.87 ***	8.71	0.64	0	3.3
V	0.56 **	25.48	-1.64	0.21	4.1	0.89 ***	8.82	0.68	0	0.99
VI	0.54 **	25.61	-1.79	0.22	2.03	0.88 ***	8.77	0.67	0	1.96
VII	0.52 **	24.06	-1.53	0.2	20.25	0.87 ***	8.55	0.68	0	0.34
VIII	0.73 ***	25.75	-1.73	0.22	1.44	0.94 ***	8.22	0.72	0	3.16
IX	0.57 **	25.14	-1.5	0.21	9.61	0.89 ***	8.81	0.69	0	1.08
X	0.56 **	25.02	-1.49	0.21	10.89	0.89 ***	8.67	0.7	0	2.34
XI	0.6 **	21.52	-2.06	0.19	40.96	0.86 ***	7.29	0.65	0	0.04
XII	0.54 **	24.82	-1.49	0.21	12.96	0.88 ***	8.79	0.69	0	0.4

The applied linear regression model, between Yd (GPC deviation of each field from the GPC annual average) and fPARd (fPAR deviation of each field from the fPAR annual average), is described by the equation 1 (Fig. 10.6.2). The linear regression model was implemented in the algorithm, as described by the equation 2. As described by equation 3, a correction factor (FC) for the under-estimation error was applied, providing a percentage increase of 28 % compared to GPC assessed with equation 2.

(1) Yd = 11.747 * fPARd + 9E-13

(2) Yi = OUT ± (11.747 * fPARd + 9E-13)

(3) Y = OUT ± (11.747 * fPARd + 9E-13) + (Yi * 0.28)

where: OUT is the GPC simulated by CERES-Wheat, equal to 9.4 % in 2010 and 10 % in 2011.

Fig. 10.6.2 Linear regression between the deviations from the annual average of GPC (Yd) and fPAR (fPARd), respectively.

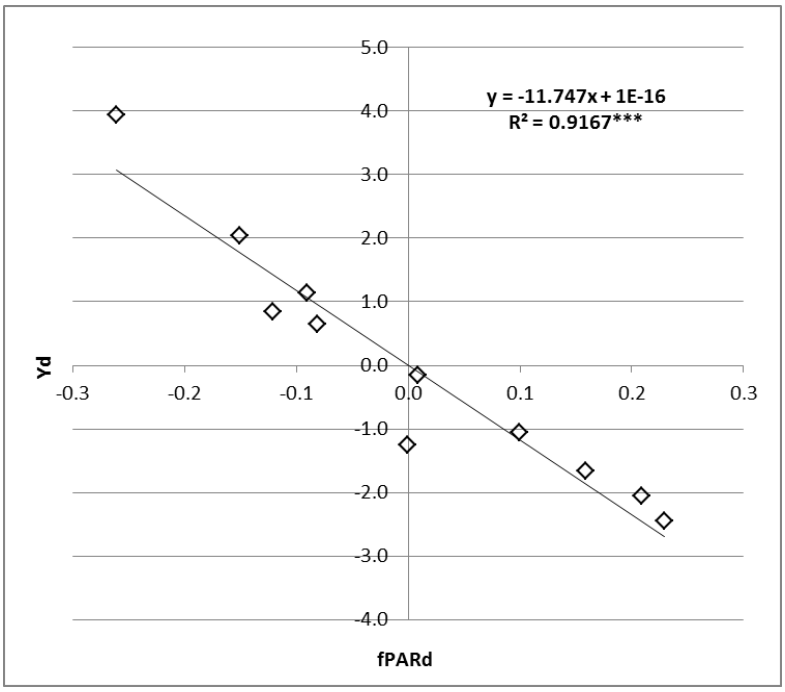

Highly significant correlation was found between Yd and fPARd (R^2 = 0.92) (Eq. 1, Fig. 10.6.2) and between the assessed and observed GPC (R^2 = 0.88) (Eq. 3, Fig. 10.6.3).

Fig. 10.6.3 Linear regression between observed GPC and that assessed on the basis of the equation 9.

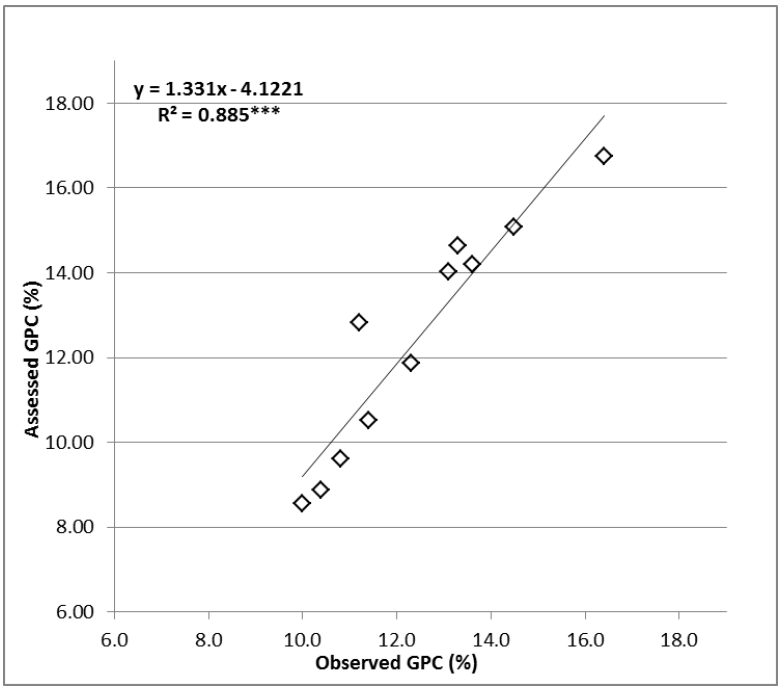

However, the algorithm, resulting from the integration between CERES-Wheat and RS data, was able to effectively simulate the GPC variability only for the fields in I and IV quartiles. These results suggested that the RS data can compensate the lack of spatial coverage of the model output only for the fields with LAI values beyond a middle range. On the other hand, the RS index was not able to provide information about the GPC variability of fields with LAI values within an intermediate range.

Finally, the algorithm was able to describe the negative impact on GPC of a yield rise, resulting from high LAI, as well as the positively impact on GPC of a yield reduction due to low LAI. Despite this the algorithm was not able to describe the impact on GPC resulting from LAI changes within a middle range.

11. CONCLUSIONS

- **Assessment of the weather impact on durum wheat yield and set up of a forecasting index with the support of crop modeling tools**

CERES-Wheat showed good performance in simulation of durum wheat yield. The complex model represented a useful tool to capture the interactions in the 'plant-soil-atmosphere' system and to determine the weather and crop variables affecting the harvest quantity.

CERES-Wheat supported the identification of the crop growth stages that were more susceptible to drought or warm stresses, and then crucial for the crop production. The yield was promoted by the water supply at tillering stage, showing highly significant correlations with the rainfall amount and distribution in March. On the other hand, the yield was negatively affected by drought and warm conditions in the late period, during the grain filling stage.

CERES-Wheat highlighted a positive and highly significant correlation between yield and plant leaf area index (LAI) at the end of the vegetative growth (ear emergence stage). The relationship was confirmed by the field data. LAI proved to be able to summarize the impact on the harvest quantity resulting from the combined effects and interactions between the environmental variables during the crop cycle.

The forecasting index showed good performance in yield prediction on the basis of the plant LAI in April and rainfall distribution in March. The index was able to provide early information about the yield, beginning in the second half of April.

Although the complex models are subject to limitations in operational applications, they can support the realization of simplified models, not subject to the same constraints. The simplified model, shown in the present study, represents a forecasting tool that is able to run with few input data, and is useful to optimize the late nitrogen fertilization at farm level. These results are particularly interesting taking into account the possibility to assess the LAI of the wheat canopy through satellite imagery, and, thus, to realize a farm supporting system based on the automated acquisition of remotely sensed and meteorological data.

- **Assessment of the weather impact on durum wheat quality and set up of a forecasting index of GPC with the support of crop modeling tools**

CERES-Wheat showed lower performance in the simulation of GPC in comparison to that of the yield. This result confirms the restrictions to which the complex models are subject in GPC simulation, highlighted in the literature (Otter-Nacke et al., 1986; Asseng et al., 1998; Meinke et al., 1998; Asseng et al., 2002). However, the new routine for GPC simulation improved the assessment of harvest quality. It was based on CERES-Wheat outputs relating the weight of the above ground biomass and grain, and the N concentration of leaves and steam, at beginning of grain filling. The new routine better described the durum wheat responsiveness in term of GPC compared to ordinary wheat, mainly through the reduction of the under-estimation error. Despite this, the correlation between observed and simulated data still showed a lower significance (R^2 = 0.4) compared to that of yield (R^2 = 0.7).

The rainfall trend affected the GPC at all development stages and, in particular, at tillering and seedling stage. The results showed an inverse relationship between the water availability and harvest quality. The temperatures had a different impact on GPC depending on the development stage of the crop. Cold weather during the crop vegetative growth promoted the harvest quality, while the GPC was improved by warm conditions during the grain filling stage. These results can be explained on the basis of the well-established negative relationship between wheat yield and GPC (Spiertz, 1977; Johnson et al., 1985; Fischer et al., 1993; Feil, 1997; Novaro et. at, 1997; Rharrabti et al., 2001a; Rharrabti et al., 2001b). Therefore, the results support the assumption that environmental conditions to the disadvantage of yield and the grain starch accumulation, involve a relative increase of GPC. Finally, CERES-Wheat seemed able to capture the interactions between the weather variables and the processes governing the GPC deposition in to the grain.

On the other hand, the model showed some deficiencies in fully capturing the interactions between plant LAI and GPC. CERES-Wheat described a significant and positive correlation between GPC and LAI value at the end of crop vegetative growth.

This result was not confirmed by the field data that instead highlighted a negative correlation between GPC and leaf expansion. As a consequence, the forecasting index was able to provide a reliable assessment of GPC only for the fields showing LAI values within an intermediate range, based on the correlations described by CERES-Wheat. For these fields, the forecasting index has supplied accurate predictions of GPC. On the other hand, the forecasting index has totally failed in the simulation of GPC for the fields with LAI values beyond the middle range. The fields for which the forecasting index was unable to describe the GPC variability, were the same that showed a significant and inverse relationship between observed GPC and yield. The results highlighted a non-linear relationship between LAI and GPC.

Increases of LAI within an middle range positively affect GPC, since GPC depends on the total N stored in the vegetative tissues (Dalling, 1985; Wang et al, 2003, Huang et al., 2004; Li et al., 2005). This type of interaction between the two variables is the basis for GPC simulation, adopted by CERES-Wheat, as well as by the other complex models (Jenner et al., 1991; Jamieson and Semenov, 2000).

Therefore, CERES-Wheat described a positive impact of a LAI rise on both GPC and yield. However, in this way, CERES-Wheat does not take into account the well-established inverse relationship between GPC and yield, that was shown in the literature (Spiertz, 1977; Johnson et al., 1985; Fischer et al., 1993; Feil, 1997; Novaro et. at, 1997; Rharrabti et al., 2001a; Rharrabti et al., 2001b), as well as by the field data.

Beyond a middle range and towards extreme LAI values, the influence of the inverse relationship between yield and GPC overrides the benefits resulting from the increasing N supply in leaf biomass. Therefore, higher LAI values, which promoted the yield, minimized the GPC, while lower LAI values, being a disadvantage for grain yield, were able to support the GPC. Finally, CERES-Wheat can be used to study the determinants for GPC, the simulation algorithms that underlie the relationships between GPC, yield and LAI must be revised. This point is particular important for durum wheat production. Indeed, in durum wheat the yield impact on GPC is emphasized more compared to common wheat (Cossani et al., 2011) and an increase of grain weight is accompanied by a higher pronounced decrease of grain N percentage (Cossani et al., 2011).

- **Integration between crop modeling tools and RS indices to monitor the harvest quantity of durum wheat**

The RS indices from MODIS imagery (NDVI, EVI, LAI and fPAR) pointed out that durum wheat reached the maximum value of canopy coverage during the period when the plants shift from the vegetative growth phase to the reproductive phase (from flag leaf stage to beginning of grain filling stage). Within this period, fPAR showed the higher significant correlation with the observed yield. These results showed the improved ability of this index in the description of the plant physiological processes underlying the wheat growth and production, compared to those of the other MODIS products.

The spatialization algorithm supplied a reliable description of the spatial and temporal variability of harvest quantity. The integration of RS data with crop modeling tools was able to improve the yield assessment in case of lack of input data with suitable level of accuracy. The good spatial coverage of RS data minimized the uncertainty in the spatial distribution of growing environment variables and improved the spatial representativeness and confidence of the model output. The simple integration approach proved to be able to translate the crop model in a tool that can run operationally for supporting applications at farm level.

- **Integration between crop modeling tools and RS indices to monitor the harvest quality of durum wheat**

The results highlighted a negative relationship between RS indices and GPC, supporting the previous assumptions: i.e. a LAI increase can involve a GPC decrease. Moreover, the result emphasized once again the relevant role of fPAR in describing the harvest variability in terms of both quality and quantity. Compared to the other indices, fPAR showed an added value. fPAR supplies a description not only of the crop canopy but also of the solar energy available for the plant processes, underlying the crop growth and production. Thanks to this, the abrupt changes in values of fPAR, due to persistent cloud cover, do not represent an element of noise anymore, but a quantification of a weather variable of major importance in determining of the harvest. The integration of MODIS imagery of fPAR with crop modeling is particular interesting, taking into account that the solar radiation is the main weather data rarely available for the crop models initialization.

However, analyzing all the data, no correlations were found with sufficient R^2 to describe the GPC variability. On the other hand, interesting results were highlighted from the analysis carried out separately per quartiles on the basis of the maximum RS value. fPAR at booting stage was able to very well capture the GPC variability for the fields having RS values beyond an middle range (I and IV quartile). Increasing or decreasing values of fPAR, above or below a threshold respectively, were found correlated to the grain quality. On the other hand, changes in LAI values within a middle range do not significantly affected the GPC.

These results confirmed the non-linear relationship between LAI and GPC. Once again the interaction between yield and GPC represented a confounding factor in the study of the relationship between LAI, or RS indices describing LAI, and harvest quality. This confounding factor resulted to be at the basis of CERES-Wheat deficiencies in GPC simulation, and must be taken into account also for the assessment of GPC on the basis of RS data. The capacity of the interaction between yield and GPC to override the impact on GPC of the nitrogen sources of the plant biomass, may cover a key role especially for durum wheat.

References

- Abbate P.E., Andrade F.H., Culot J.P., Bindraban P.S., 1997. Grain yield in wheat: effects of radiation during spike growth period. Field Crops Res. 54, 245‑257.
- Abedi T., Alemzadeh A., Kazemeini S. A., 2011. Wheat yield and grain protein response to nitrogen amount and timing. Australian Journal of Crop Science 5(3), 330-336.
- Acevedo E., Silva P., Silva H., 2002. Wheat growth and physiology. In: Bread wheat. (Eds.) Curtis B.C., Rajaram S., Gómez Macpherson H., FAO Plant Production and Protection Series 2002.
- Asrar G., Fuchs M., Kanemasu E.T., Hatfield J.L., 1984. Estimating absorbed photosynthetically active radiation and leaf area index from spectral reflectance in wheat. Agron. J. 76, 300–306.
- Asseng S., Keating B.A., Fillery I.R.P., Gregory P.J., Bowden J.W., Turner N.C., Palta J.A., Abrecht D.G., 1998. Performance of the apsim-wheat model in Western Australia. Field Crops Res. 57, 163‑179.
- Asseng S., Bar-Tal A., Bowden J.W., Keating B.A., Van Herwaarden A., Palta J.A., Huth N.I., Probert M.E., 2002. Simulation of grain protein content with APSIM-Nwheat. European Journal of Agronomy 16, 25‑42.
- Al-Khatib K., Paulsen G.M., 1984. Mode of high temperature injury to wheat during grain development. Physiologia Plantarum 61, 363-8.
- Angus J.F., Mackenzie D.H., Morton R., Schafer C.A., 1981. Phasic development in field crops. II. Thermal and photoperiodic responses of spring wheat. Field Crops Research 4, 269-83.
- Aparicio N., Villegas D., Casadesus J., Araus J.L., Royo C., 2000. Spectral vegetation indices as nondestructive tools for determining durum wheat yield. Agronomy Journal 92, 1547-1555.
- Aparicio N., Villegas D., Araus J.L., Casadesus J., Royo C., 2002. Relationship between growth traits and spectral vegetation indices in durum wheat. Crop Science 42, 1547-1555.

- Asrar, G., Myneni R.B., Choudhary B.J., 1992. Spatial heterogeneity in vegetation canopies and remote sensing of absorbed photosynthetically active radiation: a modeling study. Remote Sensing of Environment 41, 85–103.
- Babar M.A., Reynolds M.P., Van Ginkel M., Klatt A.R., Raun W.R., Stone M.L., 2006. Spectral reflectance to estimate genetic variation for in-season biomass, leaf chlorophyll, and canopy temperature in wheat. Crop Science 46, 1046-1057.
- Baez-Gonzalez A.D., Chen P., Tiscareño-Lopez M., Srinivasan R., 2002. Using satellite and field data with crop growth modeling to monitor and estimate corn yield in Mexico. Crop Sci. 42, 1943–1949,
- Bannari A., Morin D., Bonn F. Huete A. R., 1995. A review of vegetation indices. Remote Sensing Reviews13, 95-120
- Basnet B.B., Apan A.A., Kelly R.M., Jensen T.A., Strong W.M., Butler D.G., 2003. Relating satellite imagery with grain protein content. Spatial Sciences 2003, 1-11.
- Baret F., Guyot G., 1991. Potentials and limits of vegetation indices for LAI and APAR assessment. Remote Sens. Environ. 35, 161–173.
- Basnyat P., McConkey B., Lafond G.R., Moulin A., Pelcat Y., 2004. Optimal time for remote sensing to relate to crop grain yield on the Canadian prairies. Canadian Journal of Plant Science 84, 97‑103.
- Batts G.R., Ellis R.H., Morison J.I.L. and Hadley P., 1998a. Canopy development and tillering of field-grown crops of two contrasting cultivars of winter wheat (Triticum *aestivum*) in response to CO_2 and temperature. Annals of Applied Biology 133, 101–109.
- Batts G.R., Ellis R.H., Morison J.I.L., Nkemka P.N., Gregory P.J. and Hadley P., 1998b. Yield and partitioning in crops of contrasting cultivars of winter wheat in response to CO_2 and temperature in field studies using temperature gradient tunnels. Journal of Agricultural Science, Cambridge University Press 130, 17-27.
- Beck P.S.A., Jonsson P., Hogda K.A., Karlsen S.R., Eklundh L., Skidmoree A.K., 2007. A ground-validated NDVI dataset for monitoring vegetation dynamics and mapping phenology in Fennoscandia and the Kola peninsula. International Journal of Remote Sensing 28, 4311–4330.

- Becker-Reshef I., Vermote E., Lindeman M., Justice C., 2010. A generalized regression-based model for forecasting winter wheat yields in Kansas and Ukraine using MODIS data. Remote Sensing of Environment 114, 1312‑1323.
- Bellairs S.M., Turner N.C., Hick P.T, Smith R.C.G., 1996. Plant and soil influences on estimating biomass of wheat in plant breeding plots using field spectral radiometers. Australian Journal of Agricultural Research 47, 1017 – 1034.
- Benedetti R., 1993. On the use of NDVI profiles as a tool for agricultural statistics: The case study of wheat yield estimate and forecast in Emilia Romagna. Remote Sensing of Environment 45, 311–326.
- Bhatia C.R., 1975. Criteria for early generation selection in wheat breeding programmes for improving protein productivity. Euphytica 24, 789-794.
- Bhullar S.S., Jenner C.F., 1985. Differential responses to high temperatures of starch and nitrogen accumulation in the grain of four cultivars of wheat. Aust. J. Plant Physiol. 12, 363 - 375.
- Bly A.G., Woodard H.J., 2003. Foliar nitrogen application timing influence on grain yield and protein concentration of hard red winter and spring wheat. Agron J 95, 335–338.
- Blumenthal C.S., Batey I.L., Wrigley C.W., Barlow E.W.R., 1982. Seasonal changes in wheat-grain quality associated with high temperatures during grain filling. Australian Journal of Agricultural Research 42, 21–30.
- Bolten J.D., Crow W.T., Zhan X., Jackson T.J., Reynolds C.A., 2010. Evaluating the utility of remotely sensed soil moisture retrievals for operational agricultural drought Monitoring. IEEE Journal of selected topics in applied earth observations and remote sensing Vol. 3, n 1.
- Box E.O., Holben B.N., Kalb V., 1989. Accuracy of the AVHRR Vegetation Index as a predictor of biomass, primary productivity and net CO2 flux. Plant Ecology 80, 71-89
- Bronge L.B., 2004. Satellite Remote Sensing for Estimating Leaf Area Index, FPAR and Primary Production: A Literature Review. (Eds.) Svensk Kärnbränslehantering A.B..

- Brown, B.D., Petrie, S., 2006. Irrigated hard winter wheat response to fall, spring, and late season applied nitrogen. Field Crops Res 96, 260–268.
- Campbell C.A., Davidson H.R., Winkelman G.E., 1981. Effect of nitrogen, temperature, growth stage and duration of moisture stress on yield components and protein content of Manitou spring wheat. Can. J. Plant Sci. 61, 549 - 563.
- Campillo C., Fortes R., Del Henar Prieto M., 2012. Solar Radiation Effect on Crop Production. In: Solar Radiation. Chapter 11. (Eds.) Babatunde E.B, InTech Pub., March 2012.
- Casanova D., Epema G.F., Goudriaan J., 1998. Monitoring rice reflectance at field level for estimating biomass and LAI. Field Crops Research 55, 83‑92.
- Ciaffi M., Tozzi L., Borghi B., Corbellini M., Lafiandra D., 1996. Effect of Heat Shock During Grain Filling on the Gluten Protein Composition of Bread Wheat. Journal of Cereal Science 24, 91–100
- Clevers J.G.P.W., Vonder O.W., Jongschaap R.E.E., Desprats J.F., King C., Prévot L., Bruguier, N., 2002. Using SPOT data for calibrating a wheat growth model under Mediterranean conditions. Agronomie 22, 687 - 694.
- Cossani C.M., Slafer G.A., Savin R., 2011. Do barley and wheat (bread and durum) differ in grain weight stability through seasons and water–nitrogen treatments in a Mediterranean location?. Field Crops Research 121, 240-247.
- Cox M.C., Qualset C.O., Rains D.W., 1985. Genetic variation for nitrogen assimilation and translocation in wheat: II. Nitrogen assimilation in relation to grain yield and protein. Crop Sci. 25, 435–440.
- Cubadda R. E., Carcea M., Marconi E., Trivisonno M.C., 2007). Influence of gluten proteins and drying temperature on the cooking quality of durum wheat pasta. Cereal Chemistry 84, 48–55.
- Dailiang P., Lianqing Z., Jingfeng H., Bin Z., Fumin W., 2011. Rice yield estimation based on MODIS EVI and measured data derived from statistical sampling plots at province level. Transactions of the Chinese Society of Agricultural Engineering 2011-09

- Dalirie M.S., Sharifi R.S., Farzaneh S., 2010. Evaluation of yield, dry matter accumulation and leaf area index in wheat genotypes as affected by terminal drought stress. Notulae Botanicae Horti AgrobotaniciCluj-Napoca 38, 182-186.
- Dalling M.J., 1985. The physiological basis of nitrogen redistribution during grain filling in cereals. In: Exploitation of Physiological and Genetic Variability to Enhance Crop Productivity. (Eds.) Harper J.E., Schrader L.E., Howell R.W., American Society of Plant Physiologists, Rockville, MD, p. 55–71.
- Dawson I.A, Wardlaw, I.F., 1989. The tolerance of wheat to high temperatures during reproductive growth III. Booting to anthesis. Australian Journal of Agricultural Research 40, 965-980.
- D'Egidio M.G., Mariani B.M., Nardi S., Novaro P., 1993. Viscoelastograph measures and total organic matter test: Suitability in evaluating textural characteristics of cooked pasta. Cereal Chemistry 70, 67–72.
- Dente L., Satalino G., Mattia F., Rinaldi M., 2008. Assimilation of leaf area index derived from ASAR and MERIS data into CERES-Wheat model to map wheat yield. Remote Sensing of Environment 112, 1395–1407
- Dettori M., Cesaraccio C., Motroni A., Spano D., Duce P., 2011. Using CERES-Wheat to simulate durum wheat production and phenology in Southern Sardinia, Italy. Field Crops Research 120, 179–188.
- De Vita P., Di Paolo E., Fecondo G., Di Fonzo N., Pisante M., 2007. No-tillage and conventional tillage effects on durum wheat yield, grain quality and soil moisture content in southern Italy. Soil and Tillage Research 92, 69–78.
- De Wit A.J.W., Van Diepen C.A., 2007. Crop model data assimilation with the Ensemble Kalman filter for improving regional crop yield forecasts. Agricultural and Forest Meteorology, 146, 38‑56
- Doraiswamy P. C., Sinclair T.R., Hollinger S., Akhmedov B., Stern A., Pruegere J., 2005. Application of MODIS derived parameters for regional crop yield assessment. Remote Sensing of Environment 97, 192‑202.

- Doraiswamy P.C., Hatfield J.L., Jackson T.J., Akhmedov B., Prueger J., Stern A., 2004. Crop condition and yield simulations using Landsat and MODIS. Remote Sensing of Environment 92, 4548‑559.
- Dorigo W.A., Zurita-Milla R., De Wit A.J.W., Brazile J., Singh R., Schaepmanc M.E., 2007. A review on reflective remote sensing and data assimilation techniques for enhanced agroecosystem modeling. International Journal of Applied Earth Observation and Geoinformation 9, 165‑193.
- Ehdaie B., Waines J.G., 2001. Sowing date and nitrogen rate effects on dry matter and nitrogen partitioning in bread and durum wheat. Field Crops Research 73, 47–61.
- Eitzinger J., Stastna´ M., Zalud Z., Dubrovsky´ M., 2003. A simulation study of the effect of soil water balance and water stress on winter wheat production under different climate change scenarios. Agricultural Water Management 61, 195–217.
- Erekul O., Köhn W., 2006. Effect of weather and soil conditions on yield components and bread-making quality of winter wheat (*Triticum aestivum* L.) and winter triticale (*Triticosecale* wittm.) varieties in north-east Germany. Journal of agronomy and crop science 192, 452-464.
- Fang H., Liang S., Hoogenboom G., Teasdale J., Cavigelli M., 2008. Corn-yield estimation through assimilation of remotely sensed data into the CSM-CERES-Maize model. International Journal of Remote Sensing 29, 3011–3032.
- Fang H., Liang S., Hoogenboom G., 2011. Integration of MODIS LAI and vegetation index products with the CSM–CERES–Maize model for corn yield estimation. International Journal of Remote Sensing 32, 1039–1065.
- Faivre R., Goffinet B., Wallach D., 1991. Utilisation de données intermédiaires pour corriger la prédiction de modèles mécanistes. Biometrics 47, 1-12.
- Farrand E.A., 1972. Potential milling and baking value of home grown wheat. Journal of the National Institute of Agricultural Botany 12, 464-470.
- Ferris R., Ellis R.H., Wheeler T.R., Hadley P.,1998. Effect of high temperature stress at anthesis on grain yield and biomass of field-grown. Crops of Wheat Annals of Botany 82, 631-639.

- Feil B., 1997. The inverse yield-protein relationship in cereals: possibilities and limitations for genetically improving the grain protein yield. Trends Agron. 1, 103–119.
- Feller U., Crafts-Brandner S. J., Salvucci M.E., 1998. Moderately high temperatures inhibit Ribulose-1,5-Bisphosphate Carboxylase/Oxygenase (Rubisco) Activase-Mediated Activation of Rubisco. Plant Physiol. 116, 539–546.2283362
- Fensholt R., Sandholt I., Rasmussen M.S., 2004. Evaluation of MODIS LAI, fAPAR and the relation between fAPAR and NDVI in a semi-arid environment using in situ measurements. Remote Sensing of Environment 91, 490‑507
- Fernandez-Figares I., Marinetto J., Royo C., Ramos J.M., Garcıa del Moral L.F., 2000. Amino acid composition and protein and carbohydrate accumulation in the grain of triticale grown under terminal water stress simulated by a senescing agent. J. Cereal. Sci. 32, 249 - 258.
- Ferrio J.P., Villegas D., Zarco J., Aparicio N., Araus J.L., Royo C., 2005. Assessment of durum wheat yield using visible and near-infrared reflectance spectra of canopies. Field Crops Research 94, 126‑148.
- Feyereisen G.W, Sands G.R., Wilson B.N., Strock J.S., Porter P.M., 2006. Plant growth component of a simple rye growth model. Transactions of the Asabe 49, 1569‑1578.
- Field C.B., Gamon J.A., Peñuelas J., 1994Remote sensing of photosynthesis. In: Ecophysiology of photosynthesis, Ecological Studies. (Eds.) Schulze E.D., Caldwell M.M., Springer Pub., Berlin, Heidelberg, New York, p. 511‑527.
- Fischer R.A., 1975. Yield potential of dwarf spring wheat and the effect of shading. Crop Sci., 15, 607‑613.
- Fischer R.A., 1985. Number of kernels in wheat crops and the influence of solar radiation and temperature. Journal of Agricultural Science, Cambridge 105, 447–461.
- Fischer R.A., Howe G.N., Ibrahim Z.M., 1993. Irrigated spring wheat and timing and amount of nitrogen fertilizer I: Grain yield and protein content. Field Crops Research 33, 37–56.

- Fischer A., Kergoat L., Dedieu G., 1997. Coupling satellite data with vegetation functional models: review of different approaches and perspectives suggested by the assimilation strategy. Remote Sensing Reviews 15, 283-303
- Fischer R.A., 2011. Wheat physiology: a review of recent developments. Crop & Pasture Science 62, 95–114.
- Food and Agriculture Organization Statistics – FAOSTAT: http://faostat.fao.org.
- Freeman K.W., Raun W.R., Johnson G.V.,. Mullen R.W, Stone M.L., Solie J.B., 2003. Late-season prediction of wheat grain yield and grain protein. Communications in soil science and plant analysis 34, 1837–1852.
- Gallo K.P., Daughtry C.S.T, Baur M.E., 1985. Spectral estimation of absorbed photosynthetically active radiation in corn canopies. Remote Sens. Environ. 17, 221–232.
- Gallo K.P., Daughtry C.S.T., Wiegand C.L., 1993. Errors in measuring absorbed radiation and computing crop radiation use efficiency. Agron. J. 85, 1222–1228.
- Gamon J.A., Field C.B., Goulden M., Griffin K., Hartley A., Joel G., 1995. Relationships between NDVI, canopy structure, and photosynthetic activity in three Californian vegetation types. Ecological Applications 5, 28‑41.
- Gamon J.A., Serrano L., Surfus J.S., 1997. The photochemical reflectance index: an optical indicator of photosynthetic radiation use efficiency across species, functional types, and nutrient levels. Oecologia 112, 492‑501.
- Gao X., Huete A.R., Ni W., Miura T., 2000. Optical – biophysical relationships of vegetation spectra without background contamination. Remote Sensing of Environment 74, 609 – 620.
- Garabet S., Wood M., Ryan J., 1998. Nitrogen and water effects on wheat yield in a Mediterranean-type climate I. Growth, water-use and nitrogen accumulation. Field Crops Research 57, 309–318.
- Garbulsky M.F., Peñuelas J., Gamon J., Inoue Y., Filella I., 2011. The photochemical reflectance index (PRI) and the remote sensing of leaf, canopy and ecosystem radiation use efficiencies: A review and meta-analysis. Remote Sensing of Environment 115, 281‑297.

- Garbulsky M.F., Peñuelas J., Papale D., Ardö J., Goulden M.L., Kielyet G., 2010. Patterns and controls of the variability of radiation use efficiency and primary productivity across terrestrial ecosystems. Global Ecology and Biogeography19, 253‑267.
- Garcıa del Moral L.F., Boujenna A., Yanez J.A., Ramos J.M., 1995. Forage production, grain yield and protein content in dual purpose triticale grown for both grain and forage. Agron. J. 87, 902 - 908.
- Gardner F.P.; Parce R., Mitchel R.L., 1985. Carbon fixation by crop canopies. Physiology of Crop Plants xx, 31-57.
- Garrido-Lestache E., López-Bellidob R.J., L. López-Bellido, 2005. Durum wheat quality under Mediterranean conditions as affected by N rate, timing and splitting, N form and S fertilization. European Journal of Agronomy 23, 265‑278.
- Giunta F., Motzo R., Deidda M., 1993. Effect of drought on yield and yield components of durum wheat and triticale in a Mediterranean environment. Field Crops Research 33, 399-409.
- González F.G., Slafer G.A., Miralles D.J., 2005. Pre-anthesis development and number of fertile florets in wheat as affected by photoperiod sensitivity genes Ppd-D1 and Ppd-B1. Euphytica 146, 253–269.
- Gooding M.J., Ellis R.H., Shewry P.R., Schofield J.D., 2003. Effects of restricted water availability and increased temperature on the grain filling, drying and quality of winter wheat. Journal of Cereal Science 37, 295‑309.
- Guérif M., Duke C.L., 2000. Adjustment procedures of a crop model to the site specific characteristics of soil and crop using remote sensing data assimilation. Agriculture, Ecosystems and Environment 81, 57–69
- Gusta L.V., Chen T.H.H., 1987. The physiology of water and temperature stress. In: Wheat and Wheat Improvement. (Ed.) Heyne E.G., Agronomy, vol. 13. American Society of Agronomy, Inc., p. 115–150.
- Guttieri M.J., Stark J.C., Obrien K., Souza E., 2001. Relative sensitivity of spring wheat grain yield and quality parameters to moisture deficit. Crop Science 41, 327-335.

- Haboudane D., Miller J.R., Pattey E., Zarco-Tejada P.J., Strachan I., 2004. Hyperspectral vegetation indices and novel algorithms for predicting green LAI of crop canopies: modeling and validation in the context of precision agriculture. Remote Sens. Environ. 90, 337-352.
- Hamar D., Ferencz C., Lichtenberg J., Tarcsai G., Frencz-Arkos I., 1996. Yield estimation for corn and wheat in the Hungarian Great Plain using Landsat MSS data. Int. J. Remote Sens.17, 1689‑1699.
- Hansen J.W., Jones J.W., 2000. Scaling-up crop models for climate variability applications. Agricultural Systems 65, 43‑72.
- Hargreaves G.L., Hargreaves G.H., Riley P., 1985. Irrigation water requirement for the Senegal River Basin. Journal of Irrigation and Drainage Engineering, ASCE 111, 265–275.
- Hilker T., Coops N.C., Wulder M.A., Black T.A., Guy R.D., 2008. The use of remote sensing in light use efficiency based models of gross primary production: A review of current status and future requirements. Science of The Total Environment 404, 411‑423.
- Hipps L.E., Asrar G., Kanemasu E.T., 1983. Assessing the interception of photosynthetically active radiation in winter wheat. Agric. Meteorol. 28, 253–259.
- Holben B.N., 1986, Characteristics of maximum-value composite images for temporal AVHRR data. International Journal of Remote Sensing 7, 1435–1445.
- Huang W.J., Zhao C. J., Wang J.H., Wang J.D., Ma Z.H., 2004. Application of red edge variables to nutrition diagnosis and grain quality forecast of winter wheat. Transactions of The Chinese Society of Agricultural Engineering 20, 1-6.
- Huete A., Didana K., Miura T., Rodriguez E.P., Gao X., Ferreira L.G., 2002. Overview of the radiometric and biophysical performance of the MODIS vegetation indices. Remote Sensing of Environment 83, 195 – 213.
- Huete A.R., 1988. A soil-adjusted vegetation index (SAVI). Remote Sensing of Environment 25, 295 – 309.

- Hunt L.A., Van Der Poorten G., Pararajasingham S., 1991. Postanthesis temperature effects on duration and rate of grainfilling in some winter and spring wheat. Canadian Journal of Plant Science 71, 609-17.
- Hurkman W.J., McCue K.F., Altenbach S.B., et al., 2003. Effect of temperature on expression of genes encoding enzymes for starch biosynthesis in developing wheat endosperm. Plant Sci. 164, 873–881.
- Italian National Institute of Statistic– ISTAT: http://agri.istat.it
- International Pasta Organization – IPO: http://www.internationalpasta.org/
- Jamieson P.D., Semenov M.A., 2000. Modelling nitrogen uptake and redistribution in wheat. Field Crops Research 68, 21‑29.
- Jamieson P.D., Zyskowski R.F., Semenov M.A., 2004. Modelling genetic variability in wheat quality. In: VIII European Society for Agronomy Book of Proceedings, p. 275-276.
- Jenner C.F., 1991. Effects of exposure of wheat ears to high temperature on dry matter accumulation and carbohydrate metabolism in the grain of two cultivars. I. Immediate responses. Australian Journal of Plant Physiology 18, 165-77.
- Jenner C.F., Ugalde T.D., Aspinall D., 1991. The physiology of starch and protein deposition in the endosperm of wheat. Australian Journal of Plant Physiology 18, 211–226.
- Johnson V.A., Mattern P.J., Peterson C.J., Kuhr S.L., 1985. Improvement of wheat protein by traditional breeding and genetic techniques. Cereal Chem. 62, 350–355.
- Jones C.A., Kiniry J.R., 1986. In: CERES-Maize: Simulation Model of Maize Growth and Development. (Eds.) Jones C.A. and Kiniry J.R., Texas A&M University Press, College Station, TX, USA.
- Jones J.W., Hoogenboom G., Porter C.H., Boote K.J., Batchelor W.D., Hunt L.A., Wilkens P.W., Singh U., Gijsman A.J., Ritchie J.T., 2003. The DSSAT cropping system model. Eur. J. Agron. 18, 235–265.
- Jongschaap R.E.E., 2006. Run-time calibration of simulation models by integrating remote sensing estimates of leaf area index and canopy nitrogen. European Journal of Agronomy 24, 316‑324

- Jordan C.F., 1969. Derivation of leaf area index from quality of light on the forest floor. Ecology 50, 663–666.
- Jørgensen S.E., Kamp-Nielsen L., Christensen T., Windolf-Nielsen J., Westergaard B.,1986. Validation of a prognosis based upon a eutrophication model. Ecol. Model. 35, 165-182.
- Kang S., Zhang L., Liang Y., Hu X., Cai H., Gu B., 2002. Effects of limited irrigation on yield and water use efficiency of winter wheat in the Loess Plateau of China. Agricultural Water Management 55, 203-216.
- Kiliç H., Yağbasanlar T., 2010. The effect of drought stress on grain yield, yield components and some quality traits of durum wheat (*Triticum turgidum* ssp. durum) Cultivars. Notulae Botanicae Horti Agrobotanici Cluj-Napoca 38, pp 164-170.
- Knyazikhin Y., Glassy J., Privette J.L., Running S.W., Nemani R., Zhang Y., 1999. MODIS Leaf Area Index (LAI) and Fraction of Photosynthetically Active Radiation Absorbed by vegetation (*f*PAR). Product (MOD15) Algorithm Theoretical Basis Document, 1999. Website accessed 04/2007.
  Available athttp://www.ntsg.umt.edu/modis/ATBD/ATBD_MOD15_v21.pdf.
- Kobata T., Palta J.A, Turner T.C., 1992. Rate of development of post-anthesis water deficits and grain filling of spring wheat. Crop Science 32, 1238–1242.
- Kolderup F., 1975. Effects of temperature, photoperiod, and light quantity on protein production in wheat grains. Journal of the Science of Food and Agriculture 26, 583-592.
- Kramer Th., 1979. Environmental and genetic variation for protein content in winter wheat (*Triticum aestivum* L.). Euphytica 28, 209-218.
- Kumar, M., Monteith, J.L., 1981. Remote sensing of crop growth. In: Plants and the Daylight Spectrum. (Ed.) Smith H., Academic Press, London, pp. 133–144.
- Laidler G.J., Treitz P.M., Atkinson D.M., 2008. Remote sensing of arctic vegetation: relations between the spatial resolution and vegetation cover on Boothia Pninsula, Nunavut. ARCTIC Vol. 61, n. 1, 1–13.

- Landsberg J.J., Waring R.H., 1997. A generalised model of forest productivity using simplified concepts of radiation-use efficiency, carbon balance and partitioning. Forest Ecology and Management 95, 209‑228.
- Latiri K., Lhomme J.P., Annabi M., Setter T.L., 2010. Wheat production in Tunisia: progress, inter-annual variability and relation to rainfall. European Journal of Agronomy 33, 33–42.
- Launay M., Guerif M., 2005. Assimilating remote sensing data into a crop model to improve predictive performance for spatial applications. Agriculture, Ecosystems & Environment 111, 321–339.
- Lawlor D.W., Mitchell R.A.C., 2000. Crop ecosystems responses to climatic change: wheat. In: Climate Change and Global Crop Productivity. (Eds.) Reddy K.R. and Hodges H.F., CAB International, Cambridge, pp. 57–80.
- Li C., Cao W., Dai T., 2001. Dynamic characteristics of floret primordium development in wheat. Field Crops Research 71, 71–76.
- Li C., Wang J., Wang Q., Wang D., Song X., Wang Y., Huang W., 2012. Estimating wheat grain protein content using multi-temporal remote sensing data based on partial least squares regression. Journal of Integrative Agriculture 11, 1445‑1452.
- Li Q., Dong B., Qiao Y., Liu M., Zhang J., 2010. Root growth, available soil water, and water-use efficiency of winter wheat under different irrigation regimes applied at different growth stages in North China. Agricultural Water Management 97, 1676–1682.
- Li Y.X., Zhu Y., Tian Y.C., You X.T., Zhou D.Q., Cao W.X., 2005. Relationship of grain protein content and relevant quality traits to canopy reflectance spectra in wheat. Scientia Agricultura Sinica 38, 1332-1338.
- Liu W.T., Kogan F., 2002. Monitoring Brazilian soybean production using NOAA/AVHRR based vegetation condition indices. International Journal of Remote Sensing 23, 1161-1179
- Liu L., Wang J., Bao Y., Huang W., Ma Z., Zhao C., 2006. Predicting winter wheat condition, grain yield and protein content using multi-temporal EnviSat-ASAR and Landsat TM satellite images. International Journal of Remote Sensing 27, 737–753.

- Loague K., Green R.E., 1991. Statistical and graphical methods for evaluating solute transport models: overview and application. Journal of Contaminant Hydrology 7, 51 –73.
- Lobell D.B., Asner G.P., Ortiz-Monasterio J.I., Benning T.L. 2003. Remote sensing of regional crop production in the Yaqui Valley, Mexico: estimates and uncertainties. Agriculture, Ecosystems and Environment 94, 205–220.
- Lopez C.G., Banowetz G.M., Peterson C.J., Kronstad W.E., 2003. Dehydrin expression and drought tolerance in seven wheat cultivars. Crop Science 43, 577-582.
- Los S.O.,. Collatz G.J, Sellers P.J., Malmstro C.M.M, Pollack N.H., Defries R.S., Bounoua L., Parris M.T., Tucker C.J., Dazlichi D.A., 2000. A global 9-year biophysical land surface dataset from NOAA AVHRR data. J. Hydrometeorol. 1, 183–199.
- Los S.O., North P.R.J., Grey W.M.F., Barnsley M.J., 2005. A method to convert AVHRR Normalized Difference Vegetation Index time series to a standard viewing and illumination geometry. Remote Sensing of Environment 99, 400–411.
- Ludwig. F., Asseng S., 2006. Climate change impacts on wheat production in a Mediterranean environment in Western Australia. Agricultural System 90, 159–179.
- Luo C., Branlard G., Griffin W.B., McNeil D.L., 2000. The effect of nitrogen and sulphur fertilization and their interaction with genotype on wheat glutenins and quality parameters. J Cereal Sci 31, 185–194.
- Maas S.J., 1988. Use of remotely-sensed information in agricultural crop growth models. Ecological Modelling 41, 247‑268.
- Mahey R.K., Singh R., Sidhu S.S., Narang R.S., Dadhwal V.K., Parihar J.S., 1993. Preharvest state-level wheat acreage estimation using IRS-IA LISS-I data in Punjab (India). International Journal of Remote Sensing 14 1099‑1106.
- Marti J., Bort J., Slafer G.A., Araus J.L., 2007. Can wheat yield be assessed by early measurements of Normalized Difference Vegetation Index?. Annals of Applied Biology 150, 253–257

- Mariani B.M., D' Egidio M.G., Novaro P., 1995. Durum wheat quality evaluation: influence of genotype and environment. Cereal Chemistry 72, 194-197.
- Maskova Z., Zemek F., Kvet J., 2008. Normalized difference vegetation index (NDVI) in the management of mountain meadows. Boreal environment research Vol. 13, n. 5, 417-432
- McCown R.L., Hammer G.L., Hargreaves J.N.G., Holzworth D., Freebairn D.M., 1996. APSIM: a novel software system for model development, model testing and simulation in agricultural systems research. Agric. Syst. 50, 255‑271
- Mearns L.O., Rosenzweig C., Goldberg R., 1997. Mean and variance change in climate scenarios: Methods, agricultural applications, and measures of uncertainty. Climatic Change 35, 367–396.
- Meinke H., Rabbinge R., Hammer G.L., Van Keulen H., Jamieson P.D., 1998. Improving wheat simulation capabilities in Australia from a cropping systems perspective. II. Testing simulation capabilities of wheat growth. Eur. J. Agron. 8, 83‑99.
- Miller T.D., 1992. Growth stages of wheat: identification and understanding improve crop management. Better Crops with Plant Food. (Eds.) Patash & Phosphate Institute.
- Mitchell R.A.C., Mitchell V.J., Driscoll S.P., Franklin J., Lawlor D.W., 1993. Effects of increased CO_2 concentration and temperature on growth and yield of winter-wheat at 2 levels of nitrogen application. Plant Cell & Environment 16, 521–529.
- Mkhabela M.S., Mkhabela M.S., Mashinini N.N., 2005. Early maize yield forecasting in the four agro-ecological regions of Swaziland using NDVI data derived from NOAA's-AVHRR. Agricultural and Forest Meteorology 129, 1‑9
- Mkhabela M.S., Mkhabela M.S., 2000. Exploring the possibilities of using NOAA AVHRR data to forecast cotton yield in Swaziland. Uniswa J. Agr. 9 13–21.
- Mo X., Liu S., Lin Z., Xu Y., Xianga Y., McVicarc T.R., 2005. Prediction of crop yield, water consumption and water use efficiency with a SVAT-crop growth model

using remotely sensed data on the North China Plain. Ecological Modelling 183, 301–322.

- Monteith, J.L., 1972. Solar radiation and productivity in tropical ecosystems. J. Appl. Ecol. 9, 747–766.
- Monteith J.L., 1977. Climate and efficiency of crop production in Britain. Philos Trans R Soc Lond, B Biol Sci 281, 277–294.
- Monteith, J.L., Unsworth M.H., 1990. Principles of environmental physics. Edward Arnold Pub, London.
- Moriondo M., Maselli F., Bindi M., 2007. A simple model of regional wheat yield based on NDVI data. European Journal of Agronomy 26, 266–274.
- Mossedaq F., Smith D.H., 1994. Timing nitrogen application to enhance spring wheat yield in a Mediterranean climate. Agron. J. 86, 221–226.
- Moulin S., Bondeau A., Delecolle R., 1998. Combining agricultural crop models and satellite observations: From field to regional scales. International Journal of Remote Sensing 19, 1021-1036.
- Myneni R.B., Ross J., Asrar G., 1989. A review on the theory of photon transport in leaf canopies. Agric For Meteorol 45, 1‑153.
- Myneni R.B., Williams D.L., 1994. On the relationship between FAPAR and NDVI. Remote Sens. Environ. 49, 200–211.
- Myneni R.B., Maggion S., Iaquinta J., Privette J.L., Gobron N., Pinty B., Kimes D.S., Verstraete M.M., Williams D.L., 1995a. Optical remote sensing of vegetation: modeling, caveats, and algorithms. Remote Sens. Environ. 51, 169–188.
- Myneni R.B., Hall F.G., Sellers P.J., Marshak A.L., 1995b. The interpretation of spectral vegetation indexes. IEEE Transactions on Geoscience and Remote Sensing 33, 481‑486.
- Myneni R.B., Nemani R.R., Running S.W., 1997, Estimation of global leaf area index and absorbed PAR using radiative transfer models. IEEE Transaction on Geoscience and Remote Sensing 35, 1380–1393.
- Nain A.S., Kersebaum K.C., 2007. Calibration and validation of CERES model for simulating water and nutrients in Germany In: Modelling water and nutrient

dynamics in soil-crop systems. Chapter 12. (Eds) Kersebaum K.C., Hecker J.M., Mirschel W., Wegehenkel; Springer Pub., p. 161-181.

- Nash J.E., Sutcliffe J.V., 1970. River flow forecasting through conceptual model: Part I A discussion of principles. Journal of Hydrology 10, 282-290.
- Neales T.F., Anderson M.J., Wardlaw I.F., 1963. The role of the leaves in the accumulation of the nitrogen by wheat during ear development. Australian Journal of Agricultural Research 14, 725–736.
- Novaro P., D'Egidio M.G., Bacci L., Mariani B.M., 1997. Genotype and environment: their effect on some durum wheat quality characteristics. Journal of Genetics and Breeding 51, 247-252.
- Nouvellon Y., Moran M.S., Lo Seen D., Bryant R., Rambal S., Ni W.M., Begue A., Chehbouni A., Emmerich W.E., Heilman P., Qi J.G, 2001. Coupling a grassland ecosystem model with Landsat imagery for a 10-year simulation of carbon and water budgets. Remote Sensing of Environment 78, 131–149.
- Oak M. D., Sissons M., Egan N., Tamhankar S.A., Rao V.S., Bhosale S.B., 2006. Relationship between gluten strength and pasta firmness in Indian durum wheats. International Journal of Food Science and Technology 41, 538–544.
- O'Connell M.G., O'Leary G.J., Whitfield D.M., Connor D.J., 2004. Interception of photosynthetically active radiation and radiation-use efficiency of wheat, field pea and mustard in a semi-arid environment. Field Crops Research 85, 111‑124.
- Olioso A., Chauki H., Courault D., Wigneron J., 1999. Estimation of Evapotranspiration and Photosynthesis by Assimilation of Remote Sensing Data into SVAT Models. Remote Sensing of Environment 68, 341‑356.
- Ollinger S.V., Richardson A.D., Martin M.E., Hollinger D.Y., Frolking S.E., ReichP.B., 2008. Canopy nitrogen, carbon assimilation, and albedo in temperate and boreal forests: Functional relations and potential climate feedbacks. Proceedings of the National Academy of Sciences 105, 19336‑19341.
- Orlandini S., Mancini M., Grifoni D., Orlando F., Dalla Marta A., Capecchi V., 2011. Integration of meteo-climatic and remote sensing information for the analysis

of durum wheat quality in Val d'Orcia (Tuscany, Italy). Időjárás Quarterly Journal of the Hungarian Meteorological Service 115, 233-245.

- Ortiz-Monasterio J. I., Lobell D.B., 2007. Remote sensing assessment of regional yield losses due to sub-optimal planting dates and fallow period weed management. Field Crops Research 101, 80‑87.
- Otter-Nacke S., Godwin D.C., Ritchie J.T., 1986. Yield model development. Testing and validating the CERES-Wheat model in diverse environments. AGRISTARS YM-15-00407:JSC 20244. USDA-ARS Temple, TX and IFDC Muscle Shoals, AL. 147.
- Ottman M.J., Doerge T.A., Martin E.C., 2000. Durum grain quality as affected by nitrogen fertilization near anthesis and irrigation during grain fill. Agron J 92, 1035–1041.
- Pala M., Stockle C.S., Harris H.C., 1996. Simulation of durum wheat (*Triticum turgidum* ssp. durum) growth under different water and nitrogen regimes in a Mediterranean environment using CropSyst. Agricultural Systems 51, 147‑163.
- Pan J., Zhu Y., Jiang D., Dai T., Li Y., Cao W., 2006. Modeling plant nitrogen uptake and grain nitrogen accumulation in wheat. Field Crops Research 97, 322–336.
- Pecetti L., Hollington P.A., 1997. Application of the CERES-Wheat simulation model to durum wheat in two diverse Mediterranean environments. European Journal of Agronomy, 6 ,125‑139.
- Penning de Vries F.W.T., Brunsting A.H.M., Van Laar H.H., 1974. Products, requirements and efficiency of biosynthesis: A quantitative approach. J. Theor. Biol. 45, 339 - 377.
- Peterson C.J., Graybosch P.S., Baenziger. P.S, Grombacher A.W., 1992. Genotype and environment effects on quality characteristics of hard red winter wheat. Crop Science 32, 98-103.
- Pinter P.J., Hatfield J.L., Schepers J.S., Barnes E.M., Moran M.S., Daughtry C.S.T, Upchurch D.R., 2003. Remote Sensing for Crop Management. Photogrammetric Engineering & Remote Sensing, 69, 647–664.

- Pinty B., Leprieur C., Verstraete M.M., 1993. Towards a quantitative interpretation of vegetation indices, part1: biophysical canopy properties and classical indices. Remote Sensing of Environment 7, 127 – 150.
- Pleijel H., Mortensen L., Fuhrer J., Ojanpera K., Danielsson, H., 1999. Grain protein accumulation in relation to grain yield of spring wheat (*Triticum eastivum* L.) grown in open-top chambers with different concentrations of ozone, carbon dioxide and water availability. Agric. Ecosys. Environ. 72, 265 - 270.
- Porter J.R, 1993. AFRCWHEAT2: a model of the growth and development of wheat incorporating responses to water and nitrogen. Eur. J. Agron 2, 69‑82
- Porter J.R, Gawith M., 1999. Temperatures and the growth and development of wheat: a review. European Journal of Agronomy 10, 23–36.
- Prasad A.K., Chaib L., Singh R.P., Kafatos M., 2006. Crop yield estimation model for Iowa using remote sensing and surface parameters. International Journal of Applied Earth Observation and Geoinformation 8, 26–33.
- Prasad P.V.V., Staggenborg S.A., Ristic Z., 2008. Impacts of drought and/or heat stress on physiological, developmental, growth and yield: Processes of crop plants. In: Response of crops to limited water: understanding and modeling water stress effects on plant growth processes. Chapter 11 (Ed.) Advances in Agricultural Systems Modeling Series 1, p. 311-355.
- Priestley C.H.B., Taylor R.J, 1972. On the assessment of surface heat flux and evaporation large scale parameters. Monthly Weather Rev. 100, 81-82.
- Quarmby N.A., Milnes M., Hindle T.L., Silleos N., 1993. The use of multi-temporal NDVI measurements from AVHRR data for crop yield estimation and prediction. International Journal of Remote Sensing 14, 199-210
- Rawson H.M., Evans L.T., 1971. The contribution of stem reserves to grain development in a range of wheat cultivars of different height. Aust. J. Agric. Res. 22, 851–863.
- Regan K.L., Siddique K.H.M., Turner N.C., Whan B.R., 1992. Potential for increasing early vigour and total biomass in spring wheat. II: Characteristics

associated with early vigour. Australian Journal of Agricultural Research 43, 541 – 553.

- Ren J., Li S., Chen Z., Zhou Q., Tang H., 2007. Regional yield prediction for winter wheat based on crop biomass estimation using multi-source data. Conference Publications, Geoscience and Remote Sensing Symposium, IGARSS 2007. IEEE International, 23-28 July 2007, p. 805 – 808.
- Ren J., Chen Z., Zhou Q., Tang H., 2008. Regional yield estimation for winter wheat with MODIS-NDVI data in Shandong, China. International Journal of Applied Earth Observation and Geoinformation 10, 403–413.
- Ren J.Q., Liu X.R., Chen Z.X., Zhou Q.B., Tang H.J., 2009. Prediction of winter wheat yield based on crop biomass estimation at regional scale. [Article in Chinese] Ying Yong Sheng Tai Xue 20, 872-8.
- Reyniers M., Vrindts E., De Baerdemaeker J., 2006. Comparison of an aerial-based system and an on the ground continuous measuring device to predict yield of winter wheat. European Journal of Agronomy 24, 87‑94
- Rezzoug W., Gabrielle B., Suleiman A., Benabdeli K., 2008. Application and evaluation of the DSSAT-wheat in the Tiaret region of Algeria. African Journal of Agricultural Research 3, 284–296.
- Rharrabti Y., Elhani. S., Martos-Nunez. V., Garcia del Moral L.F., 2001a. Protein and lysine content, grain yield, and other technological traits in Durum Wheat under Mediterranean conditions. Journal of Agricultural and Food Chemistry 49, 3802-3807.
- Rharrabti Y., Villegas D., Garcia del Moral L.F., Aparicio N., Elhani S., Royo C., 2001b. Environmental and genetic determination of protein content and grain yield in durum wheat under Mediterranean conditions. Plant Breeding 120, 381-388.
- Rharrabti Y., Royo C., Villegas D., Aparicio N., García del Moral L.F., 2003a. Durum quality in Mediterranean environments I. Quality expression under different zones, latitudes and water regimes across Spain. Field Crop Res. 80, 123–131.
- Rharrabti Y., Villegas D., Royo C., Martos-Núñez V., García del Moral L.F., 2003b. Durum quality in Mediterranean environments II. Influence of climatic

variables and relationships between quality parameters. Field Crop Res. 80, 133‑140.

- Ritchie J.T, 1972. Model for predicting evaporation from a row crop with incomplete cover. Water Resource Research 8, 1024-1213.
- Ritchie J.T., Otter S., 1985. Description and performance of CERES-Wheat. A user-oriented wheat yield model. ARS Wheat Yield Project, ARS 38, 159–176.
- Ritchie J.T., Singh U., Godwin D.C., Bowen W.T., 1998. Cereal growth, development and yield. In: Understanding Options for Agricultural Production. (Eds.) Tsuji, G.Y., et al., Kluwer Academic Pub., Dordrecht, p. 79–98.
- Richter G.M. , Acutis M. , Trevisiol P. , Latiri K. , Confalonieri R., 2010. Sensitivity analysis for a complex crop model applied to Durum wheat in the Mediterranean. European Journal of Agronomy 32, 127–136.
- Rinaldi M., 2004. Water availability at sowing and nitrogen management of durum wheat: a seasonal analysis with the CERES-Wheat model. Field Crops Research 89, 27–37.
- Rostami M.A., O'Brien L., 1996. Differences among bread wheat genotypes for tissue nitrogen content and their relationship to grain yield and protein content. Aust. J. Agric. Res. 47, 33-45.
- Rouse J.W., Haas R.H., Schell, J.A. Deering D.W., 1973. Monitoring vegetation systems in the Great Plains with ERTS. In: 3rd ERTS Symposium, NASA SP-351 I, p. 309–317.
- Royo C., Aparicio N., Villegas D., Casadesus J., Monneveux P., Araus J.L., 2003. Usefulness of spectral reflectance indices as durum wheat yield predictors under contrasting Mediterranean conditions. International Journal of Remote Sensing 24, 4403-4419
- Runyon J., Waring R.H., Goward S.N., Welles J.M., 1994. Environmental limits on net primary production and light-use efficiency across the Oregon Transect. Ecological Applications 4, 226‑237.
- Russell E.W., 1973. Soil conditions and plant growth. Long man Group Ltd, London and New York, p. 849.

- Salmon C., Clark A.J., 1913. Durum wheat. Farmers' Bulletin 534, Issued May 2, (Eds.) Washington Government Printing Office.
- Sander D.H., Allaway W.H., Olson R.A.1987. Modification of nutritional quality by environmental and production practices. In: Nutritional quality of cereal grains: genetic and agronomic improvement. (Eds.) Olson R.A and Frey K.J., Agronomy Monograph 28. ASA-CSSA-SSSA, Madison, WI, U.S.A., p 45–81.
- Schloss A.L., Kicklighter D.W., Kaduk J., Wittenberg U., 1999. Comparing global models of terrestrial net primary productivity (NPP): comparison of NPP to climate and the Normalized Difference Vegetation Index (NDVI). Global Change Biology 5, 25–34.
- Sehgal V.K., Rajak D.R., Chaudhary K.N., Dadhwal V.K., 2002. Improved regional yield prediction by crop growth monitoring system using remote seinsing derived crop phenology. The International Archives of the Photogrammetry, Remote Sensing and Spatial Information Sciences, Vol. 34, Part 7 "Resource and Environment Monitoring", Hyderabad, India, 2002.
- Sellers P.J., 1985. Canopy reflectance, photosynthesis and transpiration. Int J Remote Sens, 6, 1335–1372.
- Sellers P.J., Randall D.A., Collatz G.J., Berry J.A., Field C.B., Dazlich D.A., Zhang C., Collelo G.D., Bounoua L., 1996. A revised land surface parameterization (SiB2) for atmospheric GCMs. Part 1. Model formulation. J. Climate 9, 676–705.
- Serrano L., Filella I., Pen˜uelas J., 2000. Remote sensing of biomass and yield of winter wheat under different nitrogen supplies. Crop Sci. 40, 723–731
- Schnyder H., Baum U., 1992. Growth of the grain of wheat (*Triticum aestivum* L.). The relationship between water content and dry matter accumulation. Eur. J. Agron. 1, 51–57.
- Shaykewich C.F., 1995. An appraisal of cereal crop phenology modeling. Canadian Journal of Plant Science 75, 329-341.
- Shewry P.R., Napier J.A., Tatham A.S., 1995. Seed storage proteins: structures and biosynthesis. The Plant Cell 7, 945-956.

- Sims D.A., Luo H., Hastings S., Oechel W.C., Rahman A.F., Gamon J.A., 2006. Parallel adjustments in vegetation greenness and ecosystem CO2 exchange in response to drought in a Southern California chaparral ecosystem. Remote Sensing of Environment 103, 289‑303.
- Singh A.K., Jain, G.L., 2000. Title Effect of sowing time, irrigation and nitrogen on grain yield and quality of durum wheat (*Triticum durum*). Indian Journal of Agricultural Sciences 70, 532-533
- Slafer G.A., Rawson H.M., 1994. Sensitivity of wheat phasic development to major environmental factors: a re-examination of some assumptions made by physiologists and modellers. Australian Journal of Plant Physiology 21, 393–426.
- Slafer G.A., Whitechurch E.M., 2001. Manipulating wheat development to improve adaptation. In: Application of physiology in wheat breeding. (Eds.) Reynolds M.P., Ortiz-Monasterio J.I., McNab A. (CIMMYT: Mexico, DF), p 160–170.
- Slafer G.A., Kantolic A.G., Appendino M.L., Miralles D.J., Savin R., 2009. Crop development: genetic control, environmental modulation and relevance to genetic improvement of crop yield. In: Crop physiology: applications for genetic improvement and agronomy. (Eds.) Sadras V. and Calderini D., Academic Press, London, p 277–308.
- Smith G.P.; Gooding M.J., 1996. Relationships of wheat quality with climate and nitrogen application in regions of England (1974-1993). Annals of Applied Biology 129, 97-108.
- Sofield I., Evans L.T., Cook M.G., Wardlaw I.F., 1977. Factors influencing the rate and duration of grain filling in wheat. Australian Journal of Plant Physiology 4, 785-97.
- Spiertz J.H.J., 1977. The influence of temperature and light intensity on grain growth in relation to the carbohydrate and nitrogen economy of the wheat plant. Neth. J. Agric. Sci. 25, 182–197.
- Spiertz J.H.J., Van De Haar H., 1978. Differences in grain growth, crop photosynthesis and distribution of assimilates between a semi-dwarf and a standard cultivar of winter wheat. Neth. J. Agric. Sci. 26, 233–249.

- Steinmetz S., Guerif M., Delecolle R., Baret F., 1990. Spectral estimates of the absorbed photosynthetically active radiation and light-use efficiency of a winter wheat crop subjected to nitrogen and water deficiencies. Int. J. Remote Sens. 11, 1797–1808.
- Stoddart F. L., Marshall D. R., 1990. Variability in grain protein in Australian hexaploid wheats. Aust. J. Agric. Res. 41, 277-288.
- Stone P. J., Nicolas M. E., 1994. Wheat cultivars vary widely in their responses of grain yield and quality to short periods of post-anthesis heat stress. Australian Journal of Plant Physiology 21, 887-900.
- Stone P.J., Nicolas M.E., 1996. Effect of timing of heat stress during grain filling on two wheat varieties differing in heat tolerance. II. Fractional protein accumulation. Aust. J. Plant Physiol. 23, 739–749.
- Stone, P.J., Savin, R., 1999. Grain quality and its physiological determinants. In: Wheat: ecology and physiology of yield determination. (Eds.) Satorre E.H. and Slafer G.A., Haworth Press Inc, New York, USA, p. 85–120.
- Stone R.C., Meinke H., 2005. Operational seasonal forecasting of crop performance. Philosophical transactions of royal society B 360, 2109-2124.
- Taiz L., Zeiger E., 2010. Photosynthesis: Physiological and Ecological Considerations. In: Plant Physiology. Chapter 9, IV Ed., (Eds.) Taiz L. and Zeiger E., Sinauer Associates Pub., Inc. 2010.
- Tan B., Hu J., Huang D., Yang W., Zhang P., Shabanov N.V., Knyazikhin Y., Nemani R.R., Myneni R.B., 2005. Assessment of the broadleaf crops leaf area index product from the Terra MODIS instrument. Agricultural and Forest Meteorology 135, 124–134.
- Tashiro T., Wardlaw I.F., 1990. The effect of high temperature at different stages of ripening on grain set, grain weight and grain dimensions in the semi-dwarf wheat ‘Banks’. Annals of Botany (London) 65, pp. 51-61.
- Tester R.F., Morris W.R., Ellis R.H., Piggott J.R., Batts G.R., Wheeler T.R., Morison W.R., Hadley P., Ledward D.A., 1995. Effects of elevated growth

temperature and carbon dioxide levels on some physicochemical proprieties of wheat starch. Journal of Cereal Science 22, 63–71.

- Tian Y., Dickinson R.E., Zhou L., Zeng X., Dai Y., Myneni R.B., Knyazikhin Y., Zhang X., Friedl M., Yu H., Wu W., Shaikh M., 2004. Comparison of seasonal and spatial variations of leaf area index and fraction of absorbed photosynthetically active radiation from Moderate Resolution Imaging Spectroradiometer (MODIS) and Common Land Model. Journal of geophysical research 109, 1-14
- Tilling A. K., O' Leary G. J., Ferwerda J. G., Jones S. D., Fitzgerald G. J., Rodriguez D., Belford R., 2007. Remote sensing of nitrogen and water stress in wheat. Field Crops Research104, 77‑85.
- Timms M.F., Bottomley R.C., Ellis J.R.S., Schofield J.D., 1981. The baking quality and protein characteristics of a winter wheat grown at different levels of nitrogen fertilization. Journal of the Science of Food and Agriculture 32, 684–698.
- Toscano P., Ranieri R., Matese A., Vaccari F.P., Gioli B., Zaldei A., Silvestri M., Ronchi C., La Cava P., Porter J.R., Miglietta F., 2012. Durum wheat modeling: the Delphi system, 11 years of observations in Italy. European Journal of Agronomy 43, 108–118.
- Trnka M., Žalud Z., Eitzinger J., Dubrovský M., 2005. Global solar radiation in Central European lowlands estimated by various empirical formula. Agricultural and Forest Meteorology 131, 54–76.
- Troccoli A., Borrelli G.M., De Vita P., Fares C., Di Fonzo N., 2000. Mini review: Durum wheat quality: a multidisciplinary concept. Journal of Cereal Science 32, 99‑113.
- Tucker C.J., Holben B.N., Elgin J.H., McMurtrey J.E., 1980. Relationships of spectral data to grain yield variation. Photogrammetric Engineering and Remote Sensing 46, 657‑666.
- Tucker C. J., Holben B. N., 1981. Remote sensing of total dry-matter accumulation in winter wheat. Remote Sensing of Environment 11, 171‑189
- Tucker C.J., Sellers P.J., 1986. Satellite remote sensing of primary production. Int. J. Remote Sens. 7, 1395–1416.

- Uhlen K.A., Hafskjold R., Kalhovd A.H., Sahlstrom S., Longva A., Magnus E. M., 1998. Effects of cultivars and temperature during grain filling on wheat protein content, composition, and dough mixing properties. Cereal Chem. 75, 460-465.
- Unganai L.S., Kogan F.N., 1998. Drought monitoring and corn yield estimation in Southern Africa from AVHRR Data. Remote Sens. Environ. 63, 219‑232.
- Vandiepen C.A., Wolf J., Vankeulen H., Rappoldt C., 1989. Wofost − A simulation-model of crop production. Soil Use and Management 5, 16‑24.
- Vanevert F.K., Campbell G.S., 1994. Cropsyst − A collection of object-oriented simulation-models of agricultural systems. Agronomy Journal 86, 325‑331.
- Van Ittersum M.K., Howden S.M., Asseng S., 2003. Sensitivity of productivity and deep drainage of wheat cropping systems in a Mediterranean environment to changes in CO_2, temperature and precipitation. Agricultural Ecosystem Environment 97, 255–273.
- Van Herwaarden A.F., Farquhar G.D., Angus J.F., Richards R.A., Howe G.N., 1998. 'Haying-off', the negative grain yield response of dryland wheat to nitrogen fertiliser. I. Biomass, grain yield, and water use. Aust. J. Agric. Res. 49, 1067–1081.
- Van Keulen H., Seligman N.G., 1987. Simulation of water use, nitrogen nutrition and growth of a spring wheat crop. Simulation Monographs, Pudoc, Wageningen (1987), p. 310.
- Vos J., 1981. Agricultural Research Reports, PUDOC. (Eds.) PUDOC, Wageningen, Netherlands, 1981, p. 164.
- Wang J.H., Huang W.J., Zhao C.J., Yang M.H., Wang Z.J., 2003. The inversion of leaf biochemical components and grain quality indicators of winter wheat with spectral reflectance. Journal of Remote Sensing 7, 277—284.
- Wang Z.J., Wang J.H., Liu L.Y., Huang W.J., Zhao C.J., Wang C.Z., 2004. Prediction of grain protein content in winter wheat (*Triticum aestivum* L.) using plant pigment ratio (PPR). Field Crops Research 90, 311–321
- Wardlaw I.F., Sofield I., Carrwright P.M., 1980. Factors limiting the rate of dry matter accumulation in the grain of wheat grown at high temperature. Australian Journal of Plant Physiology 7, 387-400.

- Wardlaw I.F., Moncur L., 1995. The response of wheat to high temperature following anthesis. The rate and duration of kernal filling. Australian Journal of Plant Physiology 22, 391-7.
- Weber E.A., Graeff S., Koller W.D., Hermann W., Merkt N., Claupein W., 2008. Impact of nitrogen amount and timing on the potential of acrylamide formation in winter wheat (*Triticum aestivum* L.). Field Crops Res 106, 44–52.
- Wheeler T.R., Hong T.D., Ellis R.H., Batts G.R., Morison J.I.L., Hadley P., 1996. The duration and rate of grain growth, and harvest index, of wheat (*Triticum aestivum* L.) in response to temperature and CO_2. Journal of Experimental Botany 47, 623-630.
- Whitechurch E.M., Slafer G.A., 2002. Contrasting Ppd alleles in wheat: effects on sensitivity to photoperiod in different phases. Field Crops Research 73, 95–105.
- Whitmarsh J., Govindjee., 1999. The photosynthetic process. In: Concepts in Photobiology: Photosynthesis and Photomorphogenesis. (Eds) Singhal G.S., Renger G., Sopory S.K., Irrgang K-D., Govindjee. Narosa Pub., p. 11-51.
- Wiegand C.L., Richardson A.J., 1990. Use of spectral vegetation indices to infer leaf area, evapotranspiration and yield: II. Results. Agron. J. 82, 630–636.
- Williams J.R., 1991. Runoff and water erosion. In: Modelling plant and soil systems. (Eds.) Hanks R.J. and Ritchie J.T., Agronomy Monograph: 31, American Society of Agronomy, Madison WI, USA, 439- 455.
- Willey R.W., Holliday R., 1971. Plant population, shading and thinning studies in wheat. J. Agric. Sci., Camb. 77, 453‑461.
- Wilson D.R., Jamieson P.D., 1985. Models of growth and water use of wheat in New Zealand. In: Wheat Growth and Modelling. (Eds.) Day W. and Atkin R.K., Plenum Press, London, p. 211‑216.
- Wit C.T., 1965. Photosynthesis of leaf canopies. Agricultural Research Report 663. Pudoc, Wageningen, p. 57.
- Wu C., Niu Z., Tang Q., Huang W., Rivard B., Feng J., 2009. Remote estimation of gross primary production in wheat using chlorophyll-related vegetation indices. Agricultural and Forest Meteorology 149, 1015–1021.

- Xiao G., Zhang Q., Yao Y., Zhao H., Wang R., Bai H., Zhang F., 2008. Impact of recent climatic change on the yield of winter wheat at low and high altitudes in semi-arid northwestern China. Agriculture Ecosystems and Environment 127, 37–42.
- Xue L., Cao W., Yang L., 2007. Predicting grain yield and protein content in winter wheat at different N supply levels using canopy reflectance spectra. Pedosphere 17, 646–653.
- Yang W., Tan B., Huang D., Rautiainen M., Shabanov N.V., Wang Y., Privette J.L., Huemmrich K.F., Fensholt R., Sandholt I., Weiss M., Ahl D.E., Gower S.T., Nemani R.R., Knyazikhin Y., Myneni R.B., 2006. MODIS Leaf Area Index products: from validation to algorithm improvement. Transactions on geoscience and remote sensing 44, 1885 – 1898.
- Yi Y., Yang D., Huang J., Chen D., 2008. Evaluation of MODIS surface reflectance products for wheat leaf area index (LAI) retrieval. Journal of Photogrammetry & Remote Sensing 63, 661–677
- Yuping M., Shili W., Li Z., Yingyu H., Liwei Z., Yanbo H., Futang W., 2008. Monitoring winter wheat growth in North China by combining a crop model and remote sensing data. International Journal of Applied Earth Observation and Geoinformation 10, 426–437.
- Zadoks J.C., Chang T.T., Konzak B.F., 1974. A decimal code for the growth stages of cereals. Weed Res. 14, 415–421.
- Zhang H., Oweis T., 1999. Water-yield relations and optimal irrigation scheduling of wheat in the Mediterranean region. Agricultural Water Management 38, 195-211.
- Zhang Y., Kendy E., Qiang Y., Changming L., Yanjun S., Hongyong S., 2004. Effect of soil water deficit on evapotranspiration, crop yield, and water use efficiency in the North China Plain. Agricultural Water Management 64, 107–122.
- Zhang J., Sui X., Li B., Su B., Li J., Zhoub D., 1998. An improved water-use efficiency for winter wheat grown under reduced irrigation. Field Crops Research 59, 91-98.

- Zhao C., Liu L., Wang J., Huang W., Song X., Li C., 2005. Predicting grain protein content of winter wheat using remote sensing data based on nitrogen status and water stress. International Journal of Applied Earth Observation and Geoinformation 7, 1–9.
- Zhao C.X., He M.R., Wang Z.L., Wang Y.F., Lin Q., 2009. Effects of different water availability at post-anthesis stage on grain nutrition and quality in strong-gluten winter wheat. Comptes Rendus Biologies 332, 759–764.

Acknowledgments

I would like to thank you:

Prof. Simone Orlandini (DIPSAA – University of Florence), for giving me the opportunity to continue working in research, make useful abroad experiences and improve my skills about agro-meteorological modeling,

Dr. Marco Mancini, Dr. Anna Dalla Marta, Dr. Federico Guasconi, Dr. Francesca Natali and Dr. Marco Napoli (DIPSAA – University of Florence), for the mutual aid shown over the years, and their major contribution to the performing of the field trials and in carrying out the research,

Prof. John Qu and Prof. Raymond Motha (ESTC - George Mason University, USA), for their time and the valuable suggestions, and for providing me with their cooperation the opportunity to acquire new knowledge in the field of remote sensing,

Dr. Xianjun Hao and Dr. Rui Zhang (ESTC - George Mason University, USA), for their patience in explaining Matlab functions, and their indispensable support in imagery processing,

Dr. Daniele Grifoni and Dr. Gaetano Zipoli (CNR – IBIMET), for collaborating with professionalism and competence in the research,

Consorzio Agrario di Siena (Siena Provincial Agrarian Consortium), for the interest in the topics covered. In particular, I would like to thank Dr. Roberto Ceccuzzi and Dr. Pietro Pagliuca for the support and availability shown,

Mr. Franco Barzi, for his friendliness and his active collaboration in the set up of the field trials and in monitoring of the crop,

Dr. Luciana Becherini, for her kindness and her significant contribution to the qualitative and quantitative analysis of the harvests,

Carletti Farm, for the time and the invaluable assistance in the collection of crop production data.

Fondazione Monte dei Paschi di Siena, for the interest shown towards the addressed issues and the support to the research activities,

ARSIA (Regional Agency for Development and Innovation in the Agro-forestry Sector), for the support in the collection of agro-meteorological data,

Dr. Petr Hlavinka (University of Agriculture and Forestry, Brno), for his kindness and his patience in explaining DSSAT-CERES functions.

My roommates in USA, Riz, Merce, Femi, Steven, Mike, Rahul and Sharath that made my stay away from home more enjoyable.